Model for Spatiotemporal Organization of Biochemical Circadian Clocks

Vom Fachbereich Physik
der Technischen Universität Darmstadt
zur Erlangung des Grades
eines Doktors der Naturwissenschaften
(Dr. rer. nat.)

genehmigte

DISSERTATION

von

Dipl.-Phys. Ivona Jakovljević
aus Belgrad

Darmstadt 2011
D17

Referent:	Prof. Dr. Friedemann Kaiser
Korreferentin:	Prof. Dr. Barbara Drossel
Tag der Einreichung:	04.02.2010
Tag der Prüfung:	21.06.2010

Contents

Chapter 1

Introduction

1.1 Quantitative Modelling

Rhythmic processes in biology are present everywhere, "...occurring at all levels of biological organisation, from unicellular to multicellular organisms, with period ranging from fractions of seconds to years.", stated Albert Goldbeter in his book about biochemical oscillations [1]. They are observed as a result of interactions between open systems and external environment, with dissipation of energy and matter if a system operates sufficiently far from equilibrium [2]. In biological systems nonlinearities arise mainly from feedback processes and cooperativity that regulate genetic and metabolic networks [3].
To understand the mechanisms underlying such rhythmic biological processes arising from diverse regulatory mechanisms, it is necessary to use an interdisciplinary approach combining the knowledge of molecular biology, bioinformatics and nonlinear dynamics. New data regarding genes, proteins and cellular networks are still emerging and it is important to quantify the links between them. In the case of rhythmic phenomena it is clear that this can be done using both data analysis and mathematical and physical modelling.
Generally two main approaches can be used to model such a complex system. The reductionist approach is based on minimal models describing relevant parts of one system or modules [4]. When they are fully understood, the next step is to create and analyse complex networks of such models. Usually it results in finding new dynamical properties, the ones that were not obvious from the simple modules. The second approach, preferred by experimentalists, is based on large-scale models describing all components and relevant processes in the system. It is usually inevitable to unravel the organisation of complex cellular networks. Regardless which type of modelling approach has been chosen, the difficulties to distinguish the different scales that occur in cell biology in time, space and complexity, still remain. However, quantitative modelling, relaying on broad tools from mathematics, physics and nonlinear dynamics, can help to reduce the region of parameter values that are critical for the system that is investigated or to distinguish which aspects of the model are more or less important. Different models can be developed, with respect to their purpose. Recent studies are more focused to combine experimental and theoretical work where usually models serve as working hypotheses, followed by appropriate experiments. Besides, experimental design is usually driven by logic of modelling. Modelling as a powerful theoretical tool in biology, brings two new scientific fields into focus, systems

biology and synthetic biology.

1.2 Systems Biology and Synthetic Biology

An emergent inter-disciplinary field in bioscience that has recently received increased attention is systems biology [5, 6]. It focuses on the systematic study of complex interactions that are very difficult to comprehend using only one scientific approach. Its roots are in the quantitative modelling of enzyme kinetics, simulations in neurophysiology, control theory and cybernetics.
Systems biology is an approach to study biological system, investigating its different structures, such as gene regulatory and biochemical networks, together with their dynamics. Using quantitative and qualitative analyses it tries to understand the functioning of the system as a whole. Thus, specific testable hypotheses about biological system can be constructed, which can be also experimentally investigated. Within the systems biology, experiment and theory are very close. Main aim of systems biology is to understand complex biological processes in order to tackle many important problems with biological and medical priorities such as mechanisms of disease, pharmaceutical applications including discovery of new drugs or drug target validation. Systems biology with its quantitative and predictive understanding of a biological system, provides the analytical framework in which new emerging fields of science start to operate. One of these new fields, with their promising applications is synthetic biology.
Synthetic biology, on the other hand, combines biology with principles of engineering in order to build and design biological systems or new functions from their standardised biological building-blocks. It was developed, similar as systems biology, to expand our understanding of biological systems and their functions, by testing artificial genetic networks using interdisciplinary approach based on the theoretical biology. Elowitz and co-workers demonstrated experimentally and theoretically how gene expression should work inside living cells, by placing DNA inside living cells [7]. Their construct called repressilator, brought new insights into intracellular network regulation and proved that a novel desired function can be designed and implemented in natural systems. A similar construct was successfully developed for metabolic networks, where integration of transcriptional regulation with metabolism was studied using synthetic gene-metabolic oscillator or metabolator [8].
Using engineering approaches, different scales of biological complexity can be constructed, such as novel genes and proteins, but also new regulation mechanisms, signal sensing or enzymatic reactions to novel multi-component modules and even to completely or partially engineered cells. Synthetic biology provides a framework for predicting and evaluating the dynamics of cellular processes. Apart from constructing and testing design principles in its simple or complex form, artificial systems for gene expression have been also used to study the influence of noise on the performance of designed units and modules [9]. It is clear that the potential applications of engineered biological "devices" are wide, ranging from functional genomics, gene and cell therapy in medicine, pharmacology, to nanotechnology. The model that will be presented in this thesis will try to unreveal some of the basic properties of circadian rhythm generator, using an approach from systems biology

and synthetic biology.

1.3 The Thesis

Numerous different models have been developed to investigate circadian rhythm generator and its dynamical properties. However there is a lack of research that incorporates different levels of its organisation together with environmental influences. The aim of this thesis is to investigate the possible mechanism of circadian rhythm organisation, on a cellular and intercellular level, using minimal model approach, with the tools of nonlinear dynamics. To achieve the first goal, two different oscillators, based on simple biochemical processes needed for self-sustained oscillations, are combined. The second goal is achieved, studying a higher level of organisation via a net of elements of combined oscillators with respect to a global and diffusive coupling among elements in the net. Some basic principles of circadian rhythm generator are tested using the single element model. To incorporate the influence from the environment, this model is extended with respect to changes in the model parameters. Phenomena of synchronisation and the formation of patterns are studied due to either variability of periods or stochastic influences. These investigations are extended, when nets of oscillatory elements are entrained by changes in the environmental signals.

Outline

This thesis is organised as follows. Chapter 2 consists of two parts. The first part deals with some general principles of a mathematical description of biochemical oscillations based on ordinary and delay differential equations. Description of coupled biological oscillators is introduced with tools from data analysis, necessary for the quantitative description of multioscillator systems. Noise and variability are also characterised in this chapter. The second part of chapter 2 deals with a specific type of biological oscillators, a circadian clock oscillator and introduces a biological concept and general properties of circadian rhythms, along with an overview on the modelling of circadian rhythms. In Chapter 3, a model of a circadian rhythm generator consisting of two different biochemical oscillators is introduced. A stability analysis of the two subsystems and of the coupled system is also presented along with an extended model for the external environmental influence, with the system's response to different periods of enviromental perturbation and the corresponding phase response curves. Chapter 4 deals with a net of such coupled two component oscillators, the influence of the variability on the net due to two different types of coupling and also, environmental influences on the net. Chapter 5 represents the stochastic influence on the single element and on the net of elements, with respect to two different types of coupling and environmental influences due to two different periods of entrainment. Finally, Chapter 6 represents the summary of results with the emphases on possible future work.

Chapter 2

Formal Representation and Analysis of Biological Oscillators

This chapter gives a quantitative description of biological oscillators as a class of nonlinear systems with necessary tools to analyse rhythmic phenomena observed in populations of oscillators. Besides, basic characteristics of circadian rhythms are presented, including core molecular mechanism and phase response curves. A brief overview over some important models for circadian clocks is also given in this chapter.

2.1 Biological Oscillators

Biological rhythms observed in nature are quite diverse regarding their spatiotemporal behaviour. Their periods are ranging from milliseconds in the case of the oscillations of the membrane potential in neuronal cells, through minutes and hours in the case of glycolityc oscillations in pancreas, to weeks and months, as it is the case of mammalian ovarian cycles [1, 10]. Also the patterns observed in nature are quite remarkable, from the spatial organisation of cellular components inducing the different cell shapes, influencing the cell cycle and having the crucial role in the signalling pathways. They are the result of complex biochemical and biophysical processes, which are occurring in the biological organisms and their environment. Biological processes involve many elements and mechanisms, and they are an inevitable part of diverse cellular and physiological functions. To describe formally such processes one should start with biochemistry where a biological process is described as one or a set of biochemical reactions. A *biochemical reaction*, in its origin, is a simple chemical reaction which rate may be increased by a substance called enzyme. Enzymes are catalysts in biochemical reactions and according to their structures, represent proteins in the living cell.
Dynamics of biological processes are described as a change of concentrations of chemicals involved in the biochemical reaction with time. Chemicals observed on the cellular level, might be proteins, small molecules, DNA, RNA or other species. This change is characterised by rate laws, based on proportionality in the chemical reactions. It states that the rate of change in the concentration of a chemical component is proportional to the product of concentrations of the chemicals present in the system and the concentration of the

chemical component itself. The biological process is presented as a set of rate equations.

Ordinary Differential Equations

The theory of ordinary differential equations (ODEs) has been successfully applied to model biochemical networks of diverse systems [11], such as the cell-cycle control system, metabolic networks or circadian rhythms, [12, 13, 14]. These models are based on assumptions that the molecular concentrations are continuous and these phenomena under consideration are occurring in the homogeneous well-stirred volume at a time scale slower compared to other cellular processes such as transcription, translation or membrane transport. The ODEs are a good starting point to describe biochemical processes. One biochemical process can be transformed into a set of ordinary differential equations, formally given by

$$\frac{dx_i}{dt} = f_i(x_i, x_j, p_k) \qquad i, j = 1, ..., N, \tag{2.1}$$

where x_i are the concentrations of the chemical component $[X_i]$ involved in one biochemical process, characterised by a set of parameters p_k and by the functions f_i. The solutions of such equations are possible to obtain, knowing the parameters and the initial conditions, by integrating the differential equations using different methods. Usually, even the most simple regulatory networks are described by a set of equations and to predict the change of each component over time, many parameters, such as the rate constants that appear in the rate laws and initial conditions are needed to be known. Many are not measured, and the only way to solve such a complex behaviour of models for molecular regulatory networks is to rely on tools from nonlinear dynamics. A linear stability analysis can be used to determine the dynamics of the system due to different parameter values.

Delay Differential Equations

Dynamics of reactant involved in one biological process sometimes depends on the history of dynamics of another reactant or reactants. To describe such a process, delay differential equations (DDEs) have to be used. DDEs have many applications in the theory of control and self-oscillating systems, regarding biological, chemical and physical questions that deal with the feedback mechanisms. General theory for DDEs (linear) are presented by Hale [15], El'sgol'ts and Norkin [16]. Delay differential equation is similar to an ordinary differential equation, with the difference, that its evolution depends on the past values of the state of variables describing given system. Thus for the exact solution of delay differential equations one should know not only the current state but also the state of certain time previously. In recent decades, the application of this class of differential equations, especially in a modelling of biological systems, has increased, for example in population dynamics and epidemiology. Regarding the type of delay involved in the dynamics of some biological system, one can distinguish delay differential equations with the discrete time delays from DDE with continuous delay. Generally, they can be presented as:

$$\frac{dx(t)}{dt} = F(x(t), x(t-\tau_1), ..., x(t-\tau_n)) \tag{2.2}$$

for $\tau_1 > ... > \tau_n \geq 0$, where $\tau_1, ..., \tau_n$ are delay terms and $x(t)$ is n - dimensional vector of variables.

Ensembles of Coupled Biological Oscillators

A population of oscillators and their collective behaviour are subject of extensive studies in the various fields of science such as physics, chemistry, social sciences and biology leading to their practical applications in engineering and medicine.
Variety of rhythmic phenomena in biology are generated as the collective rhythms emerging from multicellular structures. Examples of such network organisation, are well studied rhythms in the cardiac pacemaker at the sinoatrial node [17], calcium oscillations [18] and circadian rhythms in the suprachiasmatic nucleus [19, 20]. Thus a description of biological rhythmic processes in some cases could not relay only on a single biochemical oscillator. Instead, a complete picture of the dynamics of a certain biological process can be obtained, if the network of interacting oscillators is observed.
The phenomena which are of particularly interest in biology and other systems where dynamics of two or more coupled oscillators are investigated is synchronisation. It can be described generally with tools from nonlinear dynamics regardless of the system type. Synchronisation by definition represents how two or more self-sustained periodic oscillators are adjusting their rhythms due to their weak interaction [21]. Different manifestation of synchronisation can occur, depending on the differences among oscillators and their mutual interactions.
From the biological perspective is it challenging to find the possible mechanisms of intercellular coupling that would lead to a complete synchronisation. For the case of more then two oscillating systems, the spatial order of oscillators that are interacting is important. In this work emphases is on two types of coupling in the net of coupled oscillators, global and diffusive couplings. Spatial arrangement of the oscillators is observed when they are ordered into chains, lattices or even more complicated network geometries and where each element interact only with its neighbours. Due to their mutual coupling, the elements in one neighbourhood are adjusting their frequencies. The common frequency among neighbours can be different and then one can expect some partially synchronous state. This is resulting in the formation of synchronous clusters or oscillating spatial patterns. Reaction diffusion systems are usually used to describe such nonlinear spatial systems in biology.

2.2 Data Analysis

This section reviews the standard tools to quantify the rhythmic characteristic of single biochemical oscillators and the network of oscillators. To define the dynamics of an oscillator, its period, amplitude and phase have to be obtained. Using stability analysis one can analytically obtain the period values due to the variation of bifurcation parameters, by the means of imaginary and real part of the eigenvalue for specific fixed points. However an explicit solution of the eigenvalues for some models of biochemical oscillators is not possible to obtain. Thus, one can evaluate the period from the time series obtained by numerical simulations, using the Discrete Fourier Transform (DFT) and evaluated corresponding

power spectral density.

Measure of Spatiotemporal Order in the Ensemble

Variety of synchronisation patterns can be obtained in the network of oscillators due to different types of coupling and thus there are many numerical techniques in the literature for the estimation and analysis of synchronisation. Here, two numerical methods for quantifying the measure of coherence in the population of oscillators are presented. They will be used later to analyse the data obtained by numerical simulations of model equations. These are the order parameter R for the case of globally coupled oscillators [22] and the spatial cross-correlation measure S for diffusively coupled oscillators [23].

Order Parameter

A quantity, convenient to measure a degree of the synchrony among elements in the network of globally coupled oscillators, is defined as the order parameter R. It represents the ratio of the standard deviation of the time series of the average value $\bar{X}(t)$ to the standard deviation of the local signal $X_{ij}(t)$, calculated for each element and averaged over the number of elements in the net.

$$R = \frac{\langle \bar{X}^2 \rangle_T - \langle \bar{X} \rangle_T^2}{\frac{1}{N^2} \sum_{i,j=1}^{N} (\langle X_{ij}^2 \rangle_T - \langle X_{ij} \rangle_T^2)} \tag{2.3}$$

where $\bar{X} = \frac{1}{N^2} \sum_{i,j=1}^{N} X_{ij}(t)$ is the mean field over the number of elements in the net at time t, $1 < i, j \leq N$ and the $\langle ... \rangle_T$ denotes the average over integration time T. This parameter quantifies the distribution of phases of the oscillators in the net. The values of the order parameter R can take a range between $R = 0$, when oscillators are unsynchronised and $R = 1$, when they are completely synchronised.

Spatial Cross Correlation Measure

An efficient way to detect the nearest neighbour relationships in space and time in the net of oscillating elements, is to apply the spatial cross-correlation measure S defined by Busch and Kaiser, [23]. In Chapter 4 where nearest neighbour coupling is applied to the net of interacting elements, this measure of spatial order will be used for a quantification of coherent spatial patterns induced by variability. Spatial cross-correlation S is a measure of order in the system and is defined as the space and time averaged nearest neighbour distance of all elements in the net normalised by the total spatial amplitude variance:

$$S = \langle \frac{Cov(t)}{\sigma_X^2(t)} \rangle_T \tag{2.4}$$

where $\sigma_X^2(t)$ is the spatial variance of a system variable X at time t defined as:

$$\sigma_X^2(t) = \frac{1}{N^2} \sum_{i,j=1}^{N} (X_{ij}(t) - \bar{X}(t)) \tag{2.5}$$

and $Cov(t)$ representing the spatial autocovariance of nearest neighbours at time t defined as:

$$Cov(t) = \frac{1}{N^2} \sum_{i,j=1}^{N} \frac{1}{|\mathcal{N}_{ij}|} \sum_{b_n \in \mathcal{N}_{ij}} (X_{ij}(t) - \bar{X}(t))(b_n(t) - \bar{X}(t)) \tag{2.6}$$

$\mathcal{N}_{ij}$ is the set of elements of a von Neumann neighbourhood at each lattice site X_{ij} where the neighbourhood element is defined as b_n. A neighbourhood of 4 elements is used because of the computation ease. It was shown that using different local neighbourhoods, the results are not changed significantly. Both measures mentioned above are quantifying synchronisation, with the difference that Cov also takes into account the order in the system or the local synchronisation among elements. Thus, relative measure of the order in the system is finally obtained by averaging a ratio of spatial autocovariance of the nearest neighbour $Cov(t)$ and spatial variance $\sigma_X^2(t)$ over total integration of time T. The indicator for coherent spatiotemporal patterns is the maximum value of the spatial cross correlation $S = 1$, representing the high synchronisation in space and time. In fully synchronised systems when $Cov = \sigma_X^2 = 0$ value for spatial cross correlation S is undefined due to the ratio of two spatial variance measure. When elements are uncorrelated in time and space the value of spatial cross correlation $S = 0$ is estimated, and it can reach the value of $S = -1$ for the case of strong anticorellation. A spatial cross correlation measure is one of the tools used for a quantification of the noise-induced pattern formation [23, 24].

2.3 Noise and Variability

Influence of stochastic forces on the circadian rhythm generator is investigated in this thesis, in the form of additive uncorrelated noise. It is known that noise can have a constructive role in many nonlinear systems. This can be demonstrated by various examples, such as stochastic resonance [25], coherence resonance [26], noise induced phase transitions [27] and spatiotemporal stochastic resonance [23]. However, time independent heterogeneity between elements in the net, or variability, is also capable to induce a transition between two different dynamical regimes, similar as it is the case with noise [28]. Pattern formation in nets of biochemical oscillators can be explained due to the influence of variability among elements in the net [29]. Besides, many other phenomena such as stochastic resonance, coherence of patterns and synchronisation can be also observed due to the presence of time-independent stochastic differences (variability) among elements in the net [30, 31, 32].
The influence of stochastic forces can be presented as the set of stochastic differential equations. For a single process, it can be described by the following equation:

$$\frac{dX(t)}{dt} = f(X(t)) + g(X(t))\eta(t) \tag{2.7}$$

Depending on the function $g(X(t))$, different types of noise exist. If the function is constant, the noise term is additive. For the case when the function $g(X(t))$ is dependent on the variable $X(t)$, the noise is multiplicative. Noise is determined by its probability distribution, moments and correlation function. According to the central limit theorem,

Gaussian probability distribution $P(\eta, \sigma)$ is considered. In the present thesis only zero mean additive Gaussian white noise is studied with noise strength σ. For a net consisting of $N \times N$ coupled elements, where coupling is given by coupling function K_{ij}, the above equation can be extended:

$$\frac{dX_{ij}(t)}{dt} = f(X_{ij}(t), X_{lk}(t)) + g(X_{ij}(t))\eta_{ij}(t) + K_{ij} \tag{2.8}$$

where $1 < i, j \leq N$ are indices for each element in the square net and $l, k \in \{1, ...N\}$. Assuming that the noise term $\eta_{ij}(t)$ is uncorrelated in space, one can define the correlation function as

$$\langle \eta_{ij}(t)\eta_{kl}(t') \rangle = \sigma^2 \delta_{ij,kl}\delta(t - t') \tag{2.9}$$

If one assumes that the stochastic differences between elements in the net are independent on time, variability is introduced in the net. The process can be described as:

$$\frac{dX_{ij}(t)}{dt} = f(X_{ij}(t), X_{lk}(t)) + \mu_{ij} g(X_{ij}(t)) + K_{ij} \tag{2.10}$$

where μ_{ij} denotes the parameter values of the system that are different for each element in the net, and that follow some statistical distribution. Gaussian probability distribution is chosen, where the variance ν^2 defines the variability intensity and the standard deviation ν the variability strength, respectively. Variability also can be defined as additive, if the function $g(X(t))$ is constant or otherwise, multiplicative. The correlation function for the case of variability is defined by

$$\langle (\mu_{ij} - \bar{\mu})(\mu_{kl} - \bar{\mu}) \rangle = \nu^2 \delta_{ij,kl} \tag{2.11}$$

where $\bar{\mu}$ is mean value of parameters μ_{ij}.

2.3.1 Numerical Integration

The nonlinear differential equations which are discussed in this thesis belong to the class of delay stochastic partial differential equations. They can not be solved analytically, instead numerical methods are used to calculate their solutions. Simulations of the model equations for the circadian rhythm generator are performed using an integration algorithm based on a second order Runge-Kutta method [33]. The system describing the net of diffusive elements, when stochastic terms are present, is integrated with the higher accuracy if the larger integration step size is used [27]. Integration of equations is performed using a discrete square lattice of the size $N \times N$ with grid points defined with indices $1 \leq i, j \leq N$. As rotational symmetry is chosen for the net of locally coupled elements, the discretisation is described by the 9-point Laplacian:

$$\begin{aligned} \Delta^2 X_{ij} \quad = \quad & \frac{1}{6\triangle h^2}(X_{i-1,j-1} + X_{i-1,j+1} + X_{i+1,j-1} + X_{i+1,j+1} \\ & +4(X_{i-1,j} + X_{i+1,j} + X_{i,j-1}X_{i,j+1}) - 20X_{ij}) \end{aligned} \tag{2.12}$$

The equations are integrated with spatial length of discretisation $\triangle h = 1.0$, while temporal integration step size was taken to be $\triangle t = 0.001$. To use a fast integration scheme, the

spatial integration is performed by the Forward Time Centred Space algorithm (FTCS) [33], periodic boundary conditions are applied.
Generally, discrete integration algorithm can be derived starting from the reaction diffusion equation extended for the stochastic term $\eta(t)$.

$$\frac{\partial X_{ij}(t)}{\partial t} = f(X_{ij}(t)) + D\nabla^2 X_{ij}(t) + \sum_{kl} \eta_{kl}(t) \tag{2.13}$$

In this work white additive Gaussian noise will be applied, so the following derivation will be limited for this case[2]. After discretisation of space and time, the solution can be represented as the function of solution of previous time step:

$$X_{ij}(t+\Delta t) = X_{ij}(t) + \int_t^{t+\Delta t} f[(X_{ij}(t')) + D\nabla^2 X_{ij}(t')]dt' + \sum_{kl} \int_t^{t+\Delta t} \eta_{kl}(t')dt' \tag{2.14}$$

If the reaction term $f(X_{ij})$ is expanded by Talyor series, with respect to the first order of Δt, it reduces integrals to:

$$X_{ij}(t+\Delta t) = X_{ij}(t) + f((X_{ij}(t))\Delta t + D\nabla^2 X_{ij}\Delta t + \sum_{kl} \tilde{\eta}_{kl}(t) + O(\sqrt{\Delta t^3}) \tag{2.15}$$

where $\tilde{\eta}(t)$ is the integral of the Wiener process [34]:

$$\tilde{\eta}(t) = \int_t^{t+\Delta t} \eta_{kl}(t')dt' \tag{2.16}$$

Simulation of $\tilde{\eta}$ was performed using the Gaussian number of unit variance ζ_{ij}

$$\tilde{\eta}_{ij} = \sigma\sqrt{\frac{\Delta t}{\Delta h^2}}\zeta_{ij} \tag{2.17}$$

$$\langle \tilde{\eta}_{ij}(t)\tilde{\eta}_{i'j'}(t')\rangle = \delta_{ii'jj'}\delta(t-t') \tag{2.18}$$

representing the uncorrelated noise in time and space. The above equations represent the first order Euler integration. It is improved by the Heun method, or the Runge-Kutta second order integration algorithm, that can be presented with the following set of equations:

$$X_{ij}(t+\Delta t) = X_{ij}(t) + D\nabla^2 X_{ij}\Delta t + \frac{1}{2}[f((X_{ij}(t)) + f((\tilde{X_{ij}}(t))]\Delta t + \sum_{kl} \eta_{kl}(t) \tag{2.19}$$

$$\tilde{X_{ij}} = X_{ij}(t) + f(X_{ij}(t))\Delta t + D\nabla^2 X_{ij}\Delta t + \eta_{kl}(t) \tag{2.20}$$

[2]Other cases of multiplicative and coloured noise on reaction-diffusion systems were presented in details in the book of Garcia-Ojalvo, 1999 [27] and work by H. Busch [24].

2.4 Modelling Circadian Clocks

A biological rhythm, that has a great impact in a wide range of living organisms and is a subject of intensive studies from molecular biology, plant ecology to mathematics and physics is circadian rhythm. Circadian rhythms control many aspects of metabolism, physiology and behaviour in most types of organisms from bacteria, fungi, plants to mammals [35, 36, 37]. The term circadian comes from the Latin word *circa* - about, *dian* - day and it relates to the period close to 24 h, representing the biological periodic activity that coincides with external day-night change, caused by Earth rotation. Although the circadian rhythms from various organisms are quite different in their physiological manifestations, they share some common characteristics, which are usually used for their identification. A circadian rhythm is an intrinsic process, it is endogenous to the organism, meaning that it persists even in the absence of external cues such as light and dark with periodic activity ranging from $20 - 28$ h, depending on the biological organism.
It is remarkably entrainable to the environmental stimulus such as light and temperature, although nutrient entrainment is also observed in some organisms. The influence of external cues manifests in the resetting of the clock each day with a precise period of 24 hours. The period of circadian rhythms is temperature compensated, meaning that its length remains unchanged at different but constant temperatures, taking into consideration the physiological ranges which could have different values for the different species. As most of the enzyme catalyzed processes are strongly temperature dependant, this feature of circadian clocks is complicated to explain from the point of view of biochemical processes and is subject of some studies on circadian rhythm generation [38, 39].
Generally circadian system can be represented as a pathway consisting of an input, which senses the signals from the external environment, such as light intensity and temperature, in the chronobiology literature often called the *Zeitgebers* [40], then a central pacemaker which consists of gene controlled mechanism that generates the rhythm and on the end, the output, that proceeds and controls generated rhythms as the observable or behavioural rhythms.

2.4.1 Core Molecular Mechanisms

Increase in the research in the field of molecular genetics during several decades, has given a possibility to study the origin of many biological phenomena on the molecular level, including circadian rhythms, which were by then studied only based on perturbations of behavioural rhythms [41]. The first such as report of the molecular components came from three circadian mutants in a fruit fly *Drosophila melangoster*, discovered in 1971 [42] that caused significant changes in observable daily rhythms of Drosophila.
From these days until today, with intensive studies on molecular biology of circadian rhythm, some of the important elements of the central pacemaker, as well as a number of the molecular control mechanisms, responsible for thickening of the circadian clock are identified. The research is conducted on various organisms, and it was shown that circadian rhythms have similar features among species on the molecular level, besides the above mentioned three general characteristics. Insight into molecular function of biological clocks on a genetic level brought many theories about clock components and their regulation

[43, 44, 45]. New theories are still emerging and they are subject of intensive discussions and reviews among chronobiologists. So far it has been accepted that the basics of the core mechanisms responsible for the generation of circadian rhythm consists of transcription-translation negative feedback loops, where transcription factors drive the expression of their negative regulators. The schematic general representation of such genetic regulation of the clock is presented in Fig. 2.1, where one can see that the circadian clock is presented by the transcription of clock genes, which is regulated by negative feedback loop of its product.

One of the characteristics of the negative feedback loop is the presence of delay between

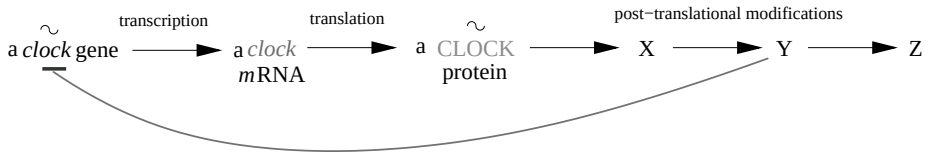

Figure 2.1: *Basic model of clock gene regulation: transcription of clock gene induces the translation of mRNA to protein, which then can be transferred into different states, X, Y or Z. They are capable of inhibit their own production by negative self regulation, ubiquitous in nature [46].*

stimuli and response. As the transcription-translation feedback cycles generally operate on time scale, which is much less than 24 hours or one circadian period, it is assumed that post-transcriptional regulations are crucial for these delays. Also, recent findings on new clock components indicate the importance of post-regulators, [47, 48]. It is shown that despite disruption of the certain clock genes, the oscillation can be saved [49]. However, if some of the regulators such as the protein kinase or phosphatase are inhibited, this can lead to the loss of the rhythmicity [50]. It opens the question, whether negative feedback alone is enough for circadian regulation. Reliability of the current model for circadian clock is also questioned by the experiments preformed on the cyanobacteria *S. elongatus* and is in detail described by the work of Tomita [51]. Although the authors have inhibited genetic transcription and translation mechanisms, they were still able to observe the circadian oscillation of the clock protein. In their later work [52] they even succeed to reconstitute the patterns of temperature compensated circadian oscillation. Thus they indicated the importance of regulators for clock machinery, which are able to form an oscillator independently from transcription of clock genes. It is clear that these results are showing the limitations of a simple feedback model, even it is the common regulatory mechanism in nature and that the current biological concept for circadian rhythms should be modified.

2.4.2 Perturbation of Circadian Systems

One of the important characteristics of circadian systems is the type of entrainment [53, 54]. Circadian clock as part of living systems can not be observed as an isolated rhythmic process, but one should consider its constant dynamic interaction with external environmental signals such as light and temperature, already defined as Zeitgebers. Due to the regular alternation between night and day, biological clocks have thus evolved from simple time

keeping mechanism to complex regulator systems. The nature of biological clocks is the best studied if it is exposed to an external perturbation. During early days in the chronobiology research [55], it was noticed that endogenous rhythm can be reset due to the application of environmental stimuli. With further studies, it was revealed that the strength, duration and point of application of stimuli are crucial and that the general response of a system due to the influence of a *Zeitgeber* can be studied by means of phase response curves (PRCs). Phase response curves are defined as the transient change in the period of oscillators caused by the perturbation on a limit cycle (a closed trajectory in phase space), as the function of the phase at which the perturbation is applied [54, 56]. It can result in an increment in the phase called a phase advance or a decrement in phase called a phase delay. In some cases, there are phase points of the PRCs where the application of stimuli induces neither delays nor advances of the phase and they are usually referred as the "dead zones" of the PRCs.
An estimation of PRCs is a very common procedure in circadian rhythm experiments and there are a number of different experimental protocols described by Aschoff [55]. The stimuli that are included in these experiments are pulses of light and temperature, but also the influence of drugs and chemicals are investigated [57]. The duration of pulses varies from 1 hour to several hours, and they are usually applied while the system is in a constant condition. Fig.2.2 illustrates the perturbation of an external signal at one arbitrary point of the oscillator phase. Generally the unperturbed or free-running period of the oscilla-

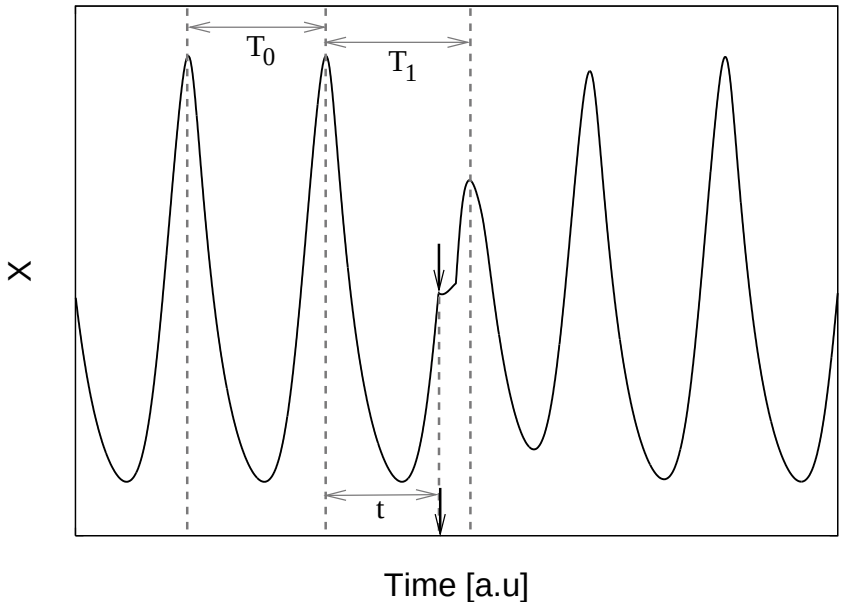

Figure 2.2: *Perturbation on a limit cycle with the endogenous period T_0 at one arbitrary phase of circadian time, which is defined as the distance t due to the reference, causes the phase shift $T_0 - T_1$. Arrows indicate the moment of time when the perturbation is applied.*

tor can be defined as T_0 and the shift caused by the perturbation, due to the reference point, defined with T_1, at the phase point which is defined $\psi = t/T_0$, where t is the time

interval between the moment of perturbation and the reference point (first maximum of unperturbed oscillation). In the terms of phases $0 < \psi < 1$ or $0 < \psi < 2\pi$ with respect to biological or mathematical formalism, the PRCs can be represented as the following function

$$F(\psi) = \frac{T_0 - T_1}{T_0} \tag{2.21}$$

In this work the PRCs will be presented as the function of unnormalised phase shifts or $(T_0 - T_1)$ due to the different phase of the perturbation defined in the units of circadian time (CT) of endogenous rhythms. This terminology is both accepted for the experimental and theoretical chronobiology. The definition of a circadian time is standardised in the experimental approach and is set as the phase in the free running rhythm when light stimuli would be applied if the system is in a natural environmental conditions. However in the field of modelling, where behavioural rhythms are rarely evaluated and the attention is on the levels of regulatory proteins and $mRNA$s, it is usually used to define the start of stimuli application at the point that will induce a very small phase shift and it is referred to the maximum of $mRNA$ concentration.
Amplitude and the type of the PRCs depends on the strength and duration of the perturbation. Two types of PRCs can be distinguished, type 0 and type 1. Type 1 represented in Fig.2.3(a) displays relatively small phase shifts, where a transition between delays and advances is continuous. Type 0, represented in Fig. 2.3(b) has significant phase shifts and usually presents a discontinuity. The terms "0" and "1" refer to the average slope of a curve that represents the function of new phase, or induced phase due to the perturbation, as the function of old phase.

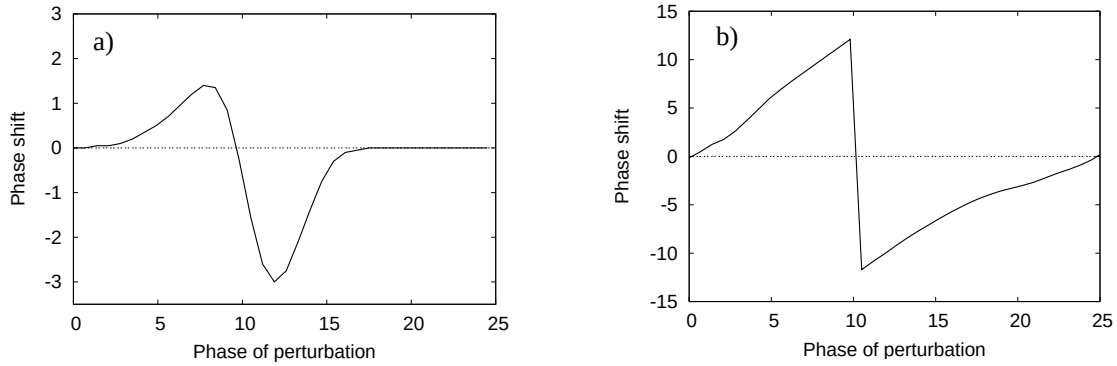

Figure 2.3: *Phase response curves: a) Phase response curve of type 1 characterised by a small amplitude of phase shifts; b) Strong perturbation resulting in the type 0 is often represented as the abrupt change in the phase shift.*

2.4.3 Models for Circadian Oscillators

Along with the development of molecular biology techniques to study the origins of a molecular and cellular mechanisms of circadian rhythms, in recent years computational biology with its theoretical models has become a significant part in understanding and

analysing complex dynamics of circadian phenomena. Two types of models can be found in the studies of circadian rhythms, general models that attempt to fit already known oscillatory model to the data and molecular models, based on biochemically reactions and a specific molecular regulation of clock genes and proteins. General models are usually approved because of their simplicity and universality, while molecular models are more valuable, due to the analogy with a specific biological system.

General Models

One of the important general models, first used by Wever [58], later modified by Kronauer is based on the Van der Pol equation and has been used for long time to model the human circadian system, with the emphases on the modelling of response of human circadian oscillations to light [59]. It is shown that this model can be used to model the effects of light on the human circadian pacemaker [59] as well, as the phase and amplitude resetting by light entrainment [60]. The Kronauer model is also applied as a basis to model the SCN as a population of self-sustained oscillators with intrinsic periods and local coupling between the oscillators. First studied for the synchronisation to 12 h light-12 h dark cycle and phase response curves [61], this model is used later by the same authors to study the stability and robustness of the overt rhythms and the phenomena of splitting, [62]. It is shown that certain aspects of circadian systems can be better explained using this extended multi-oscillator model.
A general model that is frequently used to study the synchronisation phenomena in the population of oscillators, the Kuramoto phase model, is also used to model the population of cells of cyanobacteria and to study the role of intercellular coupling for the stability of individual oscillator due to external and internal fluctuations [63]. Also an extended Kuramoto model, with drifting frequencies and a stochastic term [64] is used to study the synchronisation phenomena inspired by the data from the experimental work by Welsh and co-workers, [65].

Molecular Models

The first molecular model for circadian rhythms is based on the prediction of oscillations due to negative feedback on gene expression, proposed by Goodwin in 1965 [66]. Thirty years later Goldbeter presented the first biochemical model of the circadian system [67]. It is developed for *D. melangoster*, as it is the first organism which oscillatory molecular mechanism is studied. This early model consists of five kinetic equations, describing the negative control of the PER protein on *per* mRNA expression, including a two level phosphorylation step. Using bifurcation analysis Goldbeter showed that the oscillation period can be changed due to the rate of PER degradation. This model is well accepted because different periods are also observed in experiments with mutants representing the change in protein degradation. However, light input is not included in this model, and the model is later extended with respect to a new discovered gene *tim* and its products, where light influences the degradation of TIM protein [68]. The results of the new model included the simulation of phase response curves which exhibit good consistency with experimental data. Several studies based on this model, are also published, [69, 70] where the models under certain conditions are able to reproduce chaos and birhythmicity, interesting from

the aspect of nonlinear dynamics, but still unclear from a biological point of view.
The molecular models were also used to study the possible role of positive feedback. Such model was developed by Tyson and Hong, [71]. They proposed additional regulation of clock gene by an autocatalytic or positive feedback of homodimer PER-PER on the production of PER protein. The outcome of this model is the presence of multiple steady states.
Another class of molecular models are the models with a time delay, where details of molecular processes are in some degree incorporated in the variable which is time delayed due to the other variables in the model. For the modelling of circadian clocks, both types of time delays are used, distributed delays [72, 73] and discrete delay [74, 75], where the delay term represents the total duration of chain reactions that occur during one circadian cycle. The details of the Scheper model [74] will be presented in Chapter 4, as this model is the basis for this thesis.
Temperature effects on the circadian rhythm generator are also presented in the form of the model developed by Ruoeff and co-workers [39, 76], which is also based on the properties of Goodwin oscillator and describes the temperature compensation and phase response curves for temperature steps and temperature pulse.
Besides the single molecular cell circadian model, there are studies that incorporate intracellular and extracellular dynamics into molecular models, suggesting that the synchronisation phenomena in the cell of SCN are crucial for the rhythmicity of the single oscillator, indicating the importance of the net dynamics due to the single oscillatory process. Ueda and co-workers [77] developed a model that describes synchronisation of circadian oscillators in the realistic genetic network for *D. melangoster*. They showed the importance of the synchronisation as the important mechanism of noise resistance in the population of oscillators. The influence of synchronising processes are also demonstrated by Bernard and co-workers [78], using the singular molecular model of Becker and co-workers [79] as the basis for their network model. They show that the number of oscillators and types of coupling in the net are of the great importance for the synchronisation and rhythmic properties of the net consisting of individual oscillators whose amplitude gradually decreases (damped oscillators). A similar multioscillator model is proposed by Gonze [80], where he observes the net composed of coupled modified Goodwin oscillators. Like the model of Bernard and co-workers [78], it also suggests the interplay between oscillatory mechanism in single oscillator and coupling mechanism observed in the net. It shows that fast synchronisation can be achieved if the oscillators are driven by global coupling of the neurotransmitter concentrations, which would be damped in the case of constant forcing. Though it can demonstrate perfect entrainment with the dark-light cycles, synchronisation and the interaction between two different populations of circadian oscillators, the model lacks the period compensation. Significant change in period due to the high synchrony or increase in the coupling strength among oscillators can be observed.
However, there are also models of the circadian rhythm generator that are not based on the transcription-translational negative feedback, such as the model for CAM succulent plant *K. daigremontiana* based on the metabolic regulation and the compartmentalisation of malic acid [81].

Chapter 3

System of Coupled Genetic and Metabolic Oscillators

This chapter presents a modification of an existing molecular model for the circadian rhythm generator, obtained by the coupling to another limit cycle oscillator. The interactions between two different biochemical oscillators e.g. genetic circadian oscillator and metabolic oscillator are presented and their mutual coupling is discussed. The two clock model is also investigated from the aspect of environmental influences, introducing a model that will incorporate the influence of light and temperature signals.

3.1 Model System

The model of coupled oscillators is based on an experimental and theoretical hypothesis that more than one endogenous clock responsible for the generation of circadian rhythm exists [82], which is still an open question in chronobiology [83]. Experimental results suggest that several different cellular functions are controlled by separate circadian oscillators. The complexity of such organisation of the circadian program can be interpreted as the ability of organisms to adapt to different environmental signals, such as light and temperature. Besides, the concept of coupling circadian rhythms with other biological rhythms, such as a cell cycle [84, 85, 86] and metabolism [87, 88, 89] is also present in theory and experiment. Thus, a simple model is developed, which will incorporate the mutual influence of two autonomous biological rhythms, the circadian rhythms generator and a metabolic oscillatory process.
A two variable model for the intracellular circadian rhythm generator, discussed in detail in the work of Scheper and co-workers [74], has been shown to be relevant for representing the basic features of a circadian molecular clock. Scheper's model belongs to the class of molecular models for the circadian rhythm generator, based on experimentally established and many times proved, translation-transcription feedback loop [43, 90]. The mechanism of a biological function underlying this model of the circadian clock, consists of the protein gene regulation by a negative feedback loop with a time delay in protein synthesis and strong nonlinearities in the production of molecules. The model includes a biochemical

cascade of processes where the protein as the product of clock gene, constrains activity of the transcription factor and thus inhibits its own synthesis.
The circadian rhythms generator is mutually coupled to another autonomous biological clock, a biochemical oscillator. The Schnackenberg [91] model is chosen, which is the simplest model for a biochemical process, involving minimal numbers of reactants and which is capable of exhibiting limit cycle behaviour. According to its structure, it belongs to the class of Turing's reaction diffusion model systems [92]. This two reactant model can be used theoretically as an example of a metabolic oscillator. The coupling of two biologi-

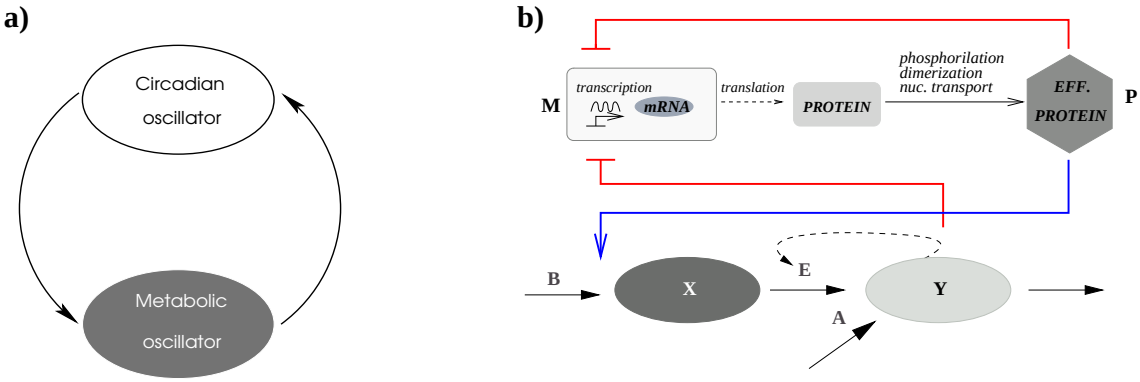

Figure 3.1: *General model for the circadian rhythm generator. a) Structure of internal, two-directional coupling between two different oscillators, genetic oscillator and metabolic oscillator. b) Schematic representation of the elements of the genetic and the metabolic oscillators and their internal coupling. Red lines represent the inhibition of the effective protein P and the substance y on the transcription of clock gene. M stands for mRNA. Blue line represents the activation of substance x. Constant input of substance x and y are defined as B and A, respectively. E represents an arbitrary enzyme that enhances the production of substance y.*

cal clocks is performed in such a way that the production of one of the reactants of the metabolic oscillator x, is activated by the effective protein of the molecular circadian clock. The coupling from the metabolic oscillator to the genetic oscillator is an additional negative feedback loop, performed in the way that the other reactant of metabolic oscillator y increases the inhibition of mRNA transcription, [Fig.3.1]. Thus a two directional coupling results in the higher regulation, where the production of substance x is not regulated only by a constant source, represented as B [Fig. 3.1(b)], but also by the activity of a clock protein. Furthermore, the generation of circadian rhythms is determined not only directly, through protein auto-regulation, but also indirectly, through some other oscillatory biochemical processes, influenced by the clock protein itself.

3.2 Scheper Model

The model for transcriptional translation feedback loop, in recent literature referred to as the translation-transcription oscillator (TTO) is presented as a set of two ordinary and delay differential equations with discrete time delay [74], where the variables $M(t)$ and $P(t)$ represent the relative abundances of mRNA and clock protein, respectively.

$$\frac{dM(t)}{dt} = \frac{p_m}{(1+P(t)^n)} - d_m M(t) \tag{3.1}$$

$$\frac{dP(t)}{dt} = p_p M^s(t-\tau) - d_p P(t) \tag{3.2}$$

The equations presented here are governed by Michaelis-Menten kinetics. The protein defined in Eq.(3.2) is represented as the effective protein [Fig.3.1(b)], in the sense that this protein has passed several posttranslational processes, such as phosphorylation, dimerisation and nuclear transport and it is capable to inhibit the transcription of clock gene. As those processes are time consuming, the time delay term τ is added. The rates of production of mRNA and protein are defined as parameters p_m and p_p, respectively. Parameter n is the Hill coefficient, while nonlinearity in the production of protein is represented through parameter s. The degradation rate constants for mRNA and protein are d_m and d_p, respectively.

3.2.1 Stability Analysis of the Scheper Model

Stability analysis of the system is already numerically obtained and discussed in detail in the work of Scheper and co-workers [74]. In the following, partially analytically obtained results are presented in order to get the conditions and relations for a Hopf bifurcation. Using a linear stability analysis, the following equation results

$$(\frac{p_p}{d_p})^n d_m M_0^{sn+1} + d_m M_0 - p_m = 0 \tag{3.3}$$

Because of the complexity of such equations, solutions can be only obtained numerically. Linearisation around the steady states leads to

$$\frac{dm(t)}{dt} = -d_m m(t) - hp(t) \tag{3.4}$$

$$\frac{dp(t)}{dt} = cm(t-\tau) - d_p p(t) \tag{3.5}$$

where new constants are defined as $h = p_m n P_0^{n-1}/(1+P_0^n)^2$ and $c = p_p s M_0^{s-1}$.
The solutions for the delay differential equations are taken to be in the form $m(t) = \hat{m}e^{\lambda t}$ and $p(t) = \hat{p}e^{\lambda t}$, substituted into the Eqs.(3.4-3.5), the following characteristic equation is obtained:

$$\lambda^2 + (d_p + d_m)\lambda + d_p - d_m + hce^{\lambda\tau} = 0 \tag{3.6}$$

Assuming the solution for the characteristic equation in the following form $\lambda = \mu + i\omega$ and taking into consideration the real and imaginary part of the equation, two equations

result. They are, after substitution the criteria for the Hopf bifurcation, with $\mu = 0$ and $\omega \neq 0$, reduced to the following form:

$$cos(\omega\tau) = \frac{\omega^2 - \rho}{hc} \tag{3.7}$$

$$sin(\omega\tau) = \frac{\kappa\omega}{hc} \tag{3.8}$$

Hopf bifurcation for the Scheper genetic oscillator occurs for the value of the production

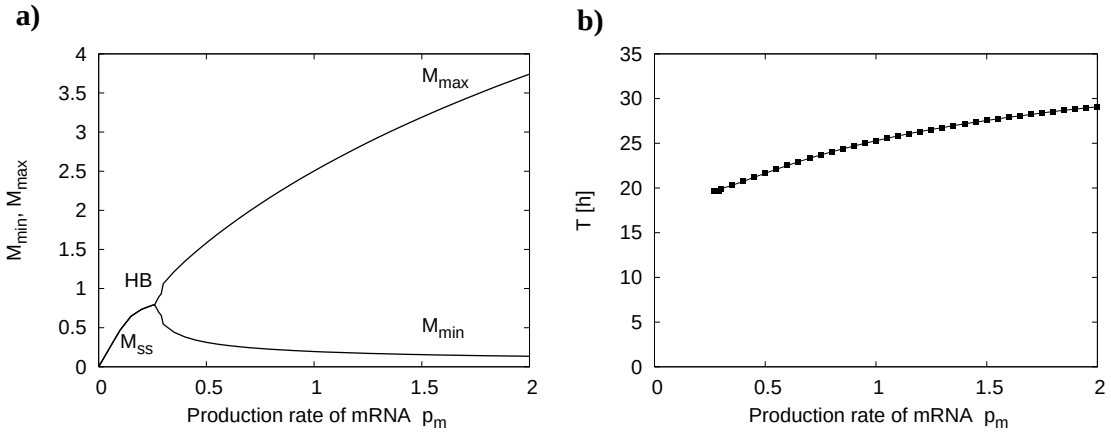

Figure 3.2: *Bifurcation diagram of the Scheper model. a) Hopf bifurcation occurs at the parameter values, p_m=0.26, where the further increase in the producation rate induces limit cycle oscillation; M_{max} maximal abundances of mRNA; M_{min}, minimal abundances of mRNA; M_{ss}, stable steady state and HB, Hopf bifurcation. b) Period of the genetic oscillator due to the variation of parameter p_m. Other model parameters are constant* $(d_m, n, p_p, s, \tau, d_p) = [0.21, 2, 0.5, 4, 4h, 0.27]$

rate of mRNA, $p_m = 0.26$, while other parameters of genetic oscillator are set to constant values. The bifurcation diagram and the period of the Hopf bifurcation point is given in Figs.3.2(a,b). Period of genetic oscillator increases from $T = 19.5$ h to $T = 29$ h as the production rate of mRNA goes from $p_m = 0.26$ to $p_m = 2$, respectively. This range of periods fits with the endogenous region of circadian clocks. Thus, the variation of parameter p_m will be used for representing a variability of circadian clocks.
The delay time τ may be taken as a bifurcation parameter, in order to stay in the endogenous region of circadian clock periods, the value of the delay term is set to $\tau = 4$ h, as it is suggested in the original model [74].

3.3 Schnakenberg Model

The Schnakenberg model is a model for a biochemical oscillator derived for an autocatalytic oscillating chemical reaction. Two ordinary differential equations, with variables $X(t)$ and $Y(t)$, are representing the relative concentrations of reactants involved in the chemical

reaction. If one considers diffusion processes, the dynamics of a system can be presented as the following set of equations:

$$\frac{\partial X(t)}{\partial t} = b - Y(t)^2 X(t) + D_x \nabla^2 X(t) \tag{3.9}$$

$$\frac{\partial Y(t)}{\partial t} = a - Y(t) + Y(t)^2 X(t) + D_y \nabla^2 Y(t) \tag{3.10}$$

For all chemical reactions constants b and a are positive $(a, b > 0)$.

3.3.1 Stability Analysis of the Schnakenberg Model

The steady state solutions (X_0, Y_0) are

$$X_0 = \frac{b}{(a+b)^2}, \qquad Y_0 = a + b \tag{3.11}$$

The result of a linear stability analysis gives the corresponding characteristic equation:

$$\lambda^2 + \lambda(k_\omega^2(D_x + D_y) + \alpha + \gamma) + k_\omega^4 D_x D_y + k_\omega^2(D_x\gamma + D_y\alpha) + \alpha = 0 \tag{3.12}$$

where parameters are $\alpha = (a+b)^2$, $\beta = 2b/(a+b)$ and $\gamma = (a-b)/(a+b)$. When diffusion of reactants is not present in the system, $D_x = D_y = 0$, one can derive the condition for the Hopf bifurcation. Then the parameters satisfy the following relations:

$$\alpha + \gamma = 0, \qquad \alpha\gamma + \alpha\beta > 0 \tag{3.13}$$

After substitution of the parameters a and b, finally, the bifurcation line is given by the equation:

$$b - a = (a+b)^3 \tag{3.14}$$

The corresponding parameter region where limit cycle solutions exist is given under the bifurcation line [Fig. 3.3]. In the case when diffusion is present in the system, one has to find which real part of the eigenvalue λ, depending on the wave number k_ω, is positive, $\Re(\lambda(k_\omega)) > 0$. For different values of diffusion constants, the dispersion relations are presented in Figs.3.4(a-c). One can see that spatial instabilities exist if diffusion of the variable X is present, while diffusion of the variable Y is set to zero. Other cases represent the spatial stability with respect to the diffusion coefficient, and thus can be further implemented in the model. For a net of elements, a case when diffusion of the reactant y is present and diffusion of the reactant x is not, will be considered.

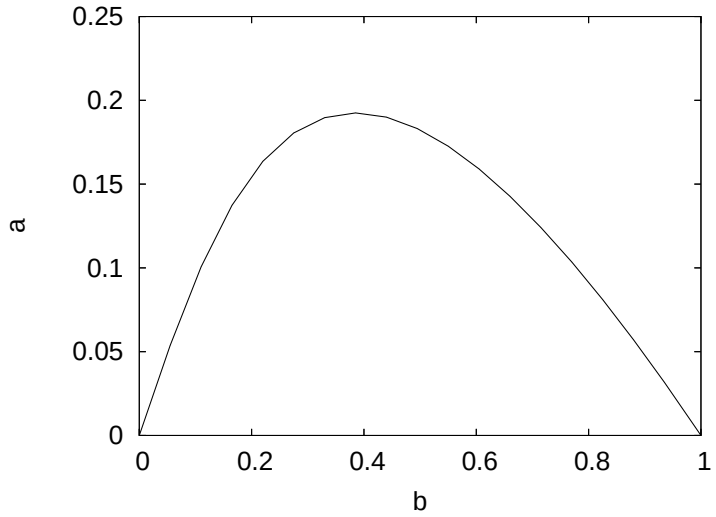

Figure 3.3: *Bifurcation diagram for the Schnakenberg model. A parameter region of the limit cycle belongs to the values of parameter, a and b under the bifurcation line. The other part of the parameter region, represents the region of fixed point.*

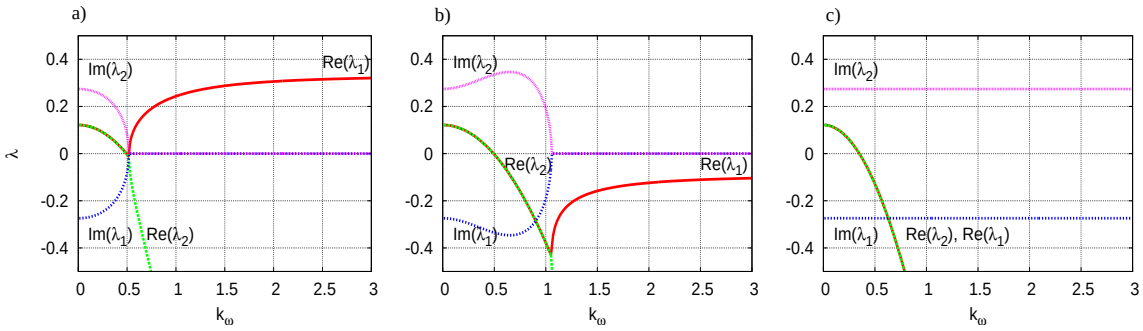

Figure 3.4: *Eigenvalues of the linearised Schnakenberg model as a function of the eigenvector κ_ω for different values of diffusion parameters: a) $D_x = 1$ and $D_y = 0$, b) $D_x = 0$ and $D_y = 1$, c) $D_x = 1$ and $D_y = 1$.*

3.4 Coupled system

The coupled system combines the Scheper and the Schnakenberg model and is presented as a set of delay and ordinary differential equations:

$$\frac{dM(t)}{dt} = \frac{1}{(1+(Y(t)/k_m)^l)}\frac{p_m}{(1+P(t)^n)} - d_m M(t) \tag{3.15}$$

$$\frac{dP(t)}{dt} = p_p M^s(t-\tau) - d_p P(t) \tag{3.16}$$

$$\frac{dX(t)}{dt} = b - Y(t)^2 X(t) + \frac{kP(t)X(t)}{f+X(t)} \tag{3.17}$$

$$\frac{dY(t)}{dt} = a - Y(t) + Y(t)^2 X(t) \tag{3.18}$$

The coupling between the metabolic and the genetic oscillators is obtained by inhibition of mRNA by the reactant Y, representing the coupling from the metabolic oscillator to the genetic oscillator. Coupling from the genetic to the metabolic oscillator is presented as the additional source of production of reactant X, caused by the activation of protein P of genetic oscillator. The coupling parameter that is referred to a mutual influence between two oscillators is the inhibition factor k_m or Michaelis parameter at which reactant Y inhibits the production of mRNA. Inhibition is also characterised by the Hill coefficient l. The activation of reactant X by protein P is characterised by a rate of the protein production k and the Michaels-Menten coefficient f, at which this activation occurs. Parameter values used for the genetic oscillator are similar to the parameters defined in the work of Scheper. The parameters that are constant throughout this thesis are given in Tab. 3.1.

parameters	k_m	d_m	l	n	p_p	s	τ	a
fixed values	3.5	0.21	2	2	0.5	4	4 h	0.1

Table 3.1: *Parameter values for the two component oscillator model of coupled genetic and metabolic oscillators. The other parameters are subject to variation.*

3.4.1 Stability Analysis of the Coupled System

The steady state solution is obtained from the set of Eqs.(3.15 - 3.18). The steady state solutions M_0 from Eq. (3.16) and X_0 from Eq. 3.18 are $M_0 = (\frac{d_p}{p_p}P_0)^{1/s}$ and $X_0 = (Y_0 - a)/{Y_0}^2$. P_0 and Y_0 can be calculated from

$$(b + a - Y_0)(f{Y_0}^2 + Y_0 - a) + kP_0(Y_0 - a) = 0 \tag{3.19}$$

$$({k_m}^l + {Y_0}^l)(1 + {P_0}^n){P_0}^{1/s} - r = 0 \tag{3.20}$$

where $r = \frac{k_m^l p_m}{d_m}(\frac{p_p}{d_p})^{1/s}$. The Eqs.(3.19-3.20) are analytically nontrivial to solve and thus they are solved numerically. Next step involved is the linearisation around those steady states. It gives a new system:

$$\begin{aligned} \dot{m} &= -d_m m - Np - Ly && (3.21)\\ \dot{p} &= cm(t-\tau) - d_p p && (3.22)\\ \dot{x} &= up + qx - \beta y && (3.23)\\ \dot{y} &= \alpha x - \gamma y && (3.24) \end{aligned}$$

with new constants, defined as

$$\begin{aligned} N = \;& h/(1+(Y_0/k_m)^l); \qquad & L = p_m k_m^l l Y_0^{l-1}/(k_m^l + Y_0^l)^2(1+P_0^n);\\ u = \;& kX_0/(f+X_0); \qquad & q = kP_0 f/(f+X_0)^2 - \alpha; \end{aligned}$$

where h and c are already introduced constants for the model of the genetic oscillator and α, β and γ are constants for the metabolic oscillator. Assuming solutions for the Eqs.(3.21-3.24) of the form $m(t) = \hat{m}e^{\lambda t}, p(t) = \hat{p}e^{\lambda t}, x(t) = \hat{x}e^{\lambda t}$ and $y(t) = \hat{y}e^{\lambda t}$ the characteristic equation reads:

$$\begin{aligned} \lambda^4 + \lambda^3((d_m+d_p)-\epsilon) + \lambda^2(\rho - (d_m+d_p)\epsilon + \theta + Nce^{-\lambda\tau}) +\\ +\lambda((d_m+d_p)\theta - d_m d_p \epsilon - \alpha\beta - \epsilon Nce^{-\lambda\tau}) + c[N\theta - \alpha(N\beta + Lu)]e^{-\lambda\tau} +\\ +d_m d_p \theta - \alpha\beta d_m = 0 \end{aligned} \qquad (3.25)$$

where $\epsilon = q - \gamma$ and $\theta = -q\gamma$. The characteristic equation, Eq.(3.25) is highly complex and thus it is impossible to solve it analytically.

A linear stability analysis is performed for the system of coupled genetic and metabolic oscillators for the given set of parameters defined in the Tab. 3.1 with $d_p = 0.27$ and for constant values of coupling parameter $k = 1$ and $f = 1$. A linear stability analysis is numerically performed in dependancy on the production rate of protein p_m and the parameter b. In Fig. 3.5(a) two dynamical regimes can be distinguished, stable focus and limit cycle. For the very small values of parameters p_m and b, ($p_m \leq 0.1, b \leq 0.1$), the system is again stable focus. The period of the coupled system for the same range of parameters, p_m and b is presented in Fig. 3.5(b). The estimated values for the new system of two coupled oscillators are around the endogenous region of circadian clock periods, when production rates of mRNA have values, which are $p_m \geq 0.26$. The period is robust with respect to the variation of parameter p_m and b in this parameter region. Values of the period for coupled system in other parameter regions ($p_m \leq 0.26$) are small. It represents a case of coupling of a limit cycle (metabolic oscillator) and a fixed point (genetic oscillator).

3.5 Different Structure of Coupling

One can distinguish four possible scenarios of coupling of the two autonomous oscillators as each of them could be in different dynamical states. Of particular interest is the coupling between two limit cycles. The bifurcation parameters in the model are p_m and b. Regarding

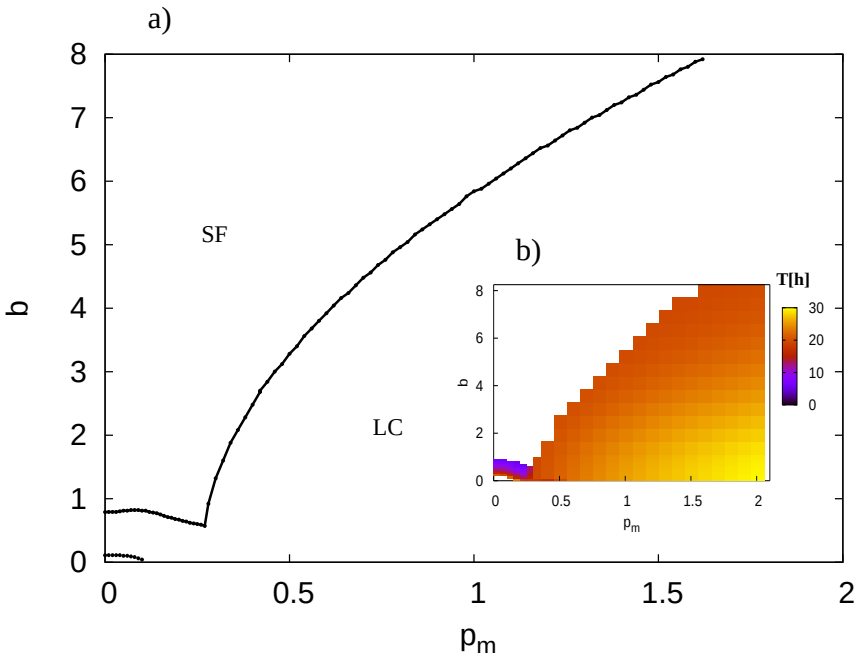

Figure 3.5: *Bifurcation diagram for the coupled system. (a) Linear stability analysis of the coupled system with $k = 1$, $f = 1$ in dependancy on the production rate of mRNA, p_m and parameter b; Parameter region for small values of bifurcation parameters ($b \leq 0.1$, $p_m \leq 0.1$) represents the stable focus; (b) Estimated period $T[h]$ for the system of coupled genetic and metabolic oscillators as a function of parameters, p_m and b.*

different values for bifurcations parameters, the four possible cases are given in Tab. 3.2. Bifurcation parameters are chosen in the way that values for the periods of genetic and metabolic oscillators are different, but that they are still in the physiological endogenous region, around $T = 24$ h. For the period of the genetic oscillator, the chosen value is $T_g = 23.7$ h and for the metabolic oscillator the value is $T_m = 24.7$ h. The first case of coupling that is investigated, is the coupling of two limit cycles, where parameters are set according to the values from Tab. 3.2. Dynamical properties of such a coupled system are investigated by the variation of parameter k which reflects the rate of activation of reactant X by the protein P. Numerical simulations are performed for three different values of Michaelis-Menten coefficients. Numerical integrations of Eqs.(3.15-3.18) give different oscillatory solutions regarding variations of coupling parameters, k and f. Oscillations are highly complex as it is presented in Fig.3.6, for small values of coupling parameter $k \leq 0.1$. The coupling between two oscillators is not strong enough and synchronisation can not be established. They also depend on the values of the Michaelis-Menten constant, f. As the value of the Michaelis-Menten constant is increased, a greater value of coupling parameter k is needed for a complete synchronisation between the genetic and the metabolic oscillators. Synchronisation between two nonidentical limit cycles is represented in Figs. 3.7(a-c) where ratios of periods of two biochemical oscillators are plotted due to the change in the coupling parameter k for the different values of Michaelis-Menten coefficients. Synchronisation between genetic and metabolic oscillators occurs for the values of the coupling parameter

$LC_g \otimes LC_m$	$LC_g \otimes FP_m$	$FP_g \otimes LC_m$	$FP_g \otimes FP_m$
$p_m = 0.75\ h^{-1}$	$p_m = 0.75\ h^{-1}$	$p_m = 0.2\ h^{-1}$	p_m =0.2 h^{-1}
$b = 0.2$	$b = 0.1$	b =0.2	b =0.1

Table 3.2: *Four different coupling situations due to different values of bifurcation parameters p_m and b for a genetic oscillator indicated with subscripts g and a metabolic oscillator indicated with subscripts m. Dynamical states of oscillators: limit cycle LC and fixed point FP, $d_p = 0.27$.*

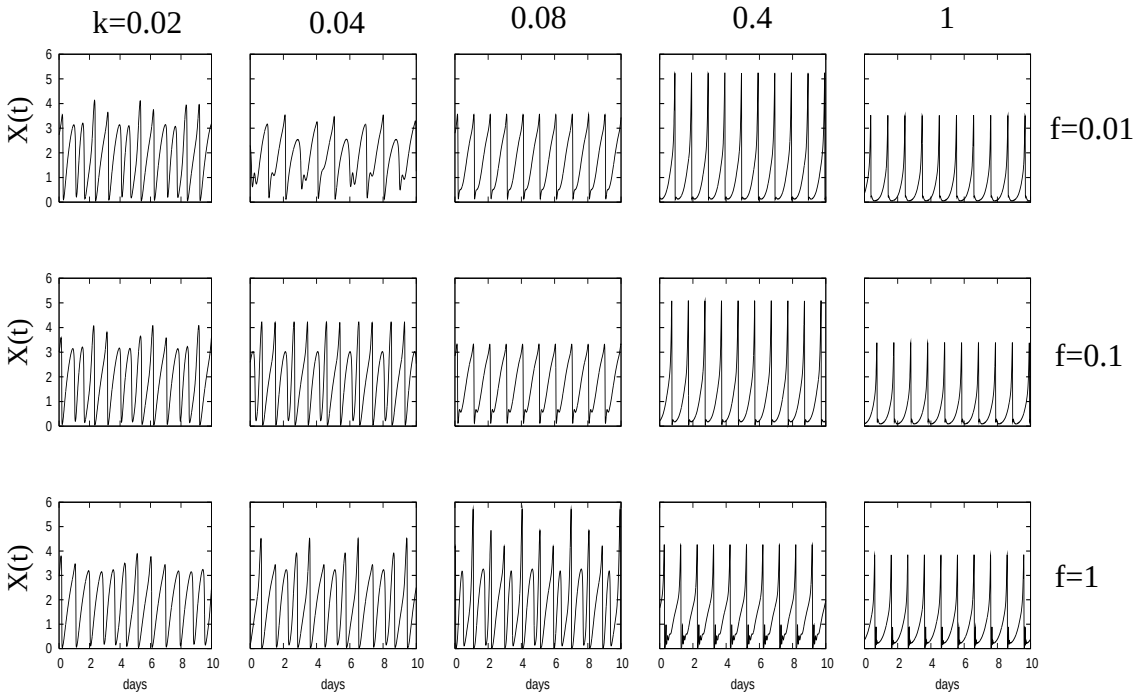

Figure 3.6: *Time series of two coupled limit cycle oscillators, for different coupling parameter values. The parameter f increases from top to bottom, while the parameter k is changed from left to right, $d_p = 0.27$.*

$k = 0.03$, $k = 0.05$ and $k = 0.1$, respectively for the different values of parameter f. The period of the coupled system depends on the values of coupling parameter k and the values of Michaelis-Menten coefficient. An increase of the coupling parameter k induces an increase in the period of coupled oscillators for different values of the Michaelis-Menten coefficient [Figs.3.8(a-c)].

In order to develop a model that will incorporate the influence of environmental signals and a model for a net of coupled elements, the case of two coupled limit cycles will be further considered with the coupling parameter $k = 1$ and the Michaelis-Menten coefficient $f = 1$. This case of coupling, thus satisfies two main requirements that reflect some of the main properties of circadian clocks. First, the period of the coupled system is robust against the variation of the coupling parameters and second, the values of maximal production of

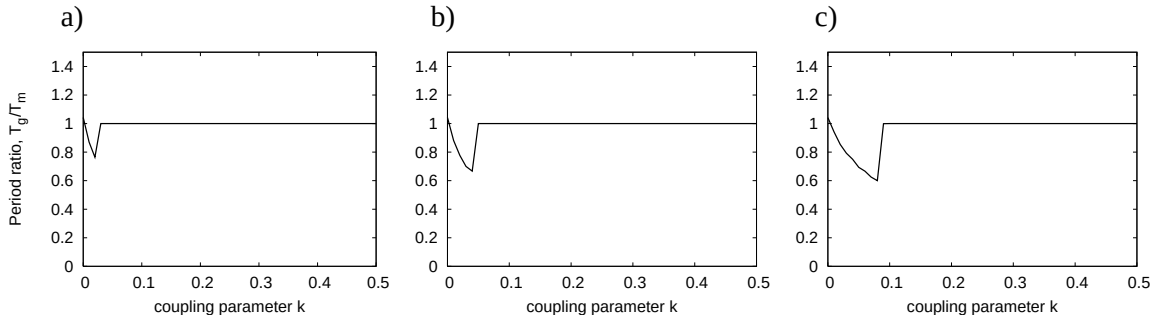

Figure 3.7: *Period ratio T_g/T_m of the coupled system of two limit cycles (genetic oscillator and metabolic oscillator) that oscillate with their own periods, $T_g = 23.7\ h$, $T_m = 24.7\ h$, due to the continously increase of the coupling parameter, k for the three different values of Michaelis-Menten coefficient f : $(a)\ f = 0.01$, $(b)\ f = 0.1$, $(c)\ f = 1$.*

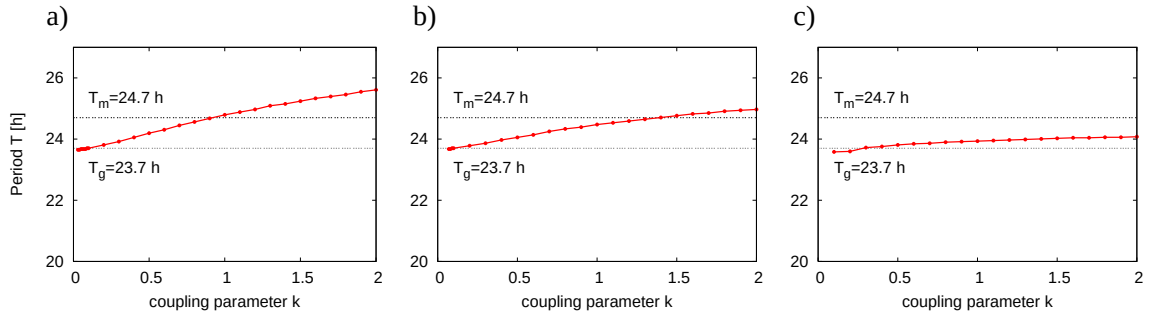

Figure 3.8: *Periods of a system composed of two coupled limit cycles (genetic oscillator and metabolic oscillator) as a function of parameter k restricted to different Michaelis-Menten coefficients f: $(a)\ f = 0.01$, $(b)\ f = 0.1$, $(c)\ f = 1$.*

reactant x by protein activation with respect to the Michaelis-Menten coefficient are in a reasonable range of biochemical values. Other cases of limit cycle behaviour, due to the coupling of oscillators when they are in different dynamical regimes, are not of interest. The periods of such systems are not robust due to parameter variations, as usually a strong decrease of periods is observed. The only case when the variation of the coupling parameter does not induce a change in the period and when the values of periods are in an endogenous physiological region is the case of the coupling of two fixed points. However, very strong coupling, e.g. high values of parameter k and small values of Michaelis-Menten coefficient are needed to obtain such a robustness.

3.6 Environmental Influences

Circadian oscillators preserve information on time in the absence of environmental cues, but they are strongly influenced by external temporal signals, such as light and temperature. Therefore, a model that will incorporate the influence of light and temperature on the activity of the internal circadian system is presented. The model combines two models

based on experimental observations, model of light influence on a transcription translation loop, [93, 94] and the model of spatiotemporal localisation, [95].Thus in the simple model presented, the assumption is that during the dark regime with low temperature, which represents night condition, the activity of effective protein does not influence the metabolic clock, so that the coupling parameter k is set to the value $k = 0$. According to experimental results light pulses enhance degradation. Therefore, degradation rate of protein is decreased also in the model presented, to the value $d_p = 0.17$. During light regime with higher temperature, which represents day conditions, the effective protein activates the production of reactant X and the coupling parameter is then set to $k = 1$, while the degradation rate of protein is increased to the value $d_p = 0.27$. Other parameter values in the model are set according to the Tab. 3.1. with (p_m, f, b)=$(0.75, 1, 0.2)$. The corresponding model is given by the schematic representation, [Fig.3.9].

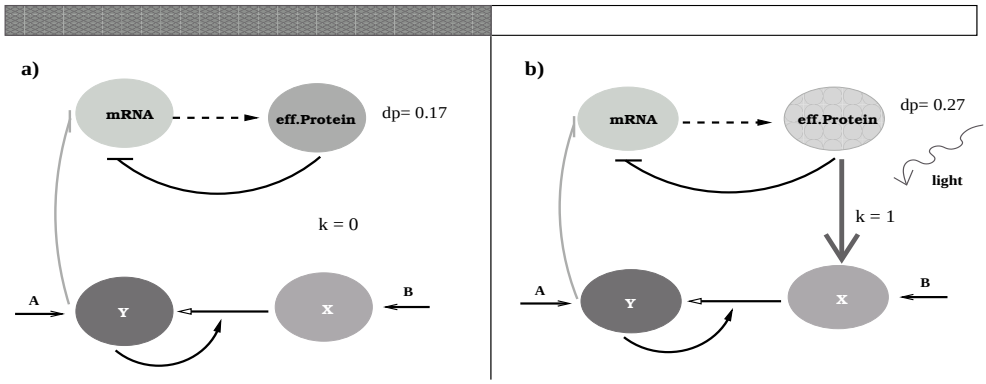

Figure 3.9: *Model for the environmental influences.* (*a*) *The system in dark regime with low temperature or night conditions (NC) is defined with parameters* $k = 0$, $d_p = 0.17$. (*b*) *The system, in light and high temperature regime, day conditions (DC) are defined with parameters:* $k = 1$, $d_p = 0.27$.

The environmental influences are studied under regular intervals of perturbation. Numerical simulations of "day-night" conditions are obtained by setting the parameters $k = 1$ and $d_p = 0.27$ for the first 12 hours of simulation and then for the next 12 hours the parameters are changed to $k = 0$ and $d_p = 0.17$. After 13 cycles of 24 hours perturbation representing the "day-night" entrainment, parameters are set to constant values for one set of parameters $k = 1$ and $d_p = 0.27$ representing the day conditions (DC), illustrated in Figs.3.10(a, b). The other set of parameters $k = 0$ and $d_p = 0.17$ represents the night conditions (NC)[Figs.3.11(a, b)].
From both figures one can see that the amplitudes of the variables representing metabolic abundances are significantly decreased comparing the same variables for the "day-night" entrainment. This is in good agreement with experimental results where it is shown that amplitudes of the variables of a circadian system are maximised during the natural change in environmental signals, Fig.3.10(b) and Fig.3.11(b) and are minimised in the constant conditions. Also, variables representing genetic oscillator are slightly increased during the continuous day regime, comparing to the "day-night" entrainment. This is also acceptable

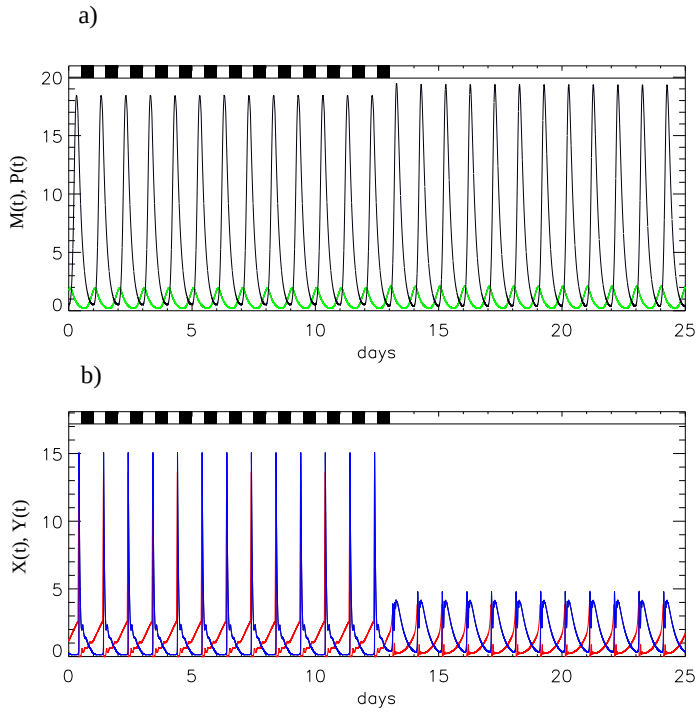

Figure 3.10: *Time series of the "day-night" entrainment for the period of change in environmental signals of $T = 24$ h for the variables (a) M, green (-) and P , black (-) and (b) X, red (-), Y, blue (-). After 13 cycles the system is set to constant "day" condition (DC).*

from the biological point, as high temperature and light enhance the activity of the gene-protein clock. On the contrary, constant "night" conditions inhibit the activity of the gene clock and thus the amplitudes of the variables for mRNA and protein abundances are also decreased.

The environmental model is also used to investigate the entrainment of the circadian system due to different periods. Numerical simulations representing the change in environmental signals with period $T = 24$ are performed for 200 oscillations and the periods of the genetic and the metabolic oscillators are estimated. The entrained system is phase and frequency locked and both oscillators are oscillating with a dominant period of $T = 24$ h, which is presented in Figs.3.12(a, b). For the case of day conditions, oscillators oscillate with the same free running period of $T = 23.9$ h, while for the case of night conditions, each oscillator oscillates with its own free running period, $T_g = 23.7$ h for the genetic oscillator and $T_m = 24.7$ h for the metabolic oscillator, respectively.

The entrainment is also investigated when the period of the environmental perturbation is set to $T = 16$ h. Numerical simulations are performed setting one set of parameters for the duration of 8 hours $(d_p, k) = (0.27, 1)$ and for the next 8 hours another set of parameters is used, $(d_p, k) = (0.17, 0)$. After 20 cycles the system is set to constant day conditions. Results from numerical simulations are illustrated in Fig.3.13, where time series of four variables are presented. Amplitudes of the variables for genetic and metabolic oscillators under the environmental perturbation period $T = 16$ hours are lower compared

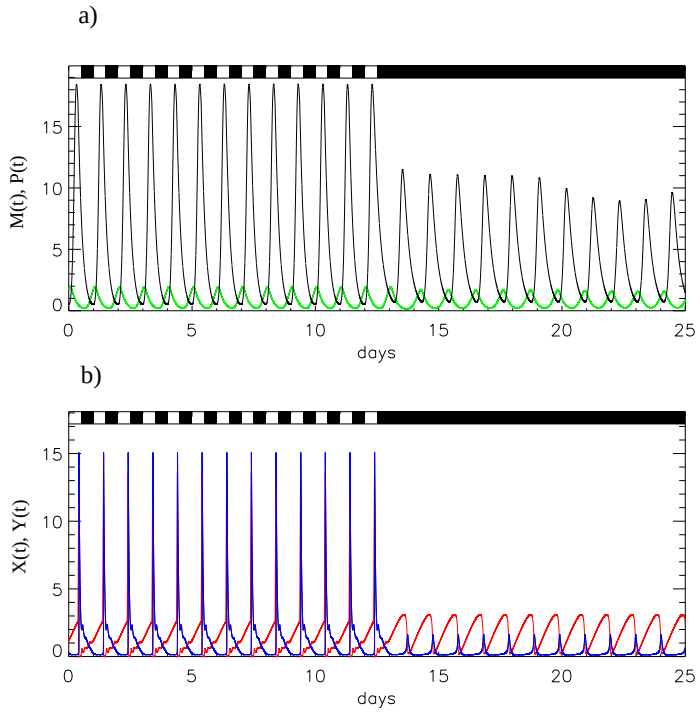

Figure 3.11: *Time series of the "day-night" entrainment for the period of change in environmental signals of $T = 24$ h for the variables (a) M, green (-) and P , black (-) and (b) X, red (-), Y, blue (-). After 13 cycles the system is set to constant "night" conditions (NC).*

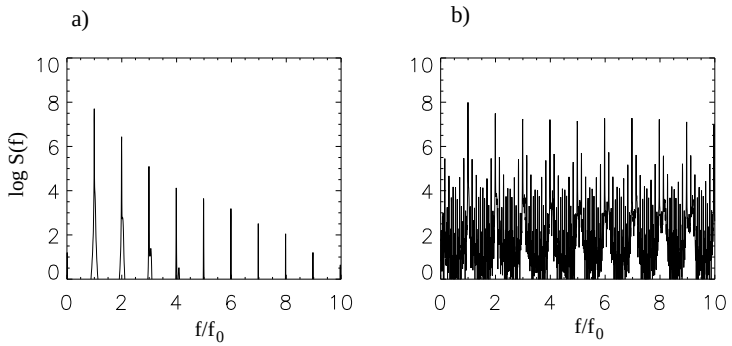

Figure 3.12: *Power spectral density $logS(f)$ obtained by the analysis of time series for the variables a) $M(t)$ of the genetic oscillator and b) $X(t)$ of the metabolic oscillator in the case of "day-night" entrainment, when the period of change in environmental signals are set to $T = 24$ h; f_0 is frequency that corresponds to the period $T_0 = 24$ h.*

to the amplitudes of the same variables for the case of environmental perturbation period $T = 24$ hours. To estimate periods of the system in this case, numerical simulations of "day-night" entrainment with period $T = 16$ h are performed and results are presented in

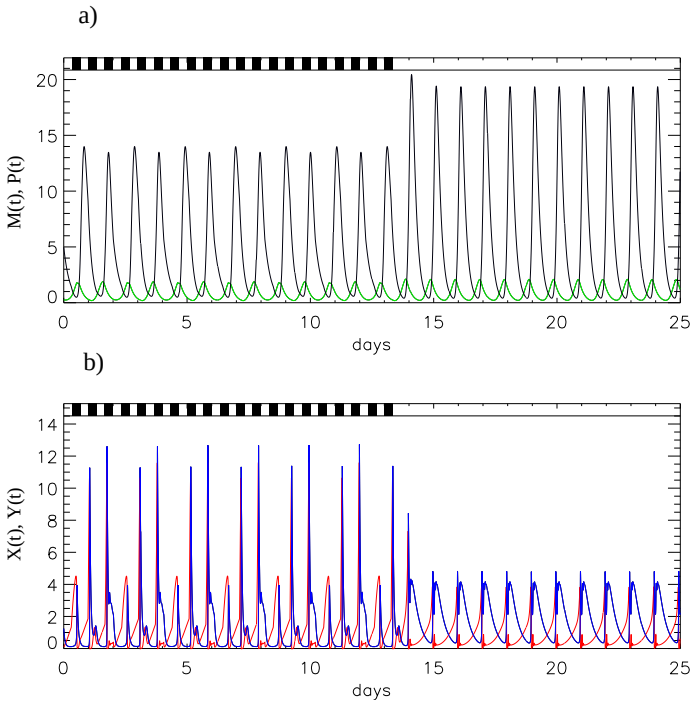

Figure 3.13: *Time series of the "day-night" entrainment for the period of change in environmental signals of* $T = 16$ *h for the variables (a)* M*, green (-) and* P *, black (-) and (b)* X*, red (-),* Y*, blue (-). After 20 cycles system is set to constant "day" condition (DC).*

Figs.3.14(a, b). From this graph one sees that the dominating period for the variable of a genetic oscillator is the free running period $T = 23.9$ h, [Fig.3.14(a)] and the variable of the metabolic oscillator oscillates with the period of the environmental perturbation $T = 16$ h, [Fig.3.14(b)]. Thus for the case of a period significantly different from 24 h, differences between variables of the genetic and metabolic oscillators are pronounced, as the variables of the metabolic oscillator partially adjust their periods to the period of environmental perturbation.

3.6.1 Phase Response Curves

System response and sensitivity due to an external perturbation are also studied by means of phase response curves. According to the model for the environmental influence and previous experimental studies, degradation rate of protein d_p is increased due to the application of light pulse. It is assumed that the coupling between two different clocks, represented here as the parameter k, is linked to both environmental signals, light and temperature.
Thus, in order to obtain phase response curves, light and temperature pulses are applied at the same time. It means that during numerical simulation, the system is perturbed for the duration of 1 hour at each point (every hour) of the oscillation phase. The zero point 0 circadian time (0 CT) is set to be at the minimum of mRNA abundances, next perturbed point (1 CT) is set 1 hour later, and further on. The perturbation is applied

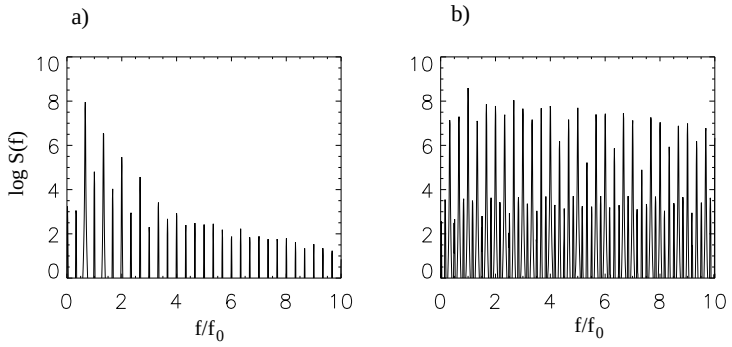

Figure 3.14: *Power spectral density obtained by the analysis of the time series for the variables a) $M(t)$ of the genetic oscillator and b) $X(t)$ of the metabolic oscillator in the case of "day-night" entrainment when the period of change in environmental signals are set $T = 16$ h; f_0 is frequency that corresponds to the period $T_0 = 16$ h.*

until a phase point for which amplitude of response is the same as the amplitude at the zero point (0 CT). Perturbation means that during one hour the parameter d_p is increased from value $d_p = 0.17$ to $d_p = 0.27$ and parameter k from value $k = 0$ to $k = 1$, taking into consideration that these changes in parameters e.g. light and high temperature pulse is applied during the constant night regime. Perturbation induces phase shifts with the respect of variables and the phase point when the perturbation is introduced. Fig.3.15(a) illustrates the phase response curve of type 1 observed for the single $1h$ light/temperature pulse for variables $M(t)$ and $P(t)$ while Fig.3.15(b) represents the phase response curve of type 0 observed for the variable $X(t)$ and $Y(t)$.
Phase advances appeared up to the value of 3.5 hours, for the first 9 hours of perturbation and then phase delays appeared up to the value of -1 hours for the next 4 hours, followed by the slow return to the reference point for the variables M and P. In the case of the metabolic variables, the PRC started also with the phase advances for the first 8 hours but up to the value of 12 h and then followed by the phase delay for the next 16 h with return to the reference point. Different types of phase response curves occur because of the application of pulses under constant night conditions, when metabolic oscillator is not influenced by genetic oscillator according to the model, $k = 0$.

To distinguish a response of the system regarding two different parameters that reflect environmental signals, d_p and k, the same kind of numerical simulation is performed, perturbing the system for the period of 1 hour by changing one parameter while setting the other parameter constant. Thus, the contribution of parameters to the phase shift for each variable can be observed. Figs.3.16(a,b) represents phase response curves for both oscillators, for a constant value $d_p = 0.17$, while the parameter k is varied form $k = 0$ to $k = 1$. The perturbation induces PRC of type 0 for the variables of the metabolic oscillator, like it is the case when both parameters are varied, and PRC of type 1 for the variables of the genetic oscillator. PRC of genetic variables has symmetric phase advances and delays. It is also characterised by a small range in the free-running cycle of genetic oscillator in which perturbation failed to induce phase shifts [Fig.3.16(a)].

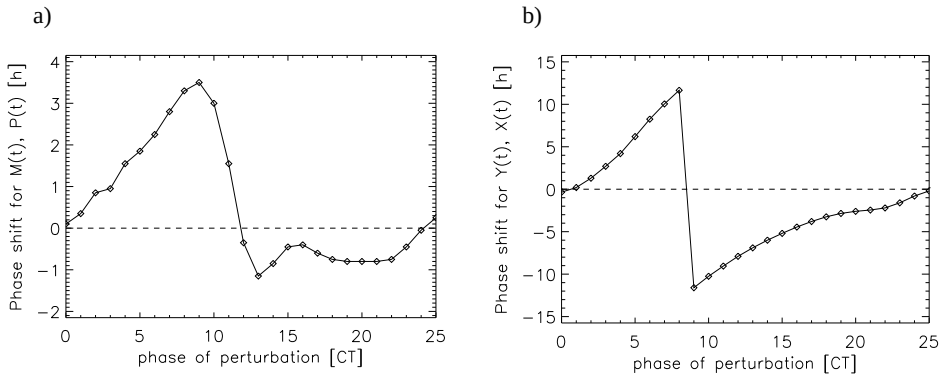

Figure 3.15: *Phase response curves of the system in night conditions (NC, $k = 0$ and $d_p = 0.17$) due to the pulse of environmental signals (DC, $k = 1$ and $d_p = 0.27$) applied for the duration of* 1 *hour for the variables (a) M and P of genetic oscillator, (b) X and Y of metabolic oscillator.*

The case when degradation rate of protein is set to the constant value, $d_p = 0.27$ and

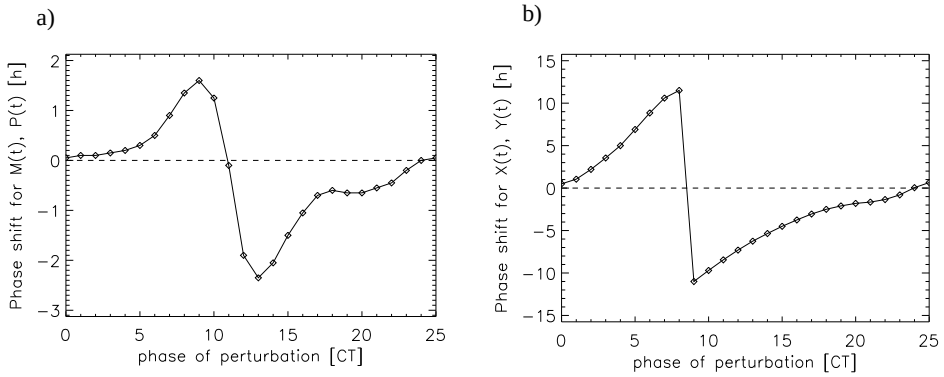

Figure 3.16: *Phase response curves of the system in night condition (NC, $k = 0$ and $d_p = 0.17$) due to the pulse ($k = 1$) applied for the duration of* 1 *hour for the variables :(a) M and P of genetic oscillator, (b) X and Y of metabolic oscillator.*

parameter k is changed from $k = 0$ to $k = 1$, is investigated to distinguish the influence of light and temperature. Most of the experimentally observed PRCs are obtained due to the perturbation in one of the external signals. The result, presented in Fig.3.17(b) represents an interesting change of PRC type in metabolic oscillator, characterised by the transition through the value zero of the phase shift. This kind of perturbation induces larger phase advances for the variables $M(t)$ and $P(t)$, with nonspecific changes in the phase shifts expected for PRC. To compare the results when only the degradation rate of the protein d_p is changed, phase response curves of 1 hour perturbation are calculated for $k = 0$, [Fig.3.18] and $k = 1$, [Fig.3.19], while parameter d_p is changed from $d_p = 0.17$ to $d_p = 0.27$. The curves are similar, resulting in the small phase advances or delays, with pronounced transition through zero phase shift.

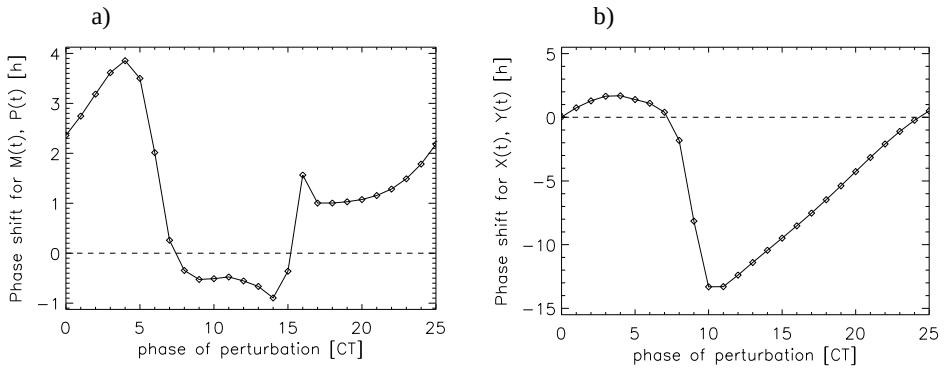

Figure 3.17: *Phase response curves of the system ($k = 0$ and $d_p = 0.27$) due to the pulse ($k = 1$) applied for the duration of 1 hour for the variables (a) M and P of genetic oscillator, (b) X and Y of metabolic oscillator.*

3.6.2 Discussions

The molecular model for circadian clock consisting of two different biochemical oscillators presented, indicates that a simple design of intracellular two oscillator "network" and variations of coupling parameters between oscillators can generate the complexity of circadian clocks. With this two clock model, some possible explanations for the rich behaviour that is usually observed in the experiments with circadian systems can be given. A fundamental question regarding the basic structure of circadian rhythms and its connection to the overt rhythms have been tackled. The model incorporates the inhibition of the metabolic reactant on the production of mRNA. Thus it includes the important issue of the additional feedback loops from the outputs of the rhythm generator to the input [83], such as the state of metabolism could interfere with the transcriptional feedback loop [87]. Model also deals with a question, whether the negative feedback loop, despite it is known as the common regulatory mechanism, is part of circadian systems that generates rhythmicity, or it is just part of the circadian pathway with simple feedback control function.
The results regarding the coupling of two biochemical oscillators and their different coupling situations reveals that some alterations in the period are possible due to the different coupling strengths and different Michaelis-Menten coefficients. This is pronounced in the case of coupling two limit cycles, where different changes in periods are observed due to variations in the coupling parameters. However, a loss of rhythmicity in genetic oscillator can result in significant change in the periods of the system, and thus can be interpreted as the loss of temperature compensation,[Figs.3.5(a,b)]. Two coupled oscillators can be also used to study the influence of environmental signals. Followed by requirements that the period of the coupled system should be robust to variations of the coupling parameter and that values of coupling coefficient k are in a reasonable range, the case of two coupled limit cycles is chosen as the basis for the environmental model. If the strength of the coupling between a genetic oscillator and a metabolic oscillator is $k = 1$ and the value of Michaelis-Menten coefficient is $f = 1$, oscillators are strongly influenced by each other. A further increase in the coupling parameter will not change the period of such a system significantly.

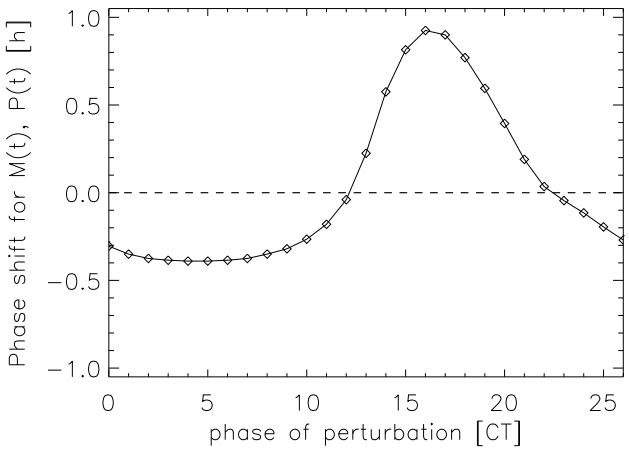

Figure 3.18: *Phase response curves of the system in night condition (NC, $k = 0$ and $d_p = 0.17$) due to a light pulse ($d_p = 0.27$) applied for the duration of 1 hour for the variables M and P of genetic oscillator. Genetic and metabolic oscillator are decoupled in one direction ($k = 0$) and PRC represents the response of genetic oscillator due to light pulse.*

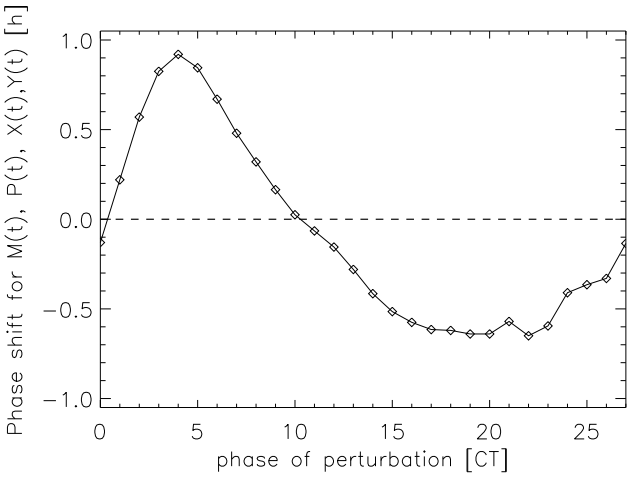

Figure 3.19: *Phase response curves of the system ($k = 1$ and $d_p = 0.17$) due to a light pulse ($d_p = 0.27$) applied for the duration of 1 hour for the variables M, P, X and Y. Genetic oscillator and metabolic oscillator are coupled ($k = 1$) and PRC represents the response of the coupled system due to light pulse.*

It is obvious that the parameter of coupling (defined as k) is an important parameter regarding the dynamics of the coupled two component oscillator, and it is varied in the model for the environmental influence. Numerical simulations of the model reveal two results due to the type of such an entrainment. According to the proposed "day-night" model the system follows the change in environmental signals if the period is 24 h. All

variables of both clock components oscillate with $T = 24$ h, as it is expected because the periods of entrainment and the system are close.
However, if the period of change of the environmental signals, $T = 16$ h, is shorter than the intrinsic period of the coupled oscillators, variables of metabolic oscillator will be partially entrained by the period imposed by external signals, $T = 16$ h. Variables of the genetic oscillator oscillate with the dominating period which is their own endogenous period. These results suggest the experimentally observed fact that different circadian clocks in a system can be distinguished due to the distinctive response caused by significantly different entrainment conditions. Thus differences of the circadian clocks in a system due to different periods of change of the environmental signals, can be only possible if the circadian system consists of two or even more clocks. Further analysis of the model due to the entrainment, obtained by numerical simulations of phase response curves revealed two typical PRCs observed in circadian systems. Comparing the results for PRCs due to the different set of parameters k and d_p, one can clearly see that the system composed of two coupled oscillators is highly sensitive to the change in the coupling parameter k, inducing the different response for the genetic and metabolic oscillator.

Chapter 4

Influence of Variability on the Net of Coupled Circadian Oscillators

The subject of this chapter is the dynamics of a net of elements. Each element consists of two coupled biochemical oscillators, a genetic and a metabolic oscillator (Chapter 3). Elements in the net oscillate with different periods. This chapter represents the investigation of synchronisation in the net with respect to different couplings among them. The net is also investigated in its response to the change in the environmental signals, such as light and temperature according to the already proposed concept for environmental influences. Different types of couplings in the net with respect to two distinct periods of change in environmental signals, are investigated.

4.1 Biological Framework

Experimental findings indicate that the higher level of cellular organisation should be considered in order to investigate the circadian rhythmicity of the whole organism. Experiments with a mammalian circadian clock show that neuronal clocks within the suprachiasmatic nuclei (SCN) form a heterogeneous network where each individual oscillator oscillates with its own frequency [19, 20, 96]. However, the output of the SCN is a coherent circadian output and is coordinated with the daily changes in the environment [97]. So far it is still unknown which coupling mechanism leads to the synchronisation of such frequency distributed oscillators, although many studies, both experimentally and theoretically are addressed in this direction [98, 99, 100, 101]. The synchronising factors which are considered in the case of circadian rhythms of SCN are biochemical substances such as neuropeptides gastrin releasing peptide (GRP), vasoactive intestinal polypeptide (VIP) as well as the neurotransmitter γ-amino butyric acid (GABA). Each of these substances could be described as global or local synchronising factors.
The question of multiple, interacting clocks in the net is also imposed in other cases of circadian systems such as the cyanobacteria [102], the unit cellular algae *Gonylaulax polyhedra* [103], succulent plant, *K. daigremontiana* [104, 105, 106], plant seedlings [107] and other plant circadian models, generally [108]. Current research on modelling circadian clocks indicates that circadian properties of such organisms can only be understood as a

result of the collective dynamics of multiple oscillators. Thus it is important to describe how cell-to-cell communication is established and what are the sufficient and necessary conditions for their synchronisation. Further subject of the investigation in this thesis is the role of a net in the collective behaviour of coupled, heterogeneous, biological oscillators.

4.2 Structure of the Net

To simulate and thus to investigate the possible mechanisms of synchronisation in a cellular network, a system of $N \times N$ elements is considered, where each element is the intracellular nonlinear oscillator composed of a genetic and a metabolic clock. The case of interest is when both oscillators are limit cycles, so the input of reactant Y is set to $b = 0.2$ and the mean value of the production rate of mRNA is set to $p_m = 0.75$. Mutually, they are coupled, with the coupling parameter $k = 1$. From a biological point of view, this set of parameters thus represents an element, the two component circadian oscillator in day conditions [Fig.3.9(b)].
As the interest is focused on a heterogeneous net, it is assumed that the elements of the net differ from each other, in the way that each element oscillates with its own frequency. The period of the oscillatory element depends on the production rate of mRNA as it is shown for the single element in Chapter 3 [cf. Fig.3.2 (b)]. The range of the parameter, p_m is chosen taking into consideration that all elements are in the limit cycle regime. Such a variability according to the model equation represents multiplicative variability [Eqs.(3.15-3.18)].

A Gaussian probability distribution $P(p_m, \nu)$, defined with mean value $p_m = 0.75$ and

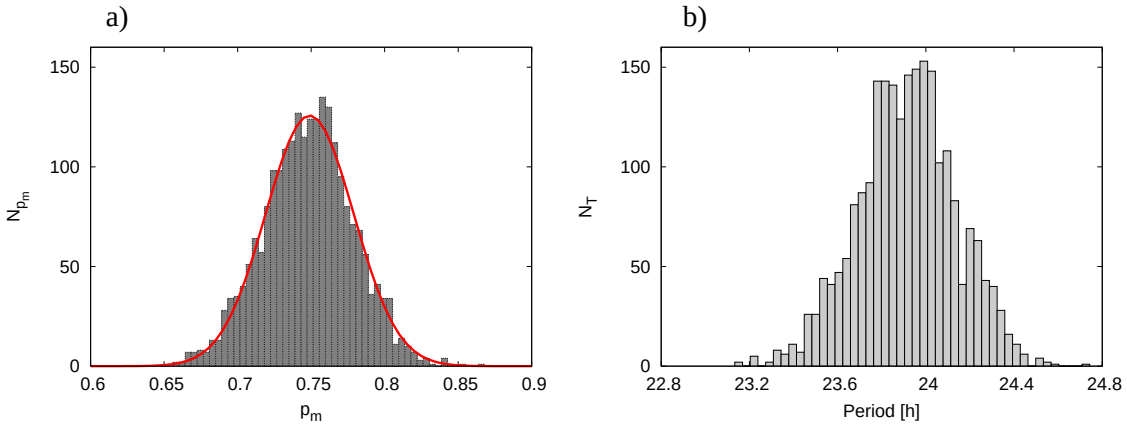

Figure 4.1: *Distribution of parameters (N_{p_m}) and periods (N_T) for the net of oscillating elements: (a) distribution of the production rate of mRNA with the mean value $\langle p_{m_{ij}} \rangle = 0.75$ and (b) corresponding distribution of periods with mean value $\langle T_{ij} \rangle = 23.9$ h for the variability strength $\nu = 0.03$ and the size of the net $N = 48$.*

standard deviation ν for a set of parameters $p_{m_{ij}}$ is used as a realistic influence. Variability of the system is quantified with the standard deviation as the measure of distribution of parameters, defined as the variability strength ν. In Figs. 4.1(a,b), it is shown how a

variability strength of $\nu = 0.03$ corresponds to the parameter range from $p_m = 0.65$ to $p_m = 0.85$, which is equivalent of the period ranging from $T = 23.1$ h to $T = 24.7$ h. The following equations represent the array of elements, where $1 \leq i, j \leq N$ are to be indices for each element in the square $N \times N$ net:

$$\frac{dM_{ij}(t)}{dt} = \frac{1}{1+(Y_{ij}(t)/k_m)^l}\frac{p_{m_{ij}}}{1+P_{ij}^n(t)} - d_m M_{ij}(t) \tag{4.1}$$

$$\frac{dP_{ij}(t)}{dt} = p_p M_{ij}^s(t-\tau) - d_p P_{ij}(t) \tag{4.2}$$

$$\frac{dX_{ij}(t)}{dt} = b - Y_{ij}^2(t)X_{ij}(t) + k\frac{X_{ij}(t)P_{ij}(t)}{f+X_{ij}(t)} \tag{4.3}$$

$$\frac{dY_{ij}(t)}{dt} = a - Y_{ij}(t) + Y_{ij}^2(t)X_{ij}(t) + K_{ij}(t) \tag{4.4}$$

Parameter values $p_{m_{ij}}$ are different for each element in the net, representing the Gaussian distributed numbers defined with mean and standard deviation,

$$\langle p_{m_{ij}} \rangle = p_m, \qquad \langle (p_{m_{ij}} - p_m)(p_{m_{kl}} - p_m) \rangle = \nu^2 \delta_{ij,kl} \tag{4.5}$$

Numerical simulations are performed with periodic boundary conditions and the same initial conditions for all elements (starting values for each variable in the above equations are set to be zero).

One of the question that arises for circadian rhythms is whether some kind of a spatial organisation of circadian clocks should be considered in the case of their mutual synchronisation. There are reports that due to the local coupling some spatial phenomena can be observed, such as pattern formation and the propagation of waves, [78]. Spatiotemporal dynamics that was in detail studied in the case of circadian rhythms of leaves of higher plant *K. diagremontinana*, show a spatial organisation of circadian clocks caused by the influence of an external driver with spatially heterogeneous amplitude and mean value [109]. The interest, lead by experimental findings of Welsh and co-workers [96], is focused on two types of couplings between elements in the net. Global coupling, where the coupling function K_{ij} is defined through the mean field where each element senses the effect of all elements in the net, and nearest-neighbour diffusive coupling, where possible local diffusion effects on the elements using discrete square lattices are investigated. Eq.(4.6) represents the coupling functions regarding diffusive coupling with coupling parameter between the elements, defined by a diffusion coefficient, D_y and Eq.(4.7), global coupling with the coupling parameter defined by a coupling coefficient, C_y:

$$K_{ij}(t) = D_y \bigtriangledown^2 Y_{i,j}(t) \tag{4.6}$$

$$K_{ij}(t) = C_y[(\frac{1}{N^2}\sum_{k,l=0}^{N} Y_{kl}(t)) - Y_{ij}(t)] \tag{4.7}$$

Coupling function is defined in the model with respect to the variable Y, because bifurcation analysis indicates that the diffusion of substance x, represented as the variable X can lead to instabilities (cf. sec. 3.3.1). Global coupling can be applied for both variables. For a comparison with diffusive coupling, only coupling of the variable Y will be used.

4.3 Global Coupling

Global coupling in the system is realized via the variable Y_{ij}. The variability is introduced via the different production rates of mRNA, for each element, with the mean value $T = 23.9$ h and normally distributed periods. The coupling coefficient is varied from $C_y = 0$ to $C_y = 1.1$ for the different spread of intrinsic frequencies. Fig.4.2 represents the order parameter R (Eq. 2.3) as a measure of synchronisation between elements in the net, for different variability strengths. If variability is not present in the net $\nu = 0$, all elements are synchronised and the order parameter has a maximum value, $R = 1$. Synchronisation is induced by an increase in the coupling coefficient C_y. Regardless of the value of the variability strength ν ($\nu > 0$) in the net, the shape of curves is almost the same. One can see that an increase in the coupling coefficient induces an increase in the order parameter or a rise of the degree of synchronisation in the population of oscillators. This

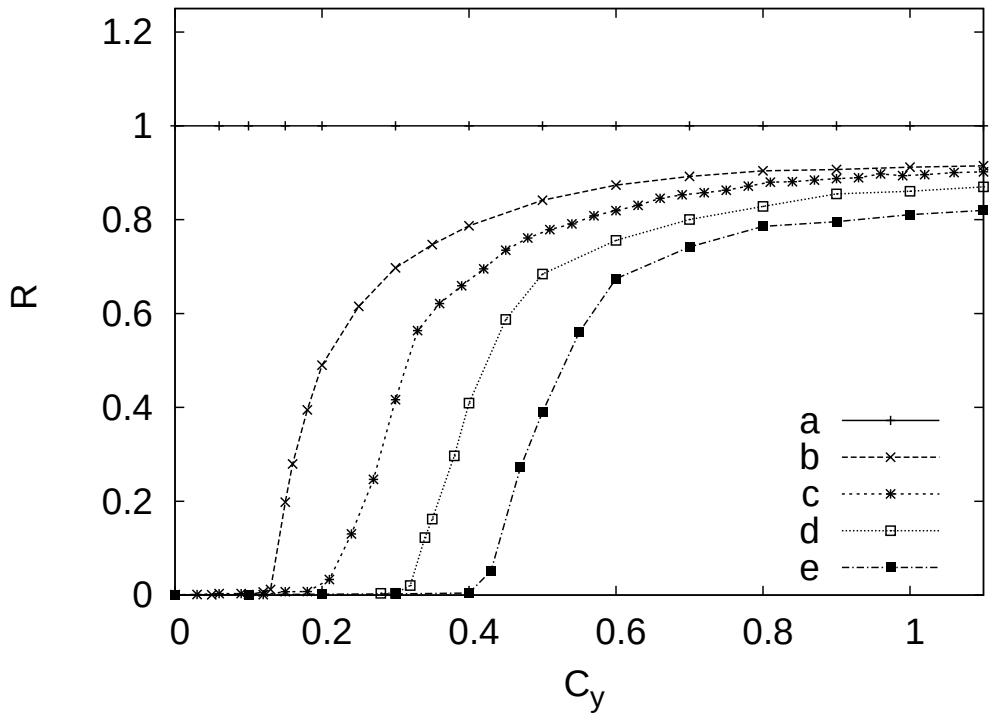

Figure 4.2: *Order parameter R as a function of the coupling coefficient C_y, for different values of the variability strength: a) $\nu = 0$, b) $\nu = 0.02$, c) $\nu = 0.03$, d) $\nu = 0.04$, e) $\nu = 0.05$; $N = 48$.*

transition from an unsynchronised to a synchronised state does not appear in a smooth, linear form. For a weak coupling, the system is not able to synchronise. If the value of the coupling coefficient reaches a certain value, which can be defined as a threshold of coupling coefficient $C_{y_{th}}$, synchronising clusters form, and with a further increase in the coupling coefficient, it increases until a complete synchronisation of the whole net of elements is reached. Figs.[4.3(a1-c1) - 4.5(a-c)] illustrate an example of such a transition for a net with $N = 48$ and for a variability strength $\nu = 0.03$. The transition starts

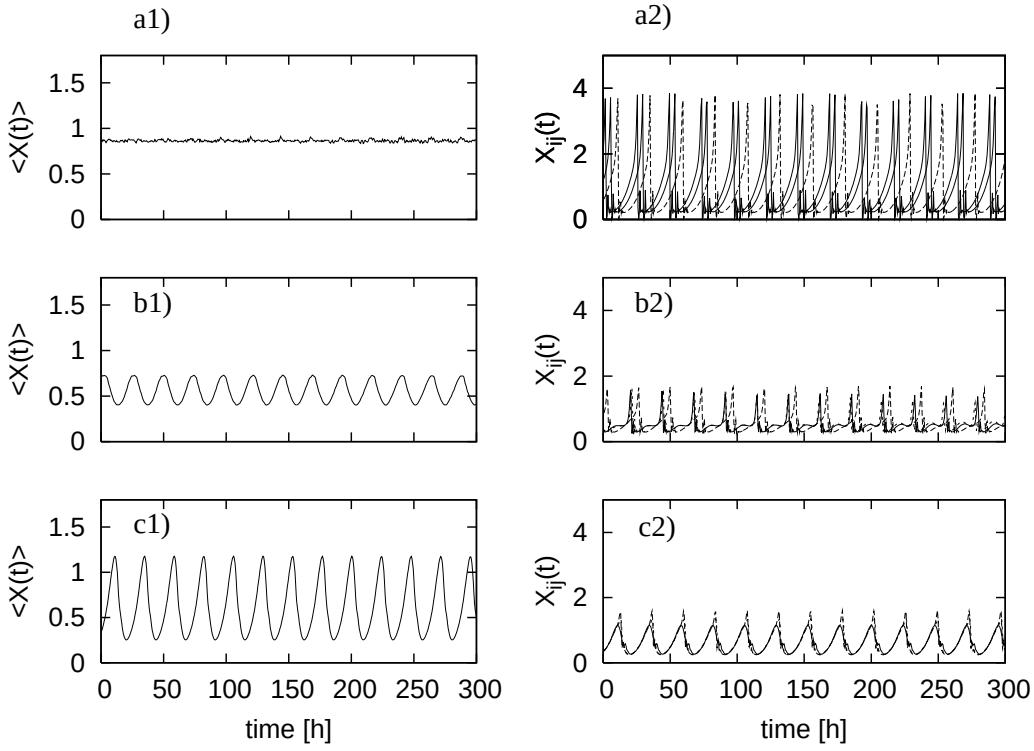

Figure 4.3: *Time series of the averaged value of X of globally coupled oscillators in the net $\langle X(t)\rangle$ for different values of the coupling coefficient: (a1) $C_y = 0$, (b1) $C_y = 0.24$, (c1) $C_y = 0.7$; Time series of variable $X_{ij}(t)$ for three randomly chosen elements and for different values of the coupling coefficient: (a2) $C_y = 0$, (b2) $C_y = 0.24$, (c2) $C_y = 0.7$, $\nu = 0.03$, $N = 48$.*

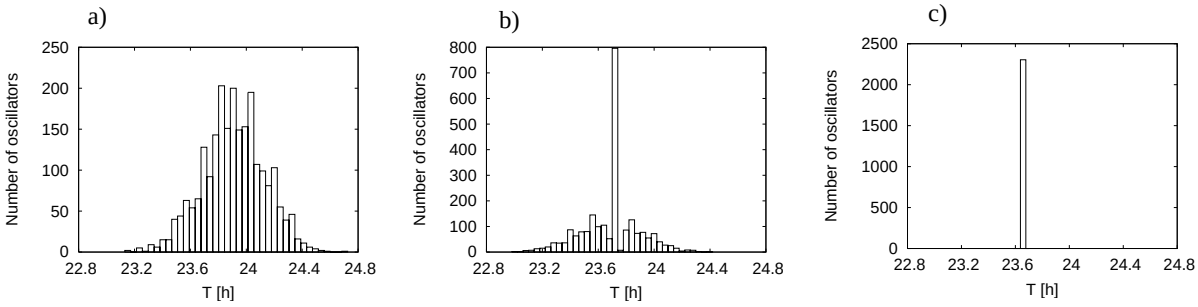

Figure 4.4: *Distribution of periods in the population of globally coupled oscillators in the net for different values of the coupling coefficient (a) $C_y = 0$, (b) $C_y = 0.24$ and (c) $C_y = 0.7$, $\nu = 0.03$, $N = 48$.*

from a completely unsynchronised regime when the coupling in the system is not present $C_y = 0$, the amplitude of the averaged value of the variable X is almost constant due to the distribution of phases [Fig.4.3 (a1)] and the periods are distributed according to the initial conditions, [Fig.4.4 (a)]. Further increase in the coupling coefficient induces partially synchronisation in the net, and the value of the coupling coefficient $C_y = 0.24$

induces an increase in the amplitude of the averaged value of X [Fig.4.3 (b1)]. For this value of the coupling coefficient, most of the elements in the net start to synchronise with a dominant period $T = 23.7h$ [Fig.4.4(b)]. Finally, the synchronised regime is reached, when the value of the coupling coefficient is $C_y = 0.7$. Then, the averaged amplitude increases further [Fig.4.3(c1)] and the single period of $T = 23.65$ h is the same for all elements in the net [Fig.4.4(c)]. Amplitudes of the variable X_{ij} of a randomly chosen element decrease due to global coupling, [Fig.4.3(a2-c2)]. Snapshots of the system, representing the net of elements in one arbitrary moment is presented in Figs.4.5(a-c), where one can clearly see the influence of variability on the system and the effects of global coupling for the different coupling strengths. In the absence of coupling $C_y = 0$ [Fig.4.5(a)], the differences between

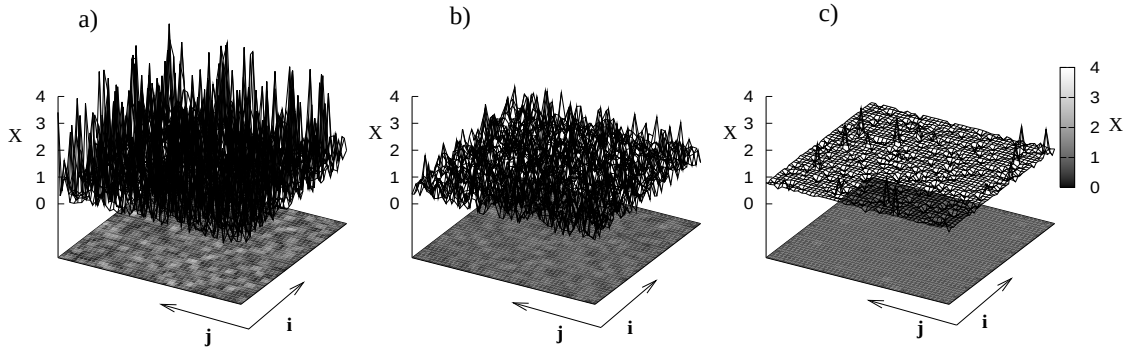

Figure 4.5: *Snapshots of the net with globally coupled elements, taken for an arbitrary moment of time, for different values of the coupling coefficient: (a) $C_y = 0$, (b) $C_y = 0.24$ and (c) $C_y = 0.7$, $\nu = 0.03$, $N = 48$.*

the relative concentrations of product X among elements are significant, they are decreased with the increase of the coupling in the net, $C_y = 0.24$, [Fig.4.5(b)] and almost vanished as the coupling reached a value $C_y = 0.7$, [Fig.4.5(c)]. The value of the coupling coefficient where transitions to a synchronised regime are starting to emerge, when the increase of the order parameter is significant and when elements starts to synchronise, strongly depends on the spread of intrinsic frequencies. As it is expected, the smaller value of the variability strength is applied in the system, and thus the more similar the individual oscillators are, the smaller values of the coupling coefficient are needed for elements to start to synchronise and thus to oscillate with the same period. Fig.4.6 shows dependency of the threshold of the coupling coefficient $C_{y_{th}}$ due to the variability strength ν. This dependency is linear.

4.4 Diffusive Coupling

The effect of diffusive coupling and the existence of spatial patterns are calculated by means of the spatial cross correlation S, for the fixed variability strength $\nu = 0.03$ and the net size $N = 64$. Spatial patterns, forming due to variability, strongly depend on the values of the diffusion coefficient. Fig.4.7 shows shows an increase of the spatial cross correlation S for an increase in a diffusion coefficient D_y. Spatial coherence is emerging with the amount of the diffusion present in the system, which results in the formation of

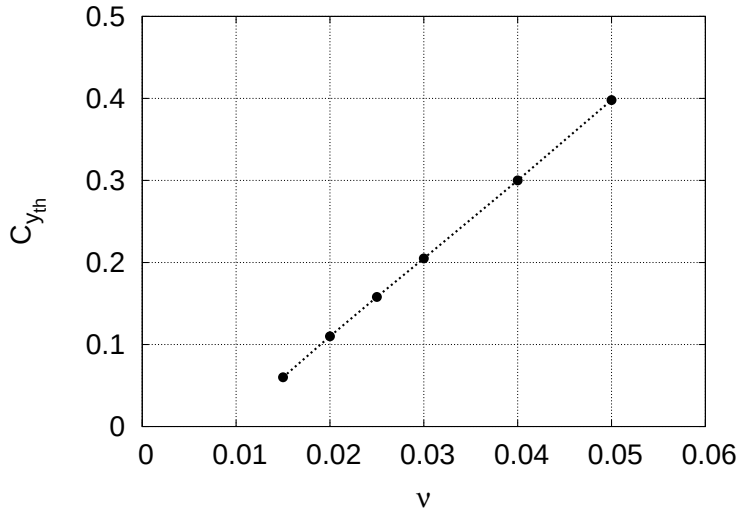

Figure 4.6: *Threshold of the coupling strength $C_{y_{th}}$ as a function of the variability strength ν, $N = 48$.*

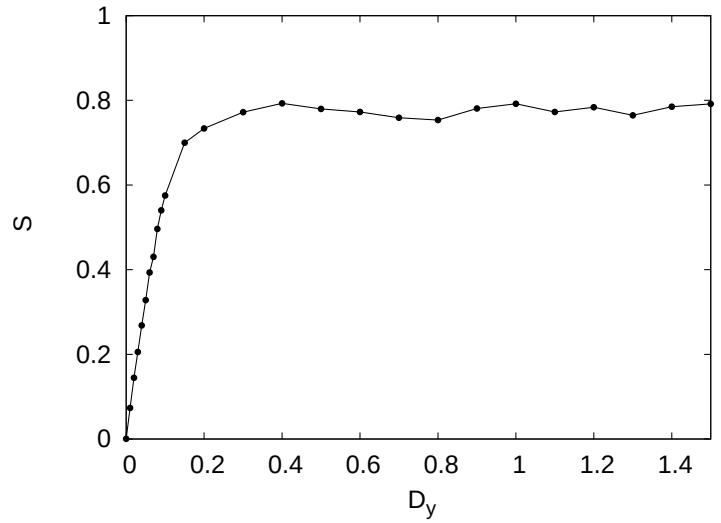

Figure 4.7: *The spatial cross correlation S as a function of the diffusion coefficient D_y, for a net of diffusively coupled elements, $\nu = 0.03$ and $N = 64$.*

patterns, illustrated in Fig.4.8. For the value of diffusion coefficient $D_y = 0.3$ the value of the spatial cross correlation reaches some plateau and ordered patterns in the system of diffusive coupled elements starts to emerge. With a further increase in the amount of diffusion in the system, the size of the patterns is increasing. Local synchronisation among elements and the pattern forming process can also be represented by comparing the time series of the global output $\langle X(t) \rangle$ and of some individual oscillators $X_{ij}(t)$ for different values of the diffusion coefficient as it is shown in Figs.4.9(a1-d2), as well as snapshots of the net taken at an arbitrary time unit [Figs.4.10(a-d)]. Same as it is the case for global

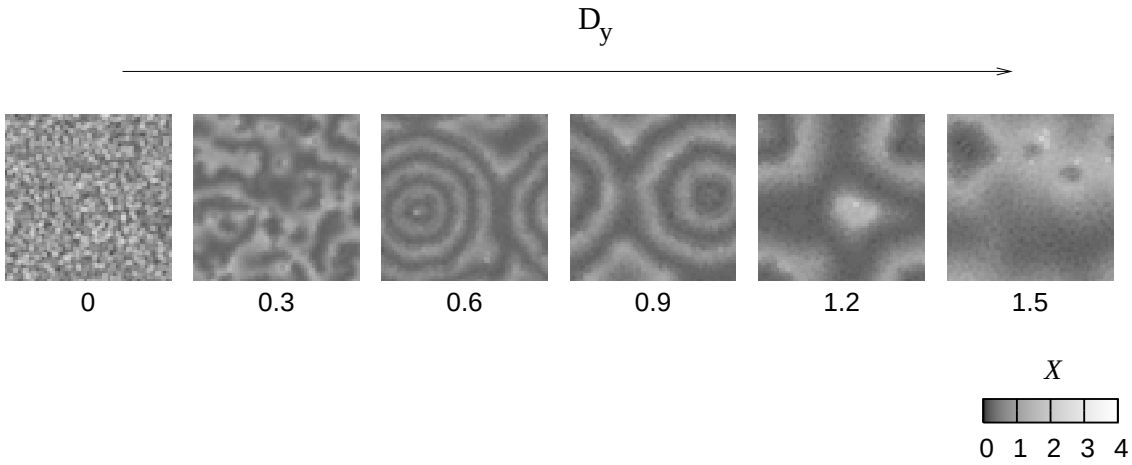

Figure 4.8: *Pattern formation of diffusively coupled oscillatory elements. Snapshots of the variables $X_{ij}(t)$ of a net of coupled elements for various diffusion coefficients $D_y = [0, 0.3, 0.6, 0.9, 1.2, 1.5]$ for the same moment of time, $\nu = 0.03$ and $N = 64$.*

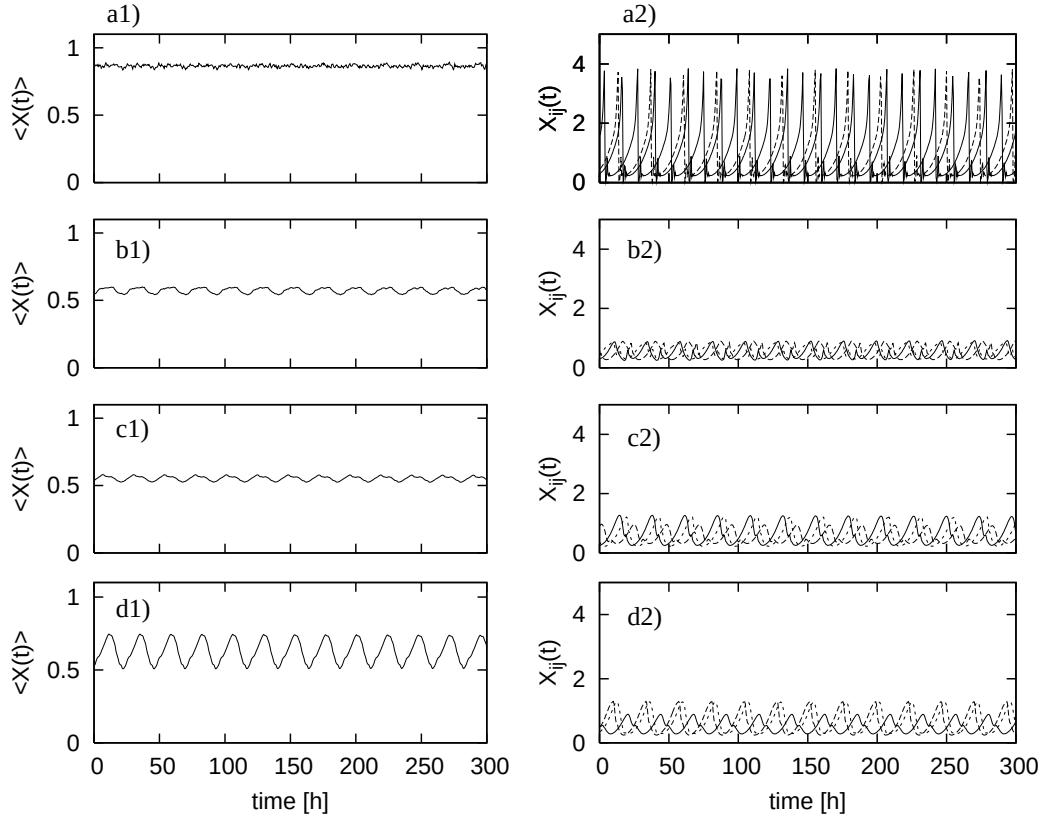

Figure 4.9: *Time series of the averaged value of X, $\langle X(t) \rangle$ for different diffusion coefficients: a1) $D_y = 0$, b1) $D_y = 0.3$, c1) $D_y = 0.6$, d1) $D_y = 1.2$; time series of the variable $X_{ij}(t)$ for three randomly chosen elements for different diffusion coefficients: a2) $D_y = 0$, b2) $D_y = 0.3$, c2) $D_y = 0.6$ and d2) $D_y = 1.2$; $\nu = 0.03$ and $N = 64$.*

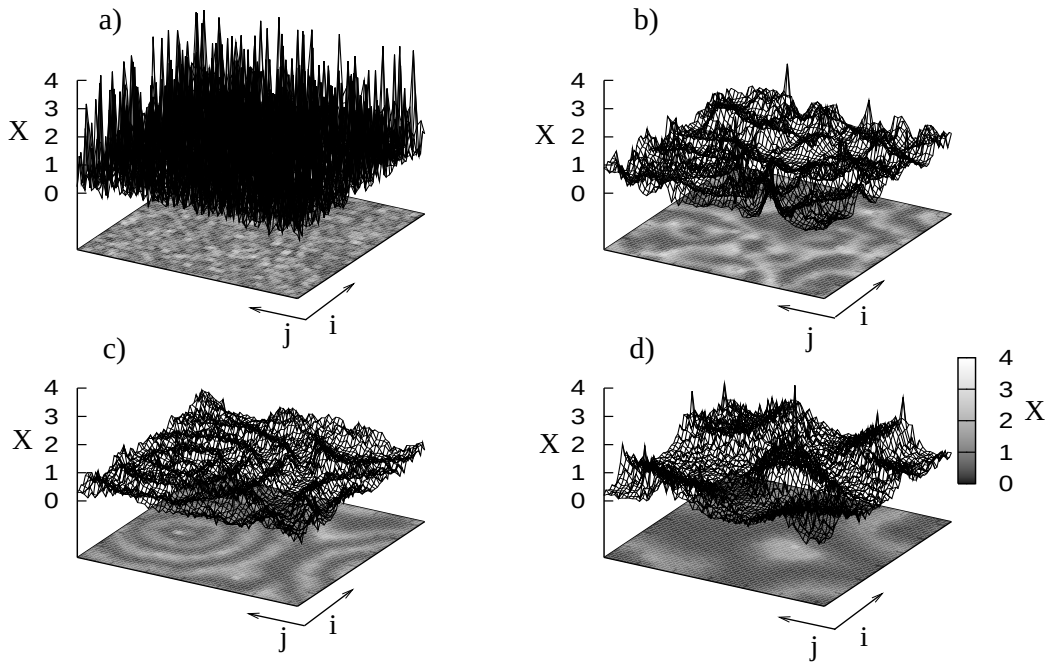

Figure 4.10: *Snapshots of the net of diffusively coupled elements, for different values of diffusion coefficients: a)* $D_y = 0$*, b)* $D_y = 0.3$*, c)* $D_y = 0.6$ *and d)* $D_y = 1.2$*,* $\nu = 0.03$ *and* $N = 64$.

coupling, the period distribution around the average value induces a phase distribution and thus the amplitude of the averaged value of X is almost constant when diffusion is not present in the net, which can be seen in Fig.4.9(a1). Snapshots of the uncoupled net, when $D_y = 0$, is presented in Fig.4.10(a). However as diffusive coupling gets stronger, for values of diffusion coefficients $D_y = 0.3$ and $D_y = 0.6$, one can observe a small increase in the amplitude of the averaged value of X, illustrated in Figs.4.9(b1, c1). Snapshots of such a coupled net indicate that diffusion induces an order in the system, [Figs.4.10(b, c)] and spatial coherence in the form of target patterns starts to appear when the diffusion coefficient reaches $D_y = 0.6$, [Fig. 4.10(c)]. A further increase of the diffusion coefficient gives higher amplitude of the mean field as it is illustrated in Fig. 4.9(d1) and larger patterns, or higher coherence among elements, that can be seen in Fig.4.10(d). Comparing the amplitudes of variables of randomly chosen elements of uncoupled and coupled net, one can see that the amplitudes decrease due to the diffusive coupling in the net, [Figs.4.9(a2-d2)]. In Fig. 4.11, snapshots of the variable $X_{ij}(t)$ due to intermediate strength of coupling ($D_y = 0.6$) for different consecutive times t of 5 hours show the temporal evolution of the net dynamics. The patterns are oscillating with small amplitude which is also presented in a time series graph, [Fig.4.9(c1)].

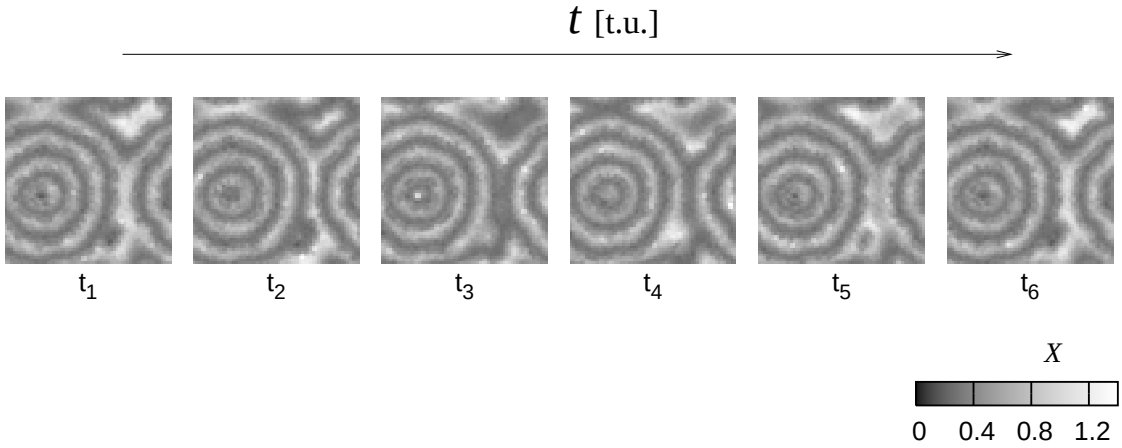

Figure 4.11: *Snapshots of the variable $X_{ij}(t)$ of a net of diffusively coupled elements, for different consecutive times ($\Delta t = t_{i+1} - t_i = 5h$), $D_y = 0.6$, $\nu = 0.03$ and $N = 64$.*

4.4.1 Spatial Patterns Versus Network Size

From the previous section, it is clear that diffusive coupling among oscillators leads to a spatial organisation, for a fixed size of the net. Now different numbers of interacting oscillators and different values for the diffusion coefficient are discussed. Of particular interest is the connection between the size of the patterns, the diffusion strength and the size of the population of oscillators.

In order to recognise which size of the net is sufficient to observe a synchronisation of elements and the phenomena of pattern formation, numerical simulation for the different diffusion coefficient and varied size of the net is performed for a fixed value of variability strength, the same used in the previous simulations $\nu = 0.03$. Both measures for synchronisation is calculated. Figs.4.12(a, b) represent the spatial cross correlation S and the order parameter R as a function of the size of the net for three different diffusion coefficients. One can see that regardless of the values of the diffusion coefficient, the spatial cross correlation increases with the size of the net and between $N = 50$ and $N = 60$ it reaches some constant values, indicating the presence of spatiotemporal patterns, [Fig.4.12(a)]. However, the order parameter as a measure for global synchronisation in the population of oscillators, decreases, with respect to different values of the diffusion coefficient, [Fig.4.12(b)]. For a small value of the diffusion coefficient, $D_y = 0.2$, [Fig. 4.12(b)], the elements are unsynchronised, no matter which size of the net is used. With a further increase in the diffusion coefficient $D_y = 1$ and $D_y = 2$, one sees from Fig. 4.12 (b) that the values of the order parameter are high for a small size of net.

Besides, the size of the target patterns increases with an increase in the diffusion coefficient in the net of elements. However, for a small size of the net, spatial patterns can not exist. Instead, global synchronisation is observed due to the small number of coupled elements. Therefore, the size of the net $N = 64$ will be used for the numerical simulations. Fig.4.13 exhibits examples for different sizes of N. It represents snapshots for a fixed value of the diffusion coefficient $D_y = 1$ with respect to three different sizes of the net. For small values ($N = 32$) there is no difference between the amplitudes of the oscillators, but for the

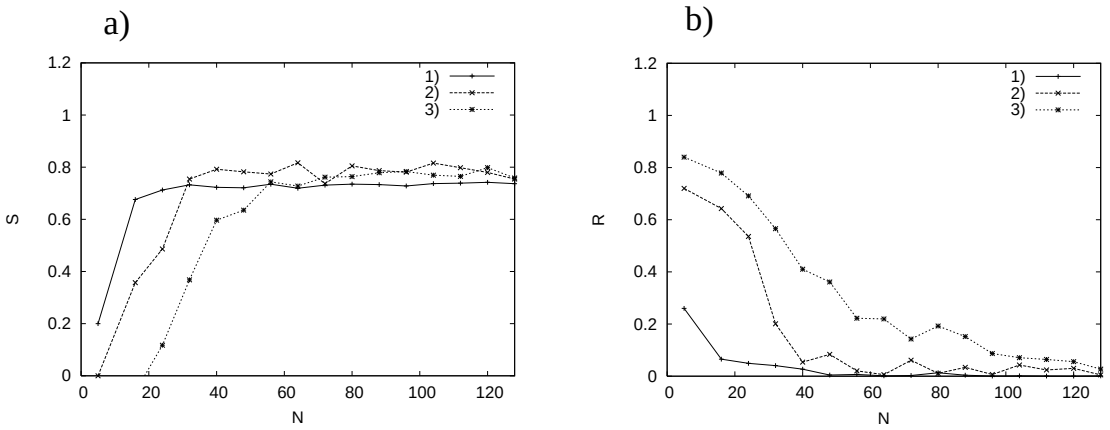

Figure 4.12: *Spatial cross correlation S (a) and order parameter R (b) as a function of the size of the net, N for different diffusion coefficients: 1) $D_y = 0.2$, 2) $D_y = 1$ and 3) $D_y = 2$, $\nu = 0.03$.*

larger net, patterns start to emerge. If the size of a net is set to $N = 128$, this difference is highly pronounced, and target patterns may be observed.

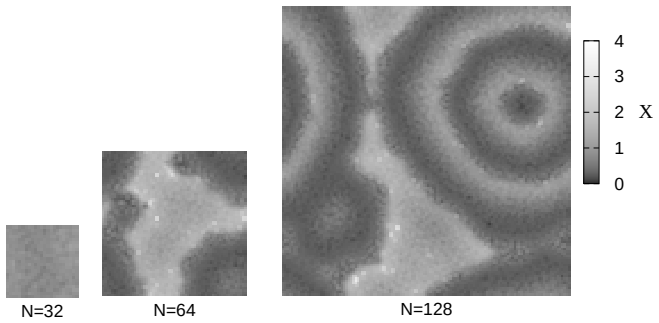

Figure 4.13: *Pattern formation and the size of the net of oscillating elements. Snapshots of the net of diffusively coupled elements with the coupling strength $D_y = 1$, at an arbitrary moment of time for $N = 32, 64, 128$.*

4.4.2 Influence of Period Variability on the Pattern Formation

The influence of different strengths of variability on the net of diffusively coupled elements is studied. This influence is investigated by means of the spatial cross correlation (Eq. 2.4). A measure for spatial coherence is calculated for a fixed value of the diffusion coefficient $D_y = 0.6$, as a function of the variability strength ν, which is varied from $\nu = 0.005$ to $\nu = 0.05$. The results are presented in Fig.4.14, where one can see that the spatial cross correlation decreases with the increase in the variability strength. The calculation of spatial cross correlation is extended for different diffusion coefficients D_y, for the same

range of variability strengths and fixed size of the net $N = 64$. Diffusion coefficient is varied from $D_y = 0$ to $D_y = 1.8$. From Fig. 4.15 one can see that for small differences in

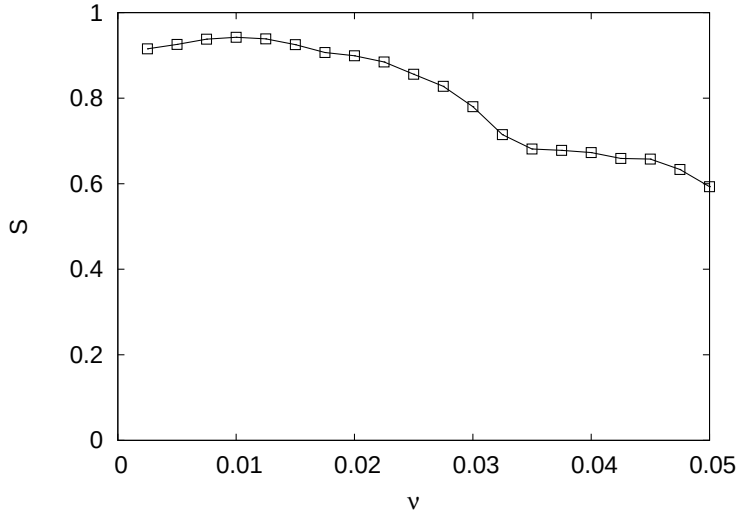

Figure 4.14: *Spatial cross correlation S, for diffusively coupled elements, as a function of the variability strength ν for a fixed value of the diffusion coefficient, $D_y = 0.6$, $N = 64$.*

periods between the elements, i.e. the values of the variability strength ν are small, lower values of the diffusion coefficient is needed for coherent structures to start to form. With the increase in the variability, patterns are detected, but their structure changes due to greater differences in the periods of the oscillators, which is illustrated in Fig.4.15. The quantification of coherent structures is illustrated in more detail in Fig. 4.16 where values of the spatial cross correlations are presented for different values of the variability strength and for different diffusion coefficients. The most coherent structures are obtained for diffusion coefficients ranging from $D = 0.3$ to $D = 0.9$ and variability strengths $\nu < 0.03$.

4.5 Environmental Influences

Change of Environmental Signals with Period $T = 24$ h

The elements in the net are influenced by a change in environmental signals, according to the proposed influence in the single element model [cf. Fig. 3.9]. Entrainment of the coupled net, for both cases of coupling, global coupling and diffusive coupling, is investigated. Numerical simulations are preformed where the coupling constants are varied from $C_y = D_y = 0$ to $C_y = D_y = 1$.
The first case which is investigated is the influence of the environmental perturbation with period $T = 24$ h on a net of diffusively coupled elements, when the elements in the net are identical ($\nu = 0$). The diffusion coefficient is set to $D_y = 0.6$ and the size of the net is $N = 64$. From Figs.4.17(a, b), one can see that the variables are entrained by a change in the environmental signal (the same result is obtained for the case of a globally coupled net,

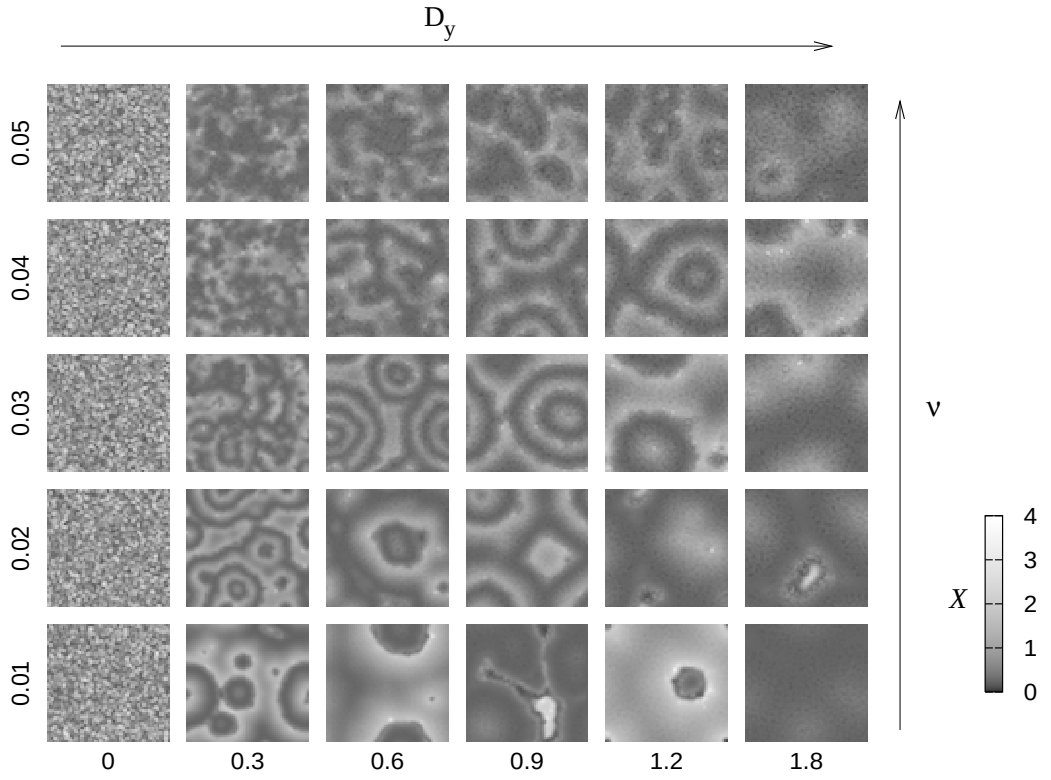

Figure 4.15: *Snapshots of a diffusively coupled net of oscillating elements, taken for an arbitrary time moment, for different diffusion coefficients D_y and different variability strengths ν, $N = 64$.*

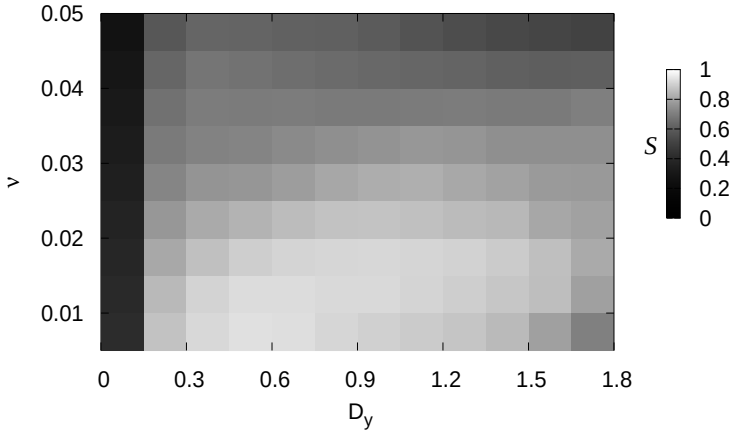

Figure 4.16: *Spatial cross correlation S as a function of the diffusion coefficient D_y and the variability strength ν for a net of oscillating elements of size $N = 64$.*

$C_y = 0.6$). Such an entrained net is synchronised and the value for the order parameter is $R = 1$. The estimation of the period, presented in Fig.4.18 is obtained numerically by

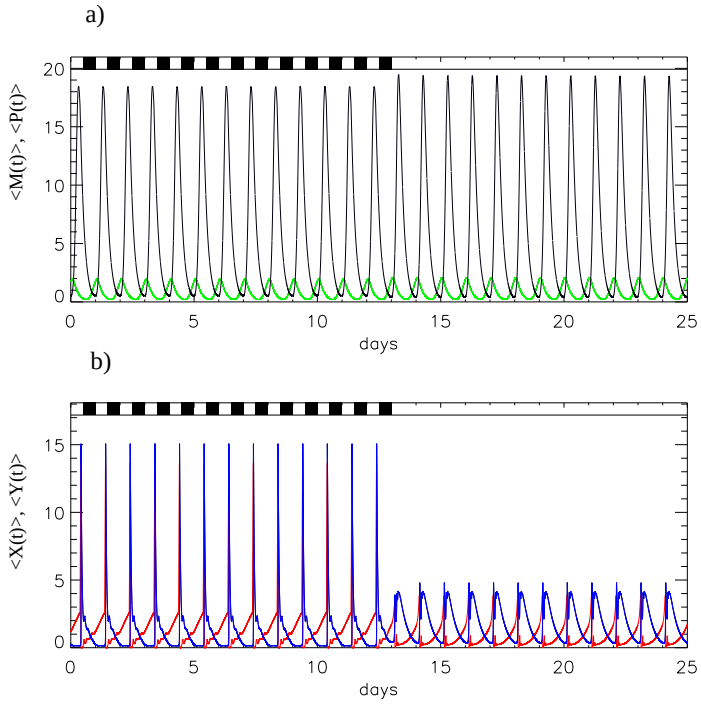

Figure 4.17: *Time series of the averaged variables for diffusively coupled elements ($D_y = 0.6$), due to the change in the environmental parameters for the period $T = 24$ h. After 13 day-night cycles the system is reset to constant day conditions. Time series for the variables, (a) $\langle M(t)\rangle$, green (-) and $\langle P(t)\rangle$, black (-) and (b) $\langle X(t)\rangle$, red (-), $\langle Y(t)\rangle$, blue (-), $\nu = 0$ and $N = 64$.*

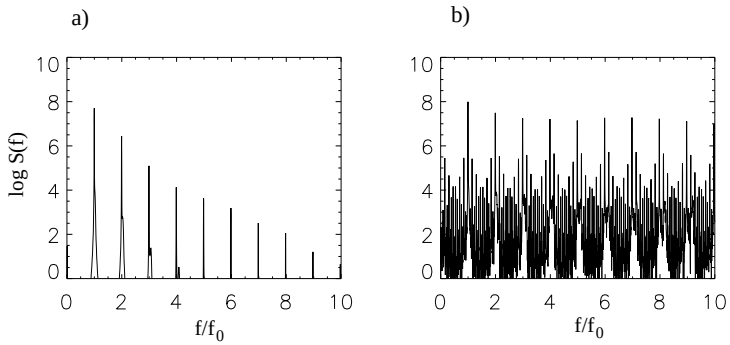

Figure 4.18: *Power spectral density $logS(f)$ obtained by the analysis of time series for the averaged variables: a) $\langle M(t)\rangle$ of the genetic oscillator and b) $\langle X(t)\rangle$ of the metabolic oscillator in the case when the period of change in environmental signals are set $T = 24$ h; f_0 corresponds to the period $T_0 = 24$ h; $D_y = 0.6$, $\nu = 0$ and $N = 64$.*

FFT analysis when the elements are under the influence of day-night conditions. Power

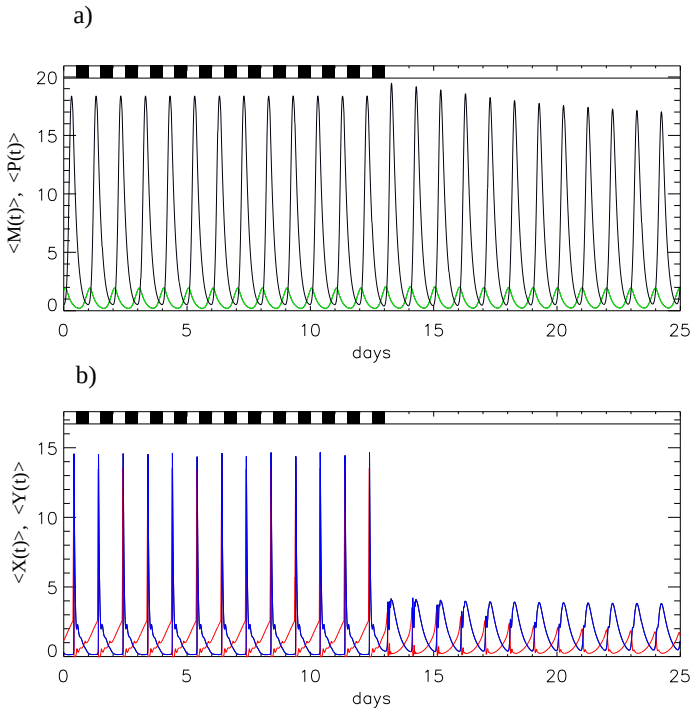

Figure 4.19: *Time series of the averaged variables for diffusively coupled elements ($D_y = 0.6$) with distributed periods ($\nu = 0.03$), due to the change in the environmental parameters for the period $T = 24$ h. After 13 day-night cycles the system is reset to constant day conditions. Time series for the variables, (a) $\langle M(t)\rangle$, green (-) and $\langle P(t)\rangle$, black (-) and (b) $\langle X(t)\rangle$, red (-), $\langle Y(t)\rangle$, blue (-), $\nu = 0.03$ and $N = 64$.*

spectral densities indicate that the variables of the net oscillate with period $T = 24$ h, which is the period of change in environmental perturbation.
In order to investigate the influence of both, variability and the environmental perturbation, numerical simulations are performed with the same conditions as previously, but with the variability strength $\nu = 0.03$. Now, each element in the net is influenced by two factors, variability and environmental perturbation. The elements oscillate with their own period and they are perturbed by environmental signals. Figs. 4.19 (a, b) illustrate the entrainment to external environmental conditions for all variables of the model, represented by the time evolution of the mean field of the variable X, when diffusion in the net of elements is set to $D_y = 0.6$. Comparing the time series of the averaged variables when diffusive coupling is present with the time series of variables for the single element and the net without variability, one can see that the mean field of all elements is also entrained by an external stimulus. Also, a small decrease in the amplitudes of the averaged variables of the metabolic oscillator is observed. When elements in the net are not under the environmental influences, the amplitudes of the averaged variables decrease after several cycles.
The estimation of the period, [Figs. 4.20 (a, b)] indicates the full entrainment of all variables by environmental signals, with a dominant period of $T = 24$ h. The same results for the estimated values of the periods for the net are obtained when global coupling among elements is introduced (data not shown). Figs. 4.21 (a, b) shows that the order parameter,

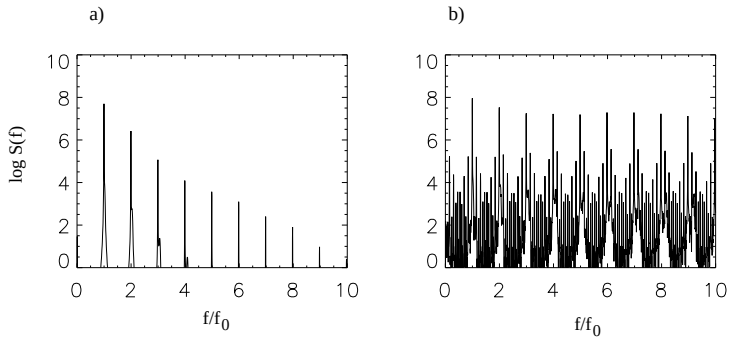

Figure 4.20: *Power spectral density $logS(f)$ obtained by the analysis of time series for the averaged variables, when elements are diffusively coupled elements. Period is estimated for the variables: a) $\langle M(t)\rangle$ of the genetic oscillator and b) $\langle X(t)\rangle$ of the metabolic oscillator in the case when the period of change in environmental signals are set $T = 24$ h; f_0 corresponds to the period $T_0 = 24$ h; $D_y = 0.6$, $\nu = 0.03$ and $N = 64$.*

estimated by numerical simulations for day-night cycles, reaches high values for each type of coupling. The elements are synchronised easily and the whole net is entrained with day-

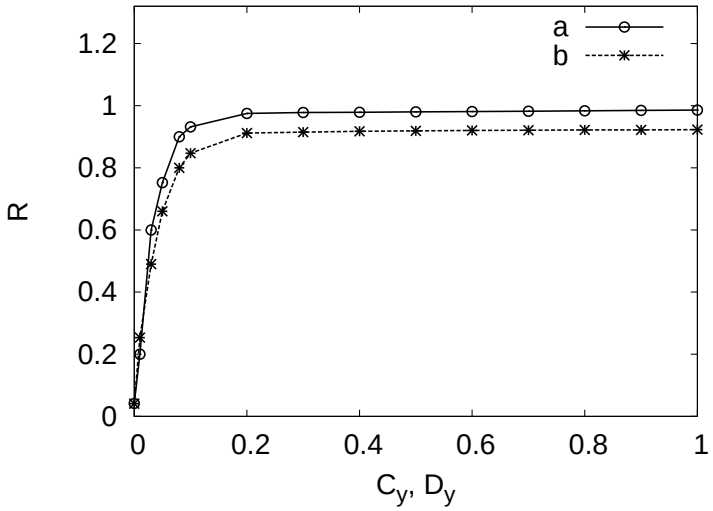

Figure 4.21: *Order parameter R for the net of coupled oscillating elements as a function of the coupling strengths for different types of coupling: a) global coupling, C_y and b) diffusive coupling, D_y. Elements in the net are entrained by the change in environmental signals (light and temperature) with period $T = 24$ h, $\nu = 0.03$ and $N = 64$.*

night alternations. Only a small amount of coupling is needed in order to get high values for the order parameter ($C_y = D_y = 0.1$). A further increase in the coupling coefficients induces a small increase in the order parameter as the interaction between elements are strong enough. However, only small differences in the values of the order parameter can be observed with respect to the different types of coupling [Fig. 4.21].

Change of environmental signals with period $T = 16$ h

The net of oscillating elements is also perturbed due to 16 hours of environmental signal changes. The same procedure used for the entrainment of a single element is used for the net of elements. The order parameter, the spatial cross correlation and the period are obtained by numerical simulations for the day-night conditions. The first case of the external influence is investigated when the variability is not present in the net, i.e. $\nu = 0$ and the diffusion coefficient is $D_y = 0.6$. Fig.4.22 represents the time series of the averaged variables, which are identical with the case for the environmental perturbation of a single element, [Fig.3.13]. Power spectral densities, presented in Fig.4.23 indicate different dominating periods for the variables of the genetic and metabolic oscillators. Variables of the genetic oscillator oscillate with the dominant period of free running conditions, $T = 23.9$ h, while the variables of the metabolic oscillator oscillate with the period of entrainment, $T = 16$ h. When variability is introduced in the net, $\nu = 0.03$ (the frequencies of elements are distributed around the frequency corresponding to the period of 24 hours), each element will respond differently due to the external perturbation of a 16-hour period. The situation of the entrainment for the net of elements to a 16 hour period, is more complex if coupling among elements of the net is present. For different realisations of coupling, several synchronisation patterns can be observed. Fig. 4.24 represents the situation of entrainment when interactions among oscillators are global, where mean field of entrained elements interacts with each oscillator, i.e. element, with coupling strength $C_y = 0.6$. The mean field amplitudes of all four variables are varied due to modulations.
The temporal evolution of the net dynamics for the case of globally coupled elements ($C_y = 0.6$) is presented in Fig. 4.25, where the time difference between two consecutive snapshots is $t = 4h$. Synchronisation occurs due to the global coupling and spatial patterns do not exist, as the values for the spatial cross correlation are around zero (data not shown). The order parameter increases with an increase in the coupling coefficient from $C_y = 0$ to $C_y = 1$ [Fig. 4.26]. One can see that the elements under the influence of environmental perturbation with the period significantly different from the periods of the elements in the net, can achieve a higher degree of synchronisation in such a complex net due to the global coupling among the elements.

Power spectral densities [Figs.4.27(a,b)], for the case of global coupling among elements ($C_y = 0.6$) show that the variables of metabolic oscillators are adjusting their frequencies to the period of external environmental signal $T = 16$, while the variables of genetic oscillators oscillate with dominating frequency which is the frequency of free running rhythm, $T = 23.9$ h. The results are the same as it is the case of the single element [Fig.3.14] and the net without variability [Fig.4.23].

Diffusive coupling, when 16 hours entrained element interacts with its neighbours via metabolic product Y is presented in Fig.4.28. From the figure one can see that the local interactions among elements can induce an increase in the mean field amplitudes of the variables of metabolic oscillator. However, the mean field amplitudes of all four variables are lower, comparing the amplitudes of the net without variability, [Fig.4.22].
Diffusive coupling in the net entrained by a 16 hours period, induces an existence of spatial patterns. The degree of spatial coherence is quantified by the spatial cross correlation measure, S for the two values of the variability strength, $\nu = 0.03$ and $\nu = 0.015$.

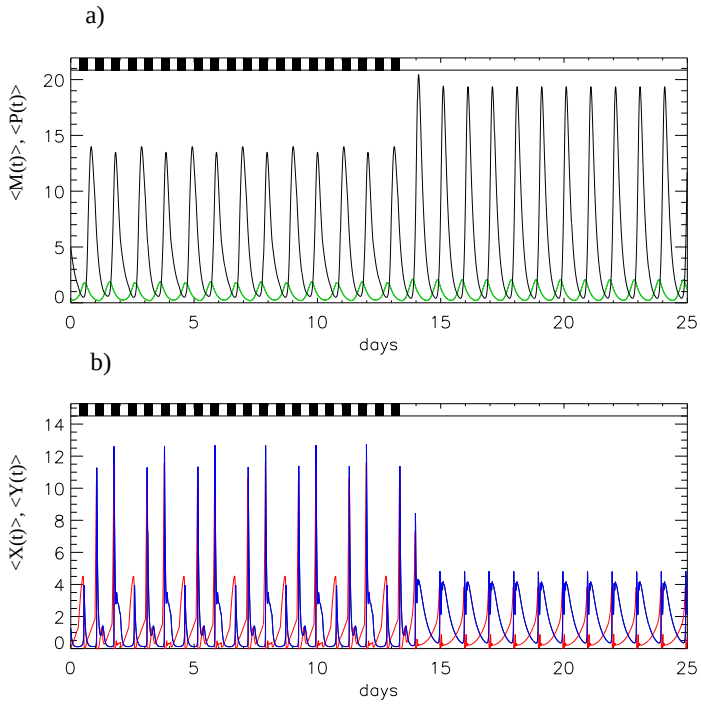

Figure 4.22: *Time series of the averaged variables for diffusively coupled elements ($D_y = 0.6$) due to the change in the environmental parameters for the period $T = 16$ h. After 20 day-night cycles the system is reset to constant day conditions. Time series for the variables, (a) $\langle M(t)\rangle$, green (-) and $\langle P(t)\rangle$, black (-) and (b) $\langle X(t)\rangle$, red (-), $\langle Y(t)\rangle$, blue (-), $\nu = 0$ and $N = 64$.*

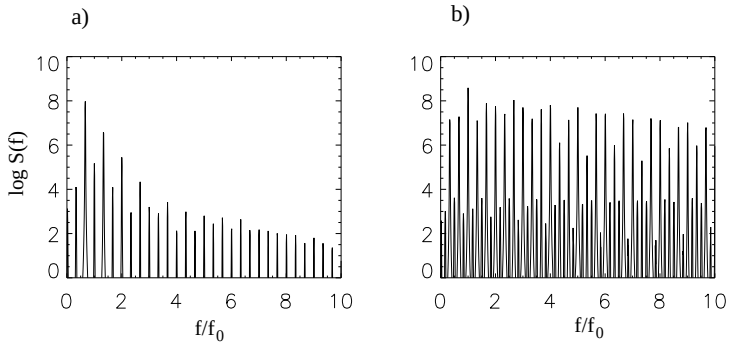

Figure 4.23: *Power spectral density $logS(f)$, obtained by the analysis of the time series for the averaged variables when the elements are diffusively coupled, for the variables: a) $\langle M(t)\rangle$ of the genetic oscillator and b) $\langle X(t)\rangle$ of the metabolic oscillator in the case when the period of change in environmental signals are set $T = 16$ h; f_0 corresponds to the period $T_0 = 16$ h; $D_y = 0.6$, $\nu = 0$ and $N = 64$.*

The diffusion coefficient is increased from $D_y = 0$ to $D_y = 1.5$ and the spatial cross correlation S is estimated [Fig.4.29]. Values for the spatial cross correlation increase with the

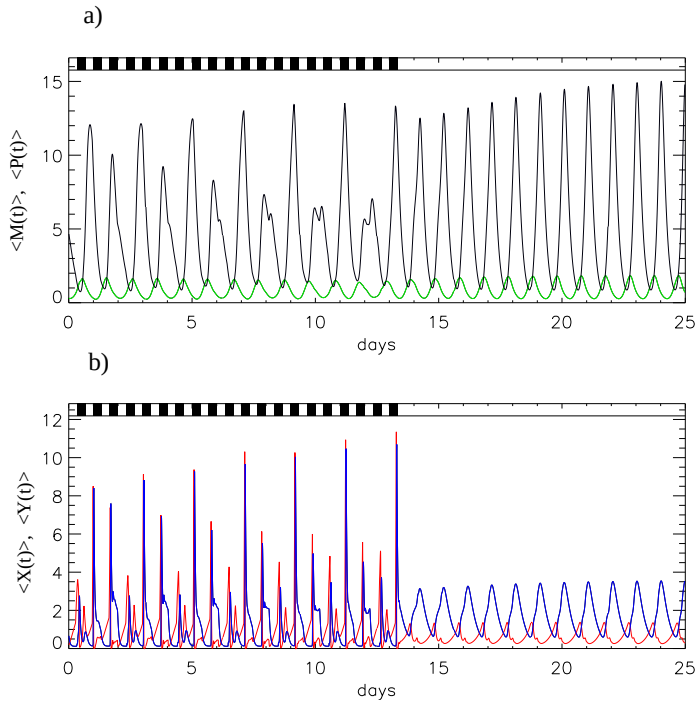

Figure 4.24: *Time series of the averaged variables of globally coupled elements ($C_y = 0.6$) with distributed periods ($\nu = 0.03$), due to the change in the environmental parameters for the period $T = 16$ h. After 20 day-night cycles the system is reset to constant day conditions. Time series for the variables, (a) $\langle M(t)\rangle$, green (-) and $\langle P(t)\rangle$, black (-) and (b) $\langle X(t)\rangle$, red (-), $\langle Y(t)\rangle$, blue (-), $N = 64$.*

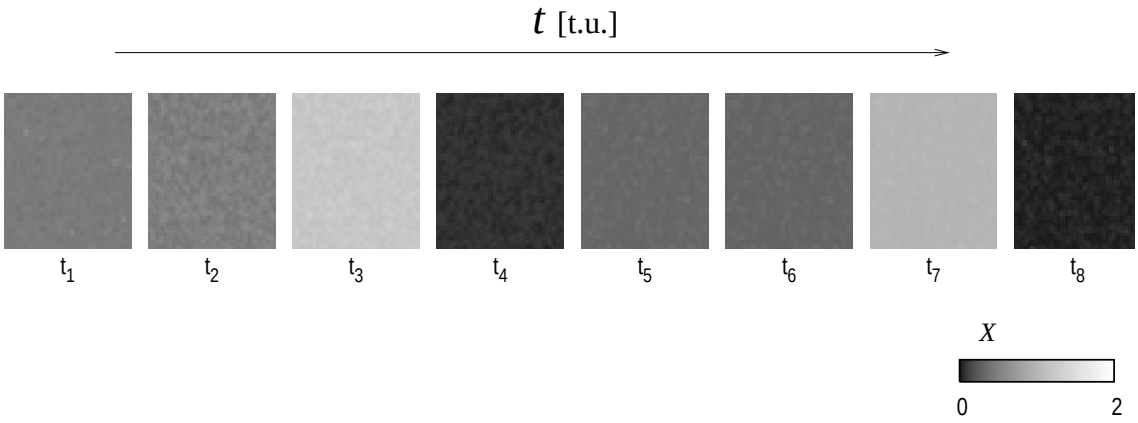

Figure 4.25: *Snapshots of the net of globally coupled elements with the coupling coefficient $C_y = 0.6$ for consecutive moments of time t, time units are hours ($\Delta t = t_{i+1} - t_i = 4h$). Oscillators are perturbed by external signals with the period of change $T = 16$ h, $\nu = 0.03$ and $N = 64$.*

increase of the strength of the local interactions among elements, and then slowly decline as the number of locally synchronised elements decreases due to the rise in the synchro-

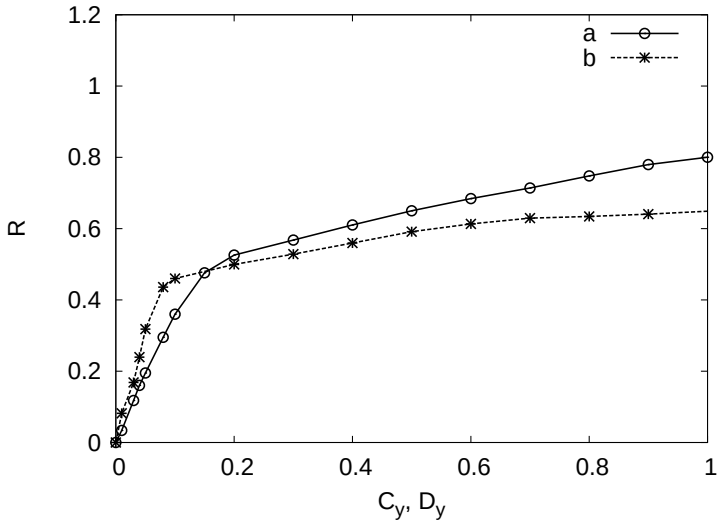

Figure 4.26: *Order parameter R of the net of coupled elements as a function of the coupling strengths, under the influence of parameter change for the period $T = 16$ h for: a) global coupling, C_y and b) local coupling, D_y, $\nu = 0.03$ and $N = 64$.*

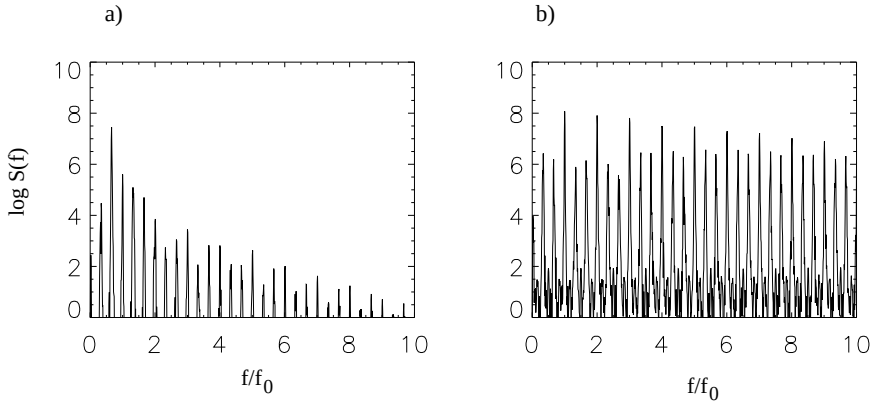

Figure 4.27: *Power spectral density $logS(f)$ obtained by the analysis of the time series for the averaged variables when the elements are globally coupled ($C_y = 0.6$), for the variables: a) $\langle M(t)\rangle$ of the genetic oscillator and b) $\langle X(t)\rangle$ of the metabolic oscillator; period of change in environmental signals is set to $T = 16$ h; f_0 corresponds to the period $T_0 = 16$ h. $\nu = 0.03$ and $N = 64$.*

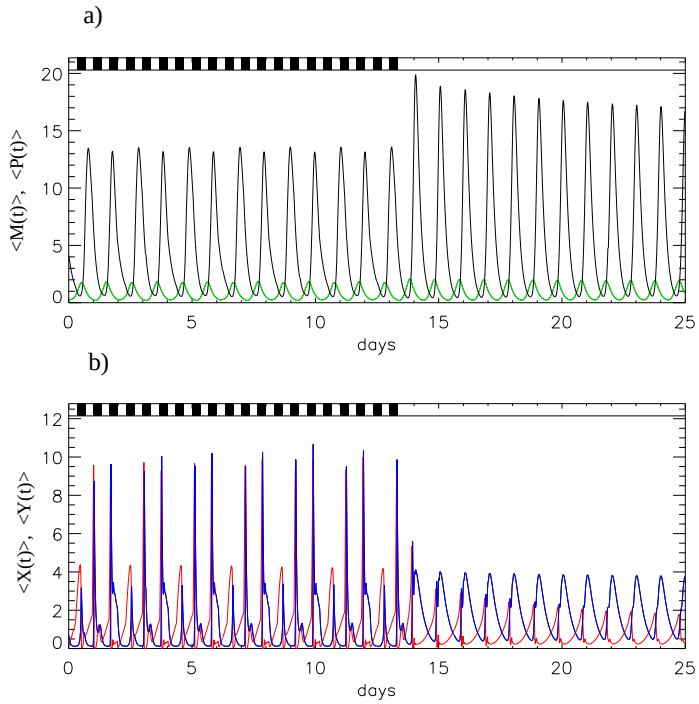

Figure 4.28: *Time series of the averaged variables for diffusively coupled elements ($D_y = 0.6$) with distributed periods ($\nu = 0.03$), due to the change in the environmental parameters for the period $T = 16$ h. After 20 cycles of parameter variation, the system is reset to constant day condition. Time series for the variables: a) $\langle M(t)\rangle$, green (-) and $\langle P(t)\rangle$, black (-) and b) $\langle X(t)\rangle$, red (-), $\langle Y(t)\rangle$, blue (-). $N = 64$.*

nisation of the whole net. For smaller values of the variability strength, the values of the spatial cross correlation are also lower. Fig.4.30 illustrates the existence of spatial patterns for the variability strength, $\nu = 0.03$. The values of the coupling strength $D_y = 0.3$ are sufficient to induce a rise in the local synchronisation or an increase in the spatial cross correlation, S. Spatial patterns arise because of pronounced phase differences in the net of elements. Differences exist not only because of the variability, as each element in the net oscillates with its own endogenous period, but also due to the coupling to the environmental signals with the period $T = 16$ h. Thus new variability in the net, caused both by the external entrainment and the period variability may induce the formation of spatial patterns, if diffusive coupling is present in the net. Time series of snapshots of the net, when a value of the diffusion coefficient is set to $D_y = 0.6$, are presented in Fig.4.31, where the time interval between two snapshots are set to 12 hours. After 48 hours patterns are repeating. Differences between the different types of coupling can be also observed due to the values of the order parameter as a function of the coupling coefficients R, as it is illustrated in Fig. 4.26. From these results, one can see the differences between diffusive and global coupling. Similar to the situation observed for the single element oscillator, the metabolic oscillator differs from the genetic oscillator due to the entrainment to a 16 hours period. According to the estimated periods, presented in Figs. 4.32 (a, b), the mean field of variables for the genetic oscillator oscillates with the dominating period, which is

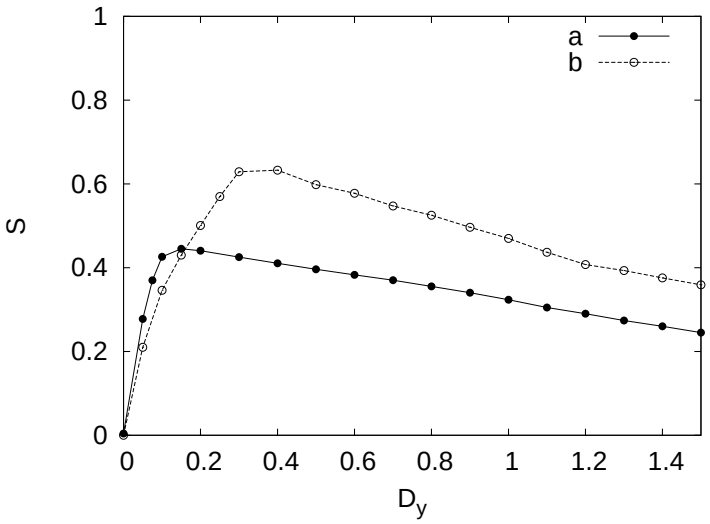

Figure 4.29: *Spatial cross correlation S as a function of the diffusion coefficient, for the net of diffusively coupled elements perturbed by a change of environmental signals with the period $T = 16$ h for variability strengths a) $\nu = 0.015$ and b) $\nu = 0.03$, $N = 64$.*

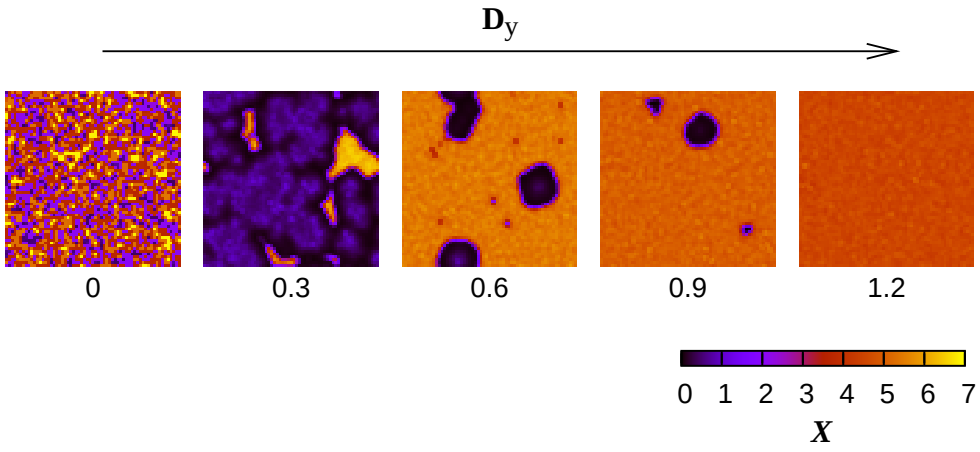

Figure 4.30: *Snapshots of the net of diffusively coupled elements for one arbitrary time moment ($t = 108$ h) for different values of diffusion coefficients $D_y = (0, 0.3, 0.6, 0.9, 1.2)$. Oscillators are perturbed by an external signals with the period of change $T = 16$ h, $\nu = 0.03$ and $N = 64$.*

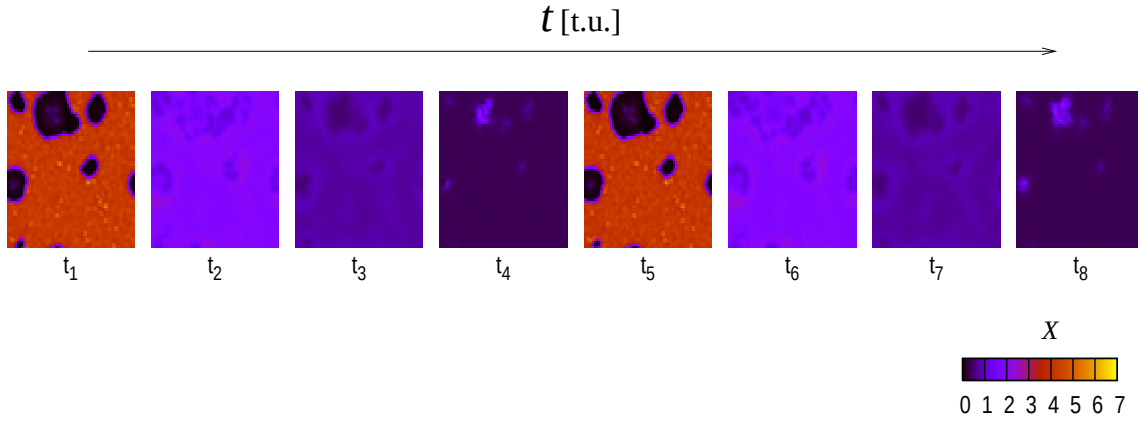

Figure 4.31: *Time series of snapshots of the net of diffusively coupled elements ($D_y = 0.6$) for consecutive moments of time ($\Delta t = t_{i+1} - t_i = 12h$). Oscillators are perturbed by an external signal with the period of change $T = 16$ h, $\nu = 0.03$ and $N = 64$.*

the period of free-running rhythm $T = 23.9$ h. The mean filed of the variables of the metabolic oscillators will follow the change in environmental signals, with dominating 16 hours period.

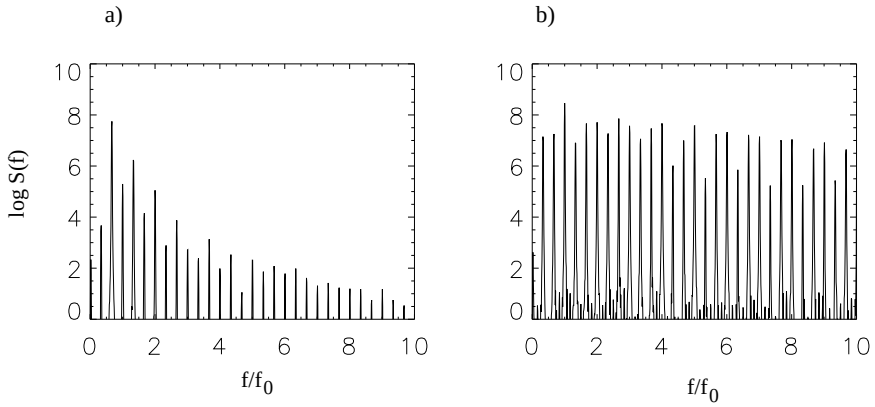

Figure 4.32: *Power spectral density $logS(f)$, obtained by the analysis of time series for the averaged variables of diffusively coupled elements ($D_y = 0.6$). Period is estimated for the variables a) $\langle M(t) \rangle$ of the genetic oscillator and b) $\langle X(t) \rangle$ of the metabolic oscillator; Period of change in environmental signals is set to $T = 16$ h; f_0 corresponds to the period $T_0 = 16h$, $\nu = 0.03$ and $N = 64$.*

4.6 Discussion

In this chapter, the further extensions of the model are discussed, introducing variability in the net of oscillating elements. The starting assumption is taken from experimentally observed facts that the output of the circadian rhythm generator is the result of a network of cellular circadian oscillators, which oscillate with slightly different periods due to each other. Two possible types of interactions among elements in the net are analysed. Numerical simulations show strong differences between global coupling and diffusive coupling in the net, for the case when the net is not entrained to external stimuli and each oscillator oscillates in free-running conditions. The order parameter, estimated for the global coupling, indicates that synchronisation in such a coupled net can be achieved if a certain threshold of coupling strengths is reached. A linear dependency of the critical coupling coefficient on the variability of the net can be observed. The more distributed the periods of the elements in the net are, the stronger the coupling which is needed in order to achieve complete synchronisation. It is shown that the increase of the coupling strength for global coupling leads to partially frequency locking of a group of oscillators, i.e. elements, with a perfect locking for high values of coupling coefficients. The period of such a synchronised net of elements is lower in comparison to the mean value of the period of the uncoupled net, though this change is not significant [Fig.4.4]. For the case of locally coupled elements, the process of diffusion between neighboring elements leads to the formation of spatial patterns due to the inhomogeneity in the net induced by the variability in the net. The size of the patterns depends on the diffusion coefficient i.e., how strong the local interactions among the elements are. The stronger the coupling is, the larger gets the area of synchronised elements. The global synchronisation also strongly depends on the number of elements that react and diffuse. Therefore, to study the phenomena of spatial pattern formation, one should determine the appropriate size of the net which provides the relevant number of oscillators capable of generating spatially coherent clusters of elements.
Whitout variability, a synchronisation of the net entrained to external day-night cycles obtained by the change of environmental signals with period $T = 24$ h or $T = 16$ h is achieved for both types of couplings. If the variability is present, differences between two types of coupling can be minimised when entrainment is imposed for 24 hours period. Then both types of net are fully entrained to the external period similar to the endogenous circadian period of both intracellular oscillators, when elements in the net are coupled. However, the differences are more pronounced if the system is entrained to a significantly different external period such as 16 hours. Mean fields of the metabolic and the genetic oscillators oscillate with different dominating periods, as it is the single element case and the case of net without variability. This is also observed for both types of coupling. In the net of diffusive coupled elements, with an increase in the diffusion coefficient, the elements start to locally interact and spatial order of elements can be observed. This is probably the result of a different response of the elements to 16 hours entrainment compared to 24 hours. The change of spatial order is not observed in the case of global coupling. Both types of coupling show an increase in order parameter with the increase in coupling coefficients.

Chapter 5

Influence of Noise on a Net of Coupled Circadian Oscillators

Introducing stochasticity in the models that are trying to mimic natural biological systems is often considered as an inevitable part of the modelling process for many biological systems. Thus in this chapter the possible influence of stochastic forces on the system of a coupled genetic and metabolic oscillator is studied in the case of the single element but also for a net of coupled oscillators. Besides entrainment to external signals on stochastic nets is discussed.

5.1 Biological Framework

Circadian systems as an example of natural systems are subject to stochastic processes such as fluctuations and various types of noise, [110, 111, 112]. The stochastic nature of circadian rhythmicity occurs at different levels of its organisation. Starting from a transcriptional regulation of clock genes, one can find the interactions between molecules as complex stochastic biochemical events. However they could also occur due to variation in the abundances of cell products set by noise in gene expression or by fluctuations of other cellular components [113, 114].
In the previous chapter the variability in a net of elements with respect to different periods of oscillation for each element in the net is investigated. Here the influence of noisy external signals are studied. For many biological systems, it is shown that the presence of noise has a beneficial and constructive role either on their dynamics, e.g. enhances the output of the system [25, 115], or on their organisation, inducing synchronisation [116] and spatiotemporal structures [27, 117]. However, the influence of noise on circadian clocks, as well as in other genetically regulated biological rhythms is not known. As the important feature of circadian systems is their ability to maintain constant, precise, periodic and coherent output, the proposed circadian models have to be structured and designed in the way that they are highly resistant and robust to noise.
The origin of noise in biochemical processes and thus its description could be quite different. If the fluctuations arise from a limited number of molecules interacting in such a process, then the biochemical system is described by birth-death stochastic processes and

is governed by master equation [2, 34, 118] . This type of noise is common in processes of gene expression and is usually described as intrinsic noise, [119]. Inherent stochasticity is investigated in details for different circadian model systems [120, 121, 122]. The other type of noise, called extrinsic noise, may originate from the differences in the output of genes and are usually referred to the activity of various regulatory proteins to polymerase and other parts of gene-regulatory circuits [123, 124]. Here, a simple biologically plausible case will be considered, where genetic noise originates from an additional, fluctuating source of mRNA.

5.2 Mathematical Description of Stochastic Dynamics for a Single Element

The two oscillator deterministic model equations (Eqs.3.15-3.18) are extended adding a stochastic driving force $\xi(t)$ into Eq.(3.15). Thus stochastic extension of the model reads:

$$\frac{dM(t)}{dt} = \frac{1}{1+(Y(t)/k_m)^l}\frac{p_m}{(1+P(t)^n)} - d_m M(t) + \xi(t) \tag{5.1}$$

$$\frac{dP(t)}{dt} = p_p M^s(t-\tau) - d_p P(t) \tag{5.2}$$

$$\frac{dX(t)}{dt} = b - Y(t)^2 X(t) + \frac{kP(t)X(t)}{f+X(t)} \tag{5.3}$$

$$\frac{dY(t)}{dt} = a - Y(t) + Y(t)^2 X(t) \tag{5.4}$$

where the additional term in the first equation represents a random process given as additive Gaussian white noise. The characteristics of such a random process is described by zero mean, noise strength σ and noise intensity σ^2:

$$\langle \xi \rangle = 0, \quad \langle \xi(t)\xi(t') \rangle = \sigma^2 \delta(t-t') \tag{5.5}$$

The parameters are set according the Tab. 3.1, and other parameters are set to $(k, d_p, b, f) =$

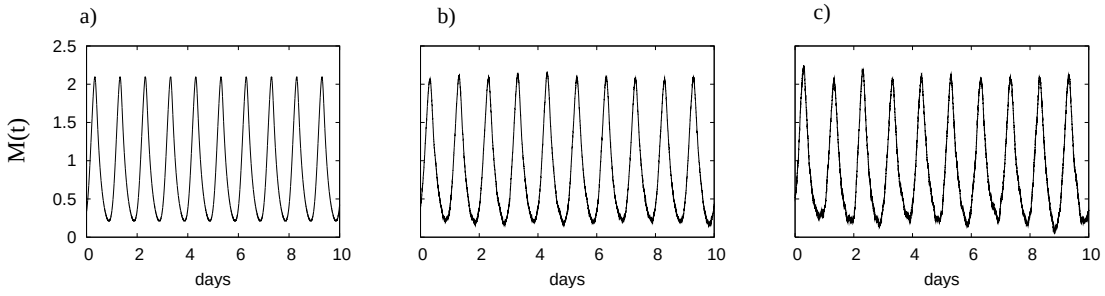

Figure 5.1: *Time series of the variable $M(t)$, for a single element for different values of noise intensities: a) $\sigma^2 = 0$, b) $\sigma^2 = 0.1$ and c) $\sigma^2 = 0.25$.*

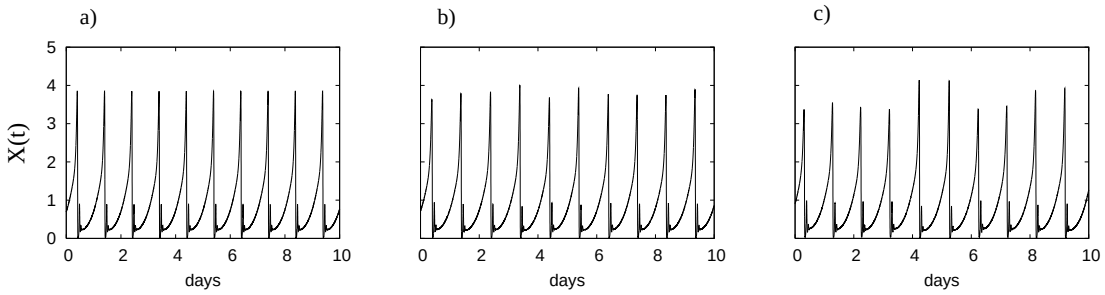

Figure 5.2: *Time series of the variable $X(t)$, for a single element for different values of noise intensities: a) $\sigma^2 = 0$, b) $\sigma^2 = 0.1$ and c) $\sigma^2 = 0.25$.*

$[1, 0.27, 0.2, 1]$. Stochastic behaviour of the coupled genetic and metabolic oscillator, using time series of variable M and X, is presented in Figs.5.1(a-c)) and Figs.5.2(a-c), respectively, for three cases. The first case represents a situation when noise is not applied to the system and others correspond to the application of noise for the two different noise intensities $\sigma^2 = 0.1$ and $\sigma^2 = 0.25$. From the figures one can see that the influence of noise on the abundance of mRNAs is expressed for the metabolic clock in the way that the amplitude of the variable of the metabolic oscillator is highly sensitive to a perturbation of the genetic oscillator, so the effect of noise results in an amplitude variation of the variable $X(t)$ over time. Small noise intensities are applied in order to avoid the appearance of negative values in the abundance of mRNAs. Using time series analysis, the periods of oscillations due to the different noise intensities are estimated for the variables, M and X. From Figs.5.3(a-c) and 5.4(a-c) one can see that dominating periods remain constant due to the variation of additive Gaussian noise for the range of noise intensities $0 \leq \sigma^2 \leq 0.25$.

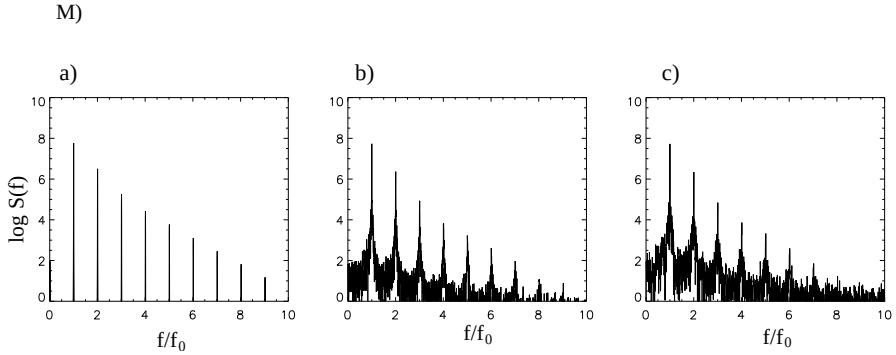

Figure 5.3: *Power spectral densities $logS(f)$ for the variable M for three different noise intensities: a) $\sigma^2 = 0$, b) $\sigma^2 = 0.1$ and c) $\sigma^2 = 0.25$. Estimated periods for all three noise intensities are the same, $T = 23.9$ h.*

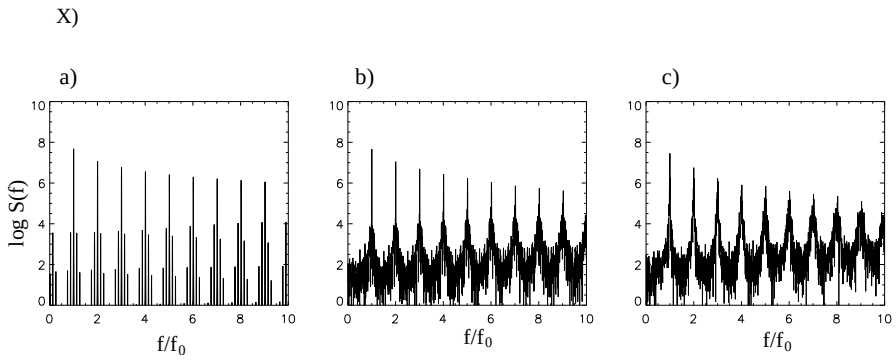

Figure 5.4: *Power spectral densities $logS(f)$ for the variable X for three different noise intensities: a) $\sigma^2 = 0$, b) $\sigma^2 = 0.1$ and c) $\sigma^2 = 0.25$. Estimated periods for all three noise intensities are the same, $T = 23.9$ h.*

5.3 Stochastic Dynamics of a Net

In this section, robustness of the population of oscillators due to the additive fluctuating source of mRNA is investigated. Each element of the net, as it was described in the previous section, is perturbed by additive Gaussian white noise. Besides, it is assumed that elements are spatially uncorrelated. The net of elements influenced by spatially uncorrelated Gaussian white noise, defined by zero mean and with stochastic term $\xi_{ij}(t)$, thus could be represented as the set of stochastic delay differential equations :

$$\frac{dM_{ij}(t)}{dt} = \frac{1}{1+(Y_{ij}(t)/k_m)^l}\frac{p_m}{1+P_{ij}^n(t)} - d_m M_{ij}(t) + \xi_{ij}(t) \tag{5.6}$$

$$\frac{dP_{ij}(t)}{dt} = p_p M_{ij}^s(t-\tau) - d_p P_{ij}(t) \tag{5.7}$$

$$\frac{dX_{ij}(t)}{dt} = b - Y_{ij}^2(t)X_{ij}(t) + k\frac{X_{ij}(t)P_{ij}(t)}{f + X(_{ij}t)} \tag{5.8}$$

$$\frac{dY_{ij}(t)}{dt} = a - Y_{ij}(t) + Y_{ij}^2(t)X_{ij}(t) + K_{ij}(t) \tag{5.9}$$

with the corresponding correlation function defined as:

$$\langle \xi_{ij} \rangle = 0, \quad \langle \xi_{ij}(t)\xi_{kl}(t') \rangle = \sigma^2 \delta_{ij,kl}\delta(t-t') \tag{5.10}$$

As it was the case with variability of the net, due to the different periods of elements, two types of coupling are also investigated in the case of additive noise, the global coupling and the diffusive coupling.

5.3.1 Global Coupling

The influence of global coupling between elements in the net is investigated with respect to the variable $Y(t)$, with the coupling function $K_{ij}(t)$ described in Chapter 4, (Eq. 4.7). It gives information how the metabolic variables sense the additional variation induced by

temporal fluctuations of the genetic system. The parameters are taken to be the same for each element in the net. The parameters which are varied are the coupling coefficient C_y and the noise intensity σ^2. Size of the net is set to $N = 64$.
Numerical simulations reveal that an increase in the coupling parameter induces an increase in the synchronisation among elements in the net proportional to the noise intensities applied in the system. Fig.5.5 shows the order parameter R as a function of the coupling parameter C_y. When the global coupling is not present in the system, a net is not synchronised and the order parameter $R = 0$. A small increase in the parameter C_y is sufficient to induce synchronisation in the net of elements, suggesting that the system of globally coupled elements composed of two oscillators is highly robust to noise.

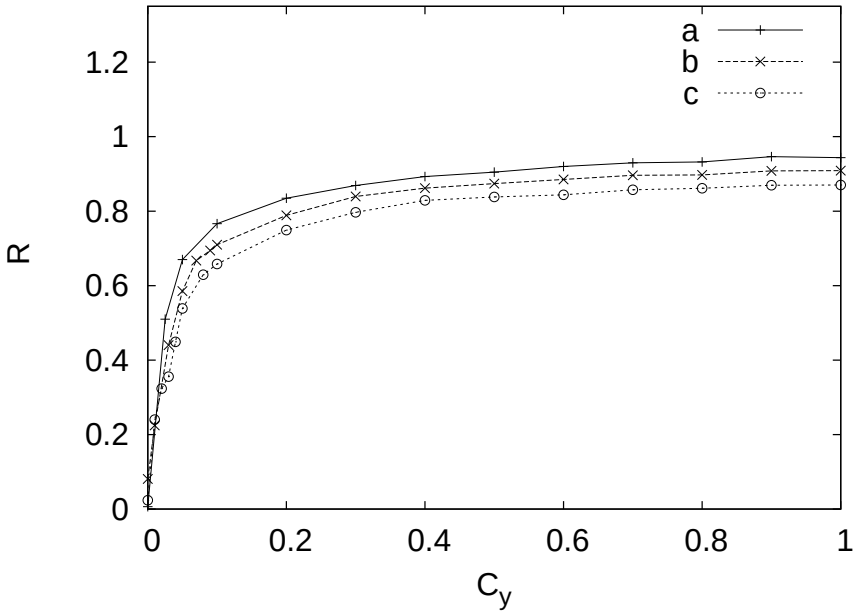

Figure 5.5: *Order parameter R as a function of coupling coefficient C_y for the net of globally coupled elements, for different noise intensities: a) $\sigma^2 = 0.05$, b) $\sigma^2 = 0.1$ and c) $\sigma^2 = 0.25$, $N = 64$.*

5.3.2 Diffusive Coupling

The influence of diffusive coupling in the net is studied by varying the diffusion coefficient and estimating the degree of synchronisation by calculating the order parameter R. Numerical simulations are conducted for four different noise intensities, represented in the Fig.5.6. The order parameter has the value $R = 0$ when diffusive coupling is not present in the system, $D_y = 0$. Similar to the case of global coupling, a small increase in the diffusion coefficient is enough to induce synchronisation among the elements in the net. For higher values of noise strength, the order parameter has smaller values, but the values of coupling coefficient, when a significant increase in the synchronisation is observed is almost the same. In Fig.5.7 mean field amplitudes are presented for the noise intensity $\sigma^2 = 0.25$.

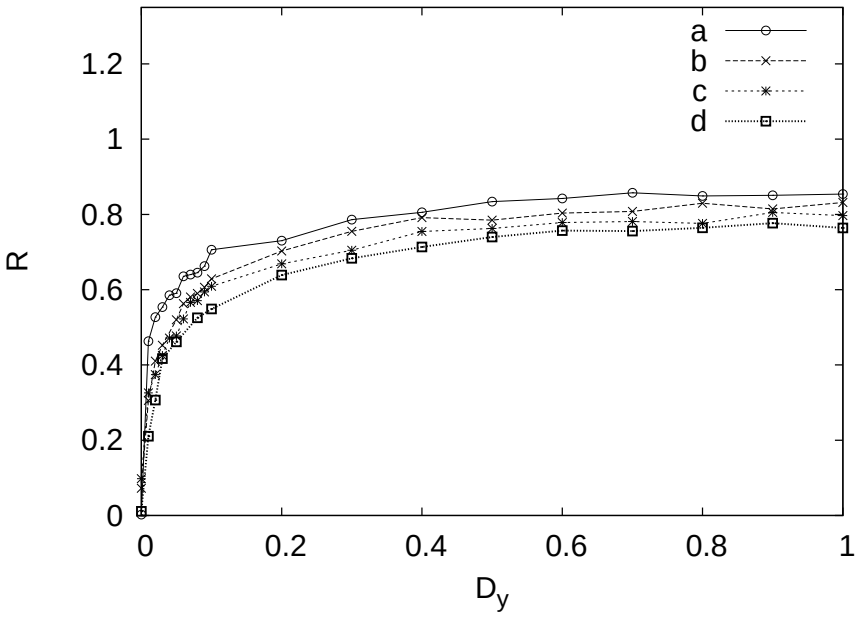

Figure 5.6: *Order parameter R as a function of the coupling coefficient for a net of diffusively coupled elements for different noise intensities: a) $\sigma^2 = 0.05$, b) $\sigma^2 = 0.1$ c) $\sigma^2 = 0.15$ and d) $\sigma^2 = 0.25$, $N = 64$.*

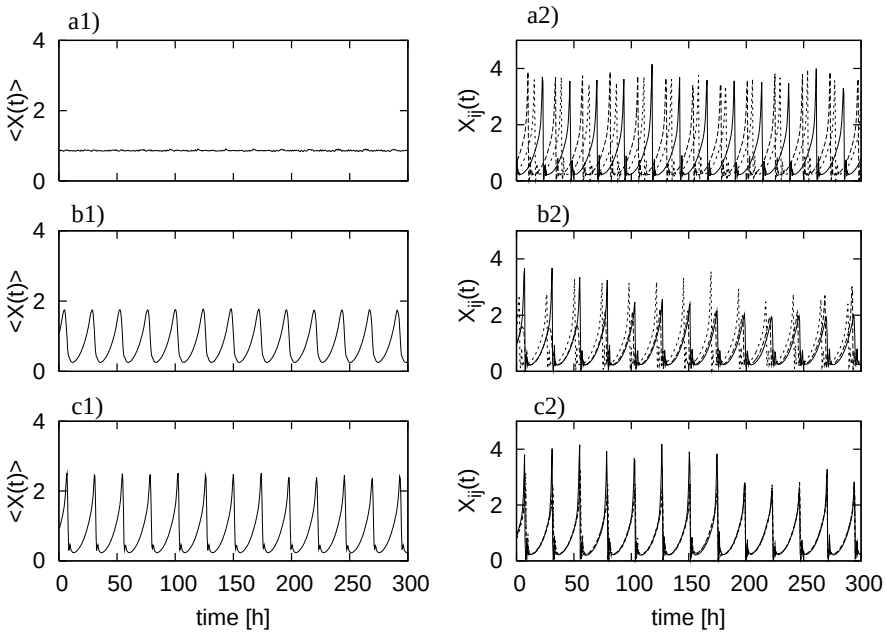

Figure 5.7: *Time series of the averaged variable of X, $\langle X(t)\rangle$ for different diffusion coefficients: a1) $D_y = 0$, b1) $D_y = 0.1$, c1) $D_y = 1$; Time series of variable $X_{ij}(t)$ for three randomly chosen elements and for different diffusion coefficients: (a2) $D_y = 0$, (b2) $D_y = 0.1$, (c2) $D_y = 1$, $\sigma^2 = 0.25$, $N = 64$.*

The mean filed amplitudes increase with an increase in the value of diffusion coefficient D_y. In the case of diffusively coupled stochastic net, one can see that the amplitudes of the variables X_{ij} of randomly chosen element do not decrease due to the diffusive coupling, as it is the case of diffusive coupling with variability, [Figs.4.9(a1-d2)]. The differences between elements in the net, induced by noise and the influence of diffusive coupling do not induce spatial patterns as it is the case when variability is considered. Estimated values of the spatial cross correlation are zero regardless which amount of diffusion is present in the net (data not shown). In order to find whether synchronisation of the elements depends on different sizes of the net, the order parameter is calculated. Fig.5.8 represents the values of the order parameter due to the variation of net size, with respect to three different diffusion coefficients. Higher values of the order parameter can be observed for a small size of the net.

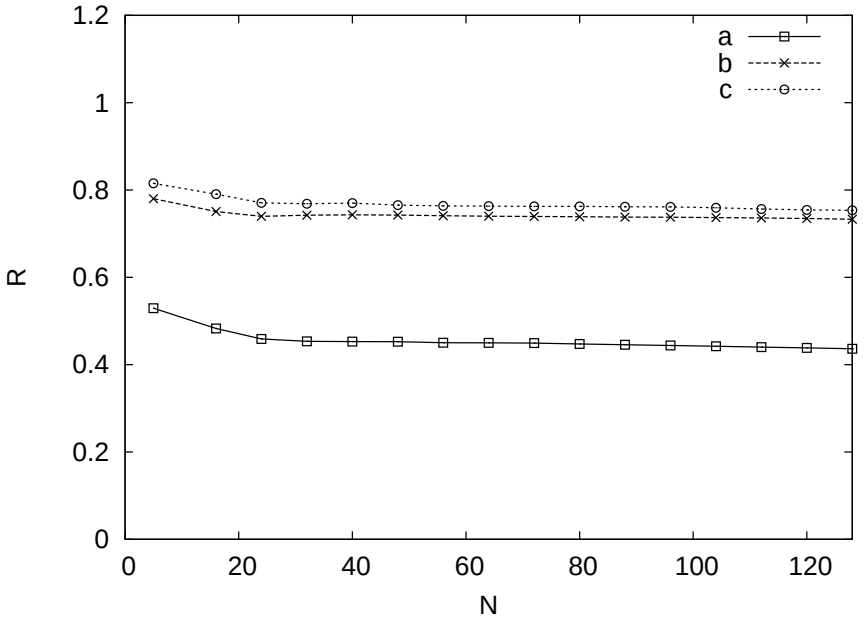

Figure 5.8: *Order parameter R as a function of net size N, for diffusively coupled elements: a) $D_y = 0.05$, b) $D_y = 0.5$ and c) $D_y = 1$, noise intensity is set to $\sigma^2 = 0.25$.*

5.4 Global Versus Local Coupling

The previous analysis indicates that the results for both types of coupling are almost the same, [Figs.5.5-5.6]. However, a small difference exists and to distinguish it, numerical simulation are performed for the same values of the coupling coefficients, while noise intensities are varied. A certain robustness of the system against an additive stochastic force for different types of coupling is presented in Fig.5.9. The graph compares the order parameters obtained by varying the noise intensity, from $\sigma^2 = 0$ to $\sigma^2 = 0.25$ for two fixed values of the coupling strength and for the two different types of coupling, diffusive coupling and global coupling. The level of synchronisation, as it is expected, depends on

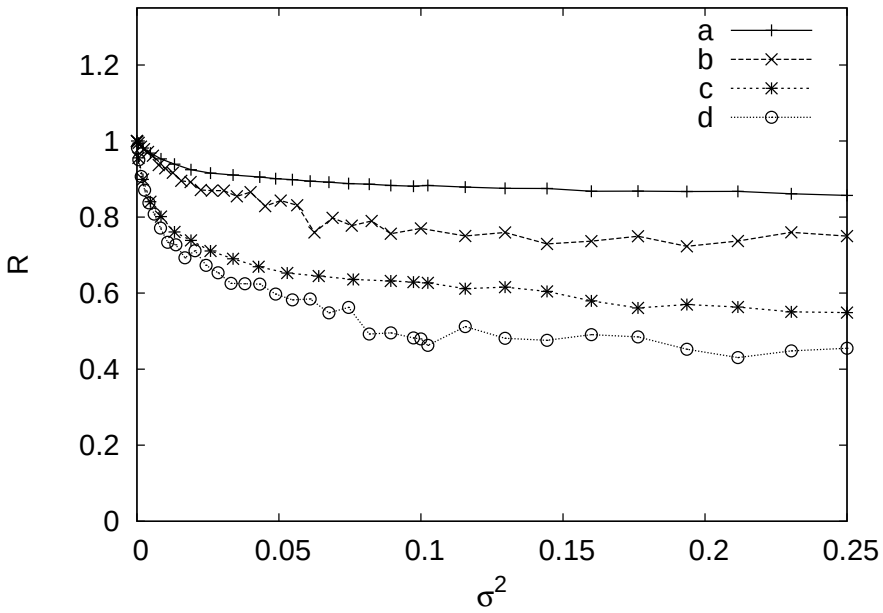

Figure 5.9: *Order parameter R as a function of noise intensity σ^2 for two different coupling strengths and two types of coupling a) $C_y = 0.5$, b) $D_y = 0.5$, c) $C_y = 0.05$ and d) $D_y = 0.05$, $N = 64$.*

the amount of coupling strength. Values of the order parameter decrease with an increase in the noise intensities, in the similar way for both types of coupling. Greater values of the order parameter R are calculated due to the global coupling for both values of coupling strength. Besides, some stronger decrease in the order parameter, due to the variation of noise intensities, can be observed in the case when diffusive coupling is present among the elements. For small values of noise intensities, the level of synchronisation is almost the same for the both coupling types. However for higher values of noise intensities, the differences between the two types of coupling are more pronounced.

5.5 Environmental Influence on the Stochastic Network

The type of entrainment with respect to different periods of change in environmental signals and thus relevant conditions for synchronisation due to the two types of interactions among elements in the net is also investigated in the case of elements under the influence of noise. Again, Gaussian white noise is applied, with a constant value of noise intensity $\sigma^2 = 0.25$. Other parameters are varied according to the already proposed model for the day night conditions which is in detail, described in Chapter 3. According to the results presented in the previous section [Fig.5.8], a net with $N = 48$ is sufficient for numerical simulations of diffusively coupled net. Numerical simulations of the entrained stochastic net are performed in a similar way as presented in the case when the entrainment of the

net is studied, with and without variability. For each element in the net, simultaneously, the parameters are changed every 12 hours representing a 24 hours entrainment, or every 8 hours representing a 16 hours entrainment.

Change of Environmental Signals with Period $T = 24$ h

Elements are influenced by two factors, Gaussian white noise and a change in the environmental signals with period $T = 24$ h. Time series of the mean field of all variables of the net are presented in Fig. 5.10 when the elements in the net are coupled by diffusion $D_y = 0.6$ and the noise intensity is set to $\sigma^2 = 0.25$. The estimation of periods is calculated

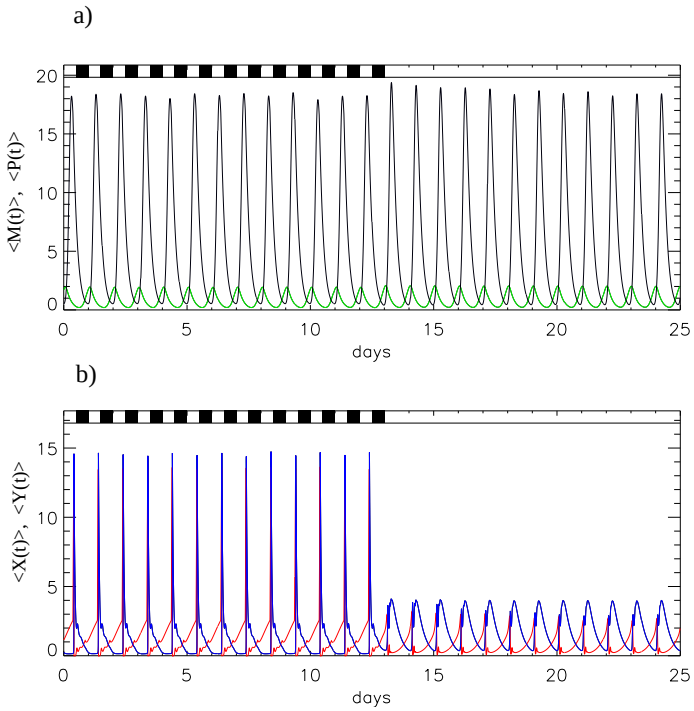

Figure 5.10: *Time series of the averaged variables for diffusively coupled elements ($D_y = 0.6$) due to the change in the environmental parameters for the period $T = 24$ h. After 13 day-night cycles, the system is reset to constant day condition. Time series for the variables, (a) $\langle M(t)\rangle$, green (-) and $\langle P(t)\rangle$, black (-) and (b) $\langle X(t)\rangle$, red (-), $\langle Y(t)\rangle$, blue (-), $\sigma^2 = 0.25$, $N = 48$.*

for day-night cycles. Figs.5.11(a,b) show that the variables of both oscillators, which are part of one element, are entrained by the period of the environmental change with period $T = 24$ h. The same results are obtained when global coupling among elements is included (data not shown). Synchronisation in the net, presented in Fig.5.12 is established due to entrainment and coupling among elements. An increase in the order parameter can be observed as the couplings between elements are getting stronger. Insignificant differences in the synchronisation measures between diffusive coupling and global coupling can be observed, similar as in the case for the net of elements influenced by variability [Fig.4.21].

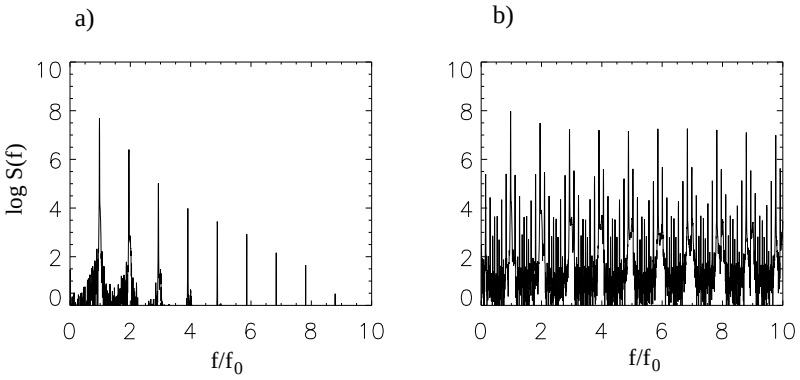

Figure 5.11: *Power spectral density $logS(f)$ obtained by the analysis of time series for the averaged variables when the elements are diffusively coupled ($D_y = 0.6$) with noise intensity $\sigma^2 = 0.25$; for the variables : a) $\langle M(t)\rangle$ of the genetic oscillator and b) $\langle X(t)\rangle$ of the metabolic oscillator; the period of change in environmental signals is $T = 24$ h; f_0 corresponds to period $T_0 = 24$ h, $N = 48$.*

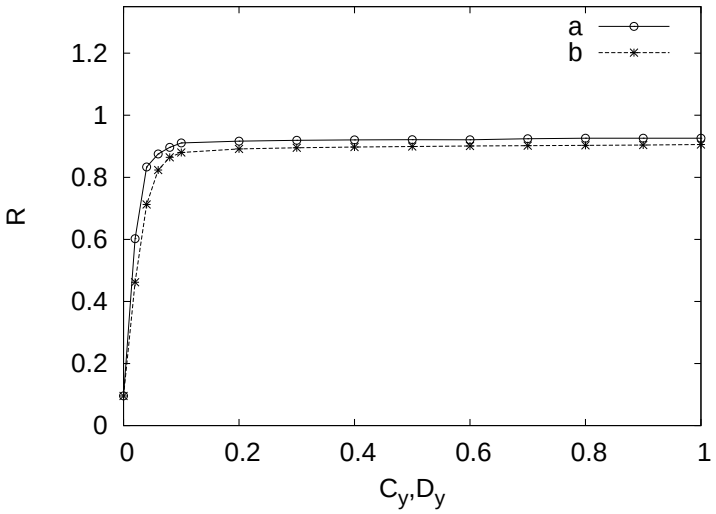

Figure 5.12: *Order parameter as a function of coupling coefficients C_y and D_y for the net of elements, influenced by a change in environmental signals with period $T = 24$ h for : (a) global coupling, C_y and (b) diffusive coupling, D_y, $\sigma^2 = 0.25$ and $N = 48$.*

Change of Environmental Signals with Period $T = 16$

When the system of noisy elements is entrained by an environmental change with a period of 16 hours, the same procedure, established for numerical simulations of 24 hours, is used, only the number of entrained cycles is increased to 20 cycles. The entrainment is illustrated in Fig.5.13. The frequencies of the averaged variables for the metabolic and the genetic oscillator are obtained by a time series analysis and are represented in Figs.5.14(a,b). The metabolic oscillator is partially entrained by the change in the parameters and it oscillates

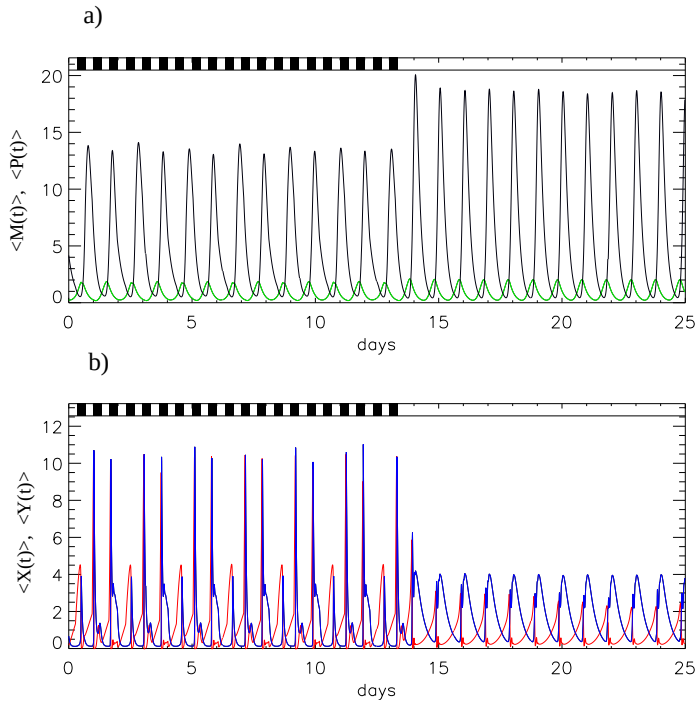

Figure 5.13: *Time series of the averaged variables for diffusively coupled elements ($D_y = 0.6$) due to the change in the environmental parameters for the period $T = 16$ h. After 20 day-night cycles, the system is reset to constant day condition. Time series for the variables, (a) $\langle M(t)\rangle$, green (-) and $\langle P(t)\rangle$, black (-) and (b) $\langle X(t)\rangle$, red (-), $\langle Y(t)\rangle$, blue (-), $\sigma^2 = 0.25$, $N = 48$.*

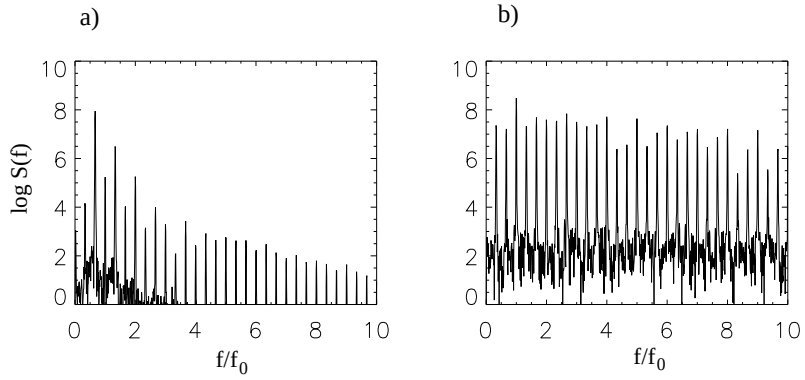

Figure 5.14: *Power spectral density $logS(f)$ obtained by the analysis of time series for the averaged variables when the elements are diffusively coupled ($D_y = 0.6$) with noise intensity, $\sigma^2 = 0.25$ for the variables: a) $\langle M(t)\rangle$ of the genetic oscillator and b) $\langle X(t)\rangle$ of the metabolic oscillator; period of change in environmental signals are set to $T = 16$ h; f_0 corresponds to period $T_0 = 16$ h, $N = 48$.*

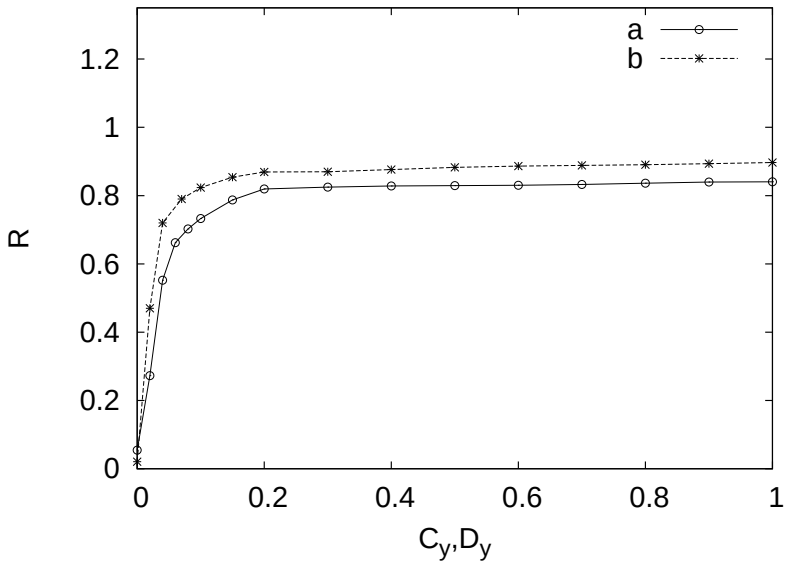

Figure 5.15: *Order parameter as a function of the coupling coefficients C_y and D_y for the net of elements, influenced by a change in environmental signals with the period $T = 16$ h for: (a) global coupling, C_y and (b) diffusive coupling, D_y, $\sigma^2 = 0.25$, $N = 48$.*

with the period $T = 16$ h. However, the genetic oscillator oscillates with the dominating period which is equal to the endogenous period $T = 23.9$ h.
Global and local interactions between elements influence the synchronisation of the entrained elements as in the case for a net with variability. The values for the order parameter are already high for very low values of coupling coefficient, suggesting that the entrainment is established. Fig. 5.15 represents an increase in the order parameter with an increase in the coupling strengths. Similar as it is the case for the 24 hours entrainment, increase in the coupling coefficients induces synchronisation in the net of elements entrained by a 16 hours period. Again, some differences due to different types of coupling can be observed as the better synchronisation is achieved for the global coupling.
Spatial patterns, observed when the net with variability is entrained by 16 hours signals, are also present in this case, as the values of the spatial cross correlation indicate. Figs.5.16 represents the spatial cross correlation as a function of the diffusion coefficient, which is increased from $D_y = 0$ to $D_y = 1$ for two different values of noise intensities, $\sigma^2 = 0.25$ and $\sigma^2 = 0.15$. Comparing the values of spatial cross correlation for the same diffusion coefficient, but for different noise intensities, one can see that the values of the spatial cross correlation are higher due to an increase in the noise intensity in the net. Fig. 5.17 illustrates an existence of spatial patterns for the values of coupling strength $D_y = 0.1$. Similar as in the case with variability, differences arise due to the influence of noise and due to the coupling to the environmental signals that change with period $T = 16$ h, which in the presence of the diffusive coupling induce the formation of spatial patterns. This is illustrated also by the time series of snapshots of the net, when the value of diffusion coefficient is set to $D_y = 0.1$ and the time interval between two snapshots is set to 12 hours [Fig.5.18].

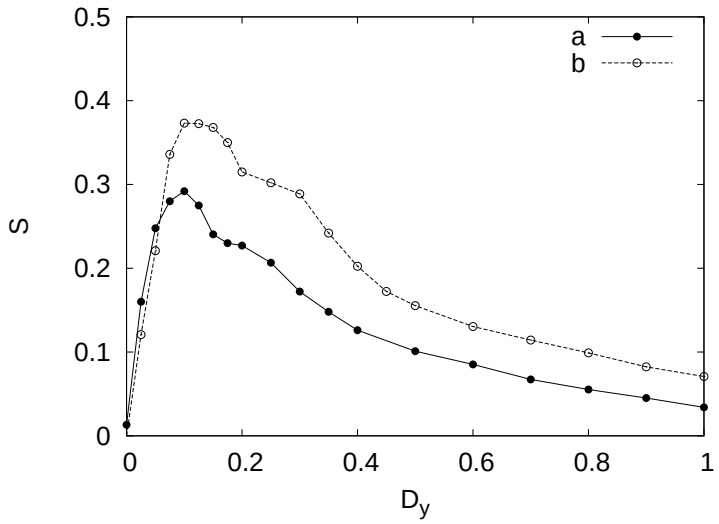

Figure 5.16: *Spatial cross correlation S as a function of diffusion coefficient, for the net of diffusively coupled elements perturbed by a change of environmental signals with the period $T = 16$ h for noise intensities: a) $\sigma^2 = 0.15$ and b) $\sigma^2 = 0.25$, $N = 48$.*

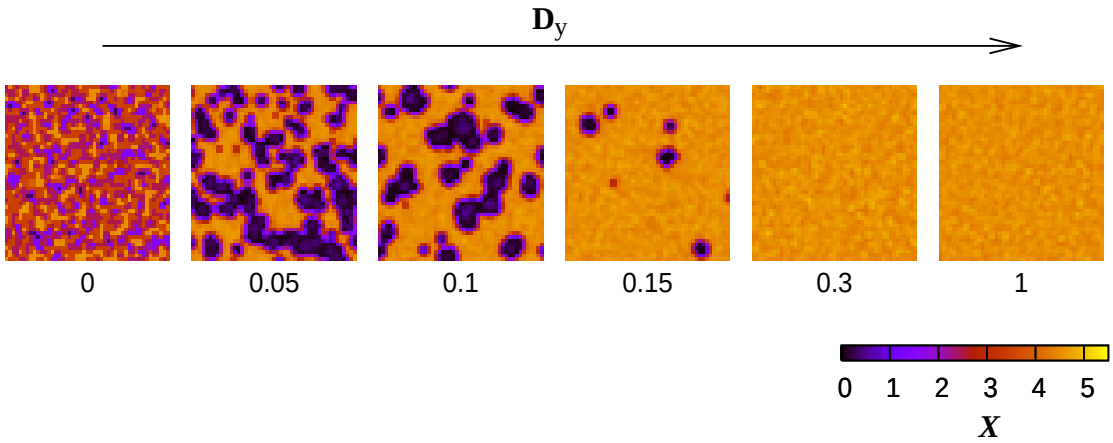

Figure 5.17: *Snapshots of the net of diffusively coupled elements for one arbitrary time moment ($t = 200$ h) for different values of diffusion coefficients $D_y = (0, 0.05, 0.1, 0.15, 0.3, 1.)$. Oscillators are perturbed by environmental signals with the period of change $T = 16$ h, $\sigma^2 = 0.25$ and $N = 48$.*

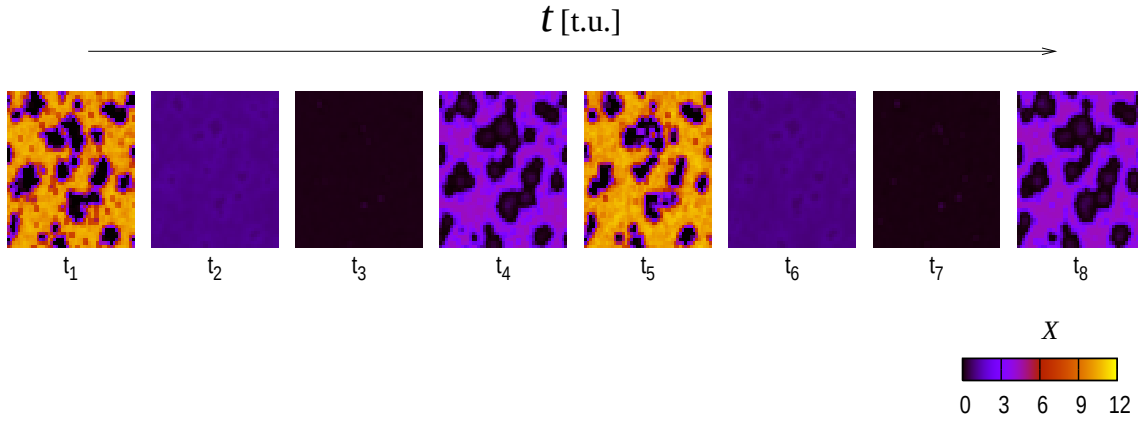

Figure 5.18: *Time series of snapshots of the net of diffusively coupled elements ($D_y = 0.1$) for consecutive moments of time ($\Delta t = t_{i+1} - t_i = 12h$). Oscillators are perturbed by environmental signals with the period of change $T = 16$ h, $\sigma^2 = 0.25$ and $N = 48$.*

5.6 Discussion

Influence of Noise

The influence of additive Gaussian white noise is analysed for a single element based on the two circadian oscillator model and also for a net of such elements. Noise induces fluctuations in the amplitude of the metabolic oscillator and the genetic oscillator. However, noise does not influence the dominating period of such a designed element. Synchronisation in a net where each element is under the influence of noise can be achieved very easily with an increase of the coupling parameter, regardless the type of couplings. A small difference can be observed for higher values of the noise intensity, where higher synchrony is achieved for global coupling. Noise in gene expression may fundamentally limit the accuracy of cellular processes, such as the circadian oscillator [122]. However, experimental evidence shows that circadian oscillations can persist for weeks with a stable oscillatory period, without extracellular entraining cues [102], which suggests that the circadian network is strongly resistant to biochemical noise. The conclusion that can be derived from an analysis of the model presented is that a system of multiple circadian oscillators where only the genetic oscillator is perturbed due to an external stochastic term can express a highly robust behaviour for a relatively small coupling.
In addition, the environmental perturbation, due to a different period of change of external perturbation also demonstrates the resistance against the influence of noise. For both types of coupling the net is synchronised to the external environmental signals. However, environmental perturbation with period $T = 16$ h induces again a different response for a genetic and a metabolic oscillator, as the variables of each oscillate with different dominating periods. Besides, formation of spatial patterns in the net of noisy elements influenced by an external entrainment is observed. They are a result of both influences in the presence of diffusive coupling, external environmetal perturbation and additive Gaussian white noise.

Variability Versus Noise

A comparison between two types of stochastic influence can be done in the case of the circadian rhythm generator. Variability in the net of elements reflects the static stochastic influence, where elements differ by their period of oscillation. Noise is expressed by the variation of the amplitudes of the clock oscillator variables in the net. A significant difference between global and diffusive couplings is observed in the net with variability, while a very small difference between couplings is expressed in the net with noisy elements. Further, a high synchronisation in a net of elements with variability and global coupling is achieved for higher values of the coupling coefficient, when a certain threshold is reached. However, the synchronisation for the net of noisy and globally coupled elements is achieved for small values of coupling coefficient. In a similar way synchronisation occurs for a net of noisy and diffusively coupled elements. On the other side in the net of diffusively coupled elements with variability, spatial patterns are induced. Spatial patterns strongly depend on the size of the net. The optimal size of the net should be established for which patterns are observed. In the case of the influence of noise on the net, the order parameter is almost constant with respect to a variation of the size of net. When the net of elements with variability is influenced by an external perturbation, which is changed with 24 hours period, the net achieves high synchrony regardless which type of coupling is applied. Estimated period of the average variable of synchronised net corresponds to the period of environmental perturbation. Almost identical results are obtained by the perturbation of the net influenced by noise. Results of numerical simulations in the case of entrainment with period of 16 hours are similar for both types of net, the net with variability and the net influenced by noise. Spatial patterns are observed in a net of diffusively coupled elements with variability, but also in a net of noisy and diffusively coupled elements. The only difference that can be noticed is the amount of diffusion at which spatial patterns starts to form. Besides, the external perturbation with the period of 16 hours in both types of net induces a different response for the genetic and the metabolic oscillator.

Chapter 6

Discussions and Perspectives

The aim of this thesis is to investigate an old hypothesis which suggests the existence of two coupled circadian oscillators [82]. It is questioned again due to the recent discoveries in the research in the field of chronobiology [52, 125]. Some experimental evidences open this question and bring the new ones regarding relevant proposed models for the circadian rhythm generator at all levels of its organisation. This thesis represents a new general model, which is based not on the detailed relations between molecular components of specific model organisms, but rather on already existing models for the transcription-translation oscillator. The extension of the model represents a simple coupling of this model with another biochemical oscillatory mechanism. It is stated that complexity of circadian clocks can arise not only because of a large number of regulatory mechanisms that interact within the clock or a large number of its components, but also due to rich dynamics observed when two different, but simple biochemical oscillators are coupled. Using computational tools, concepts from nonlinear dynamics and statistical physics, the dynamics of such a circadian rhythm generator is investigated. The model also incorporates the entrainability of such a two component system to external environmental signals. As a general picture of the higher level of organisation of such populations of circadian clocks, the synchronisation phenomena are also investigated with two different coupling mechanisms and two different fluctuating sources. One comes from the variability of individual oscillators due to the different period of oscillations, the other from an additive uncorrelated noise source of a mRNA. The entrainability is also investigated for a net of elements for all cases.

6.1 Single Circadian Oscillator Model

In particular, coupling of two different oscillatory mechanisms with a small difference in the periods is investigated. The coupling of two limit cycles reveals that the periods of the coupled system are changed due to an increase in the coupling strength between oscillators and due to an increase in the Michaelis Menten constant. Estimated periods for this case are in the endogenous regions. Synchronisation between such oscillators are possible for small values of the coupling strength. The greater the Michaelis Menten constants are, the higher degree of coupling is needed in order to reach a complete synchronisation. On the other side, the range of estimated periods due to the change in the coupling strengths are

smaller with an increase of the Michaelis Menten constants. The investigation of the circadian clock due to external signals such as temperature and light is focused on two aspects. First, the two component oscillator model is extended for the influence of environmental signals, introducing a change of two parameters simultaneously, the degradation rate of protein and the coupling parameter. Numerical simulations for the two different periods of entrainment, $T = 24$ h and $T = 16$ h, reveal relevant differences between a metabolic and a genetic oscillator. This is pronounced when the period of entrainment is significantly different from the circadian endogenous period. The variables of the metabolic oscillator oscillates with the period of environmental perturbation, while the variables of the genetic oscillator oscillates with the free running period of the system. Second, the sensitivity due to external parameters is investigated analysing the response of the system with respect to short perturbations at different phase points of the cycle, or by means of phase response curves.
The conclusion, that can be obtained from the phase response curves is that the mechanism of coupling between two different oscillators is sensitive to environmental influences. Large phase shifts or phase response curve of type 0, estimated by numerical simulations, represents an interesting result. It indicates how big is the influence of the activation of protein on the metabolic oscillator. In addition, the change of a type of phase response curves, when the coupling parameter is changed and the degradation rate is kept constant is observed. This change can be used to distinguish parameter influence. Possibly, the protein degradation rate indicates the influence of light signals on the system and the coupling parameter the influence of temperature. However, for a clear distinction whether the coupling parameter reflects only a temperature influence or light and temperature influences together, one should used a more detailed model. Reports of such a transition also exist for other models for circadian clocks, but only with respect to the duration of the applied perturbation and not due to the type of perturbation, for example in the model for circadian rhythms in *D. melangoster* [68] and in the model of net of oscillating elements [61].

6.2 Net of Circadian Oscillators

Couplings in the net of oscillating elements are investigated for the two oscillator model. The aim of a further extension of the model from a single element to a net of elements is to find out the relevant conditions for synchronisation in the case of variability and the case of stochastic influences. Some experimental and theoretical works reveal that some degree of synchrony among circadian clocks should be established in order to perform coherent physiological output. Thus the further investigation is focused on the possible network structures that could represent the circadian clock network. The usual approach is to use two common coupling schemes for the construction of such structures. Global coupling, defined through the mean field of the variable for the metabolic oscillator, shows that in the case where each element in the net oscillates with its own frequency, the synchronisation can be achieved for a strong coupling. Transition from an unsynchronised to a synchronised regime occurs for a certain value of coupling coefficient, which depends

linearly on the amount of variability present in the net. For the case of globally coupled noisy oscillators small coupling is enough to induce synchronisation in the net of elements irrespective of the noise strength.
On the other side, diffusive coupling in the net where elements oscillate with their own periods, induce spatial patterns. The size of the variability-induced patterns depends on the amount of diffusion present in the net. As the variability in the net increases, the target patterns start to change and the spatial cross corelation S decreases. In the case when noise is present in the system, amplitudes of the variables reach a high degree of synchronisation for small values of diffusion coefficients and spatial patterns are not observed. Differences between global and diffusive coupling can be observed in the case of a stochastic net. It is shown that a higher values of the order parameter R can be achieved for a global coupling. Only small differences between the two types of couplings can be observed for a small amount of noise in the system, while the differences increase with an increase of noise intensity.

Network and Environment

To complete the picture of the circadian coherent output with respect to different coupling mechanisms, the network model is also extended with respect to the influence of those environmental perturbations discussed for the single circadian model. It appears that the entrainment to the period $T = 24$ h, for the net with variability, can be established when elements are weakly coupled regardless of the type of coupling. The analysis of the order parameter shows high values for small values of the coupling coefficients. Further increase in the values of the coupling coefficients does not change the levels of synchronisation significantly. However, environmental perturbation with the period $T = 16$ h, again, as it is the case for the single element, influences the two oscillator system in the way that the variables of the metabolic oscillator oscillate with the period of perturbation. The same results are obtained for the coupled net with and without variability, also for both types of coupling. Couplings do not change the period of the entrained net, but in the case of diffusive coupling, spatial patterns are induced. They are the result of the influence of environmental perturbations and variability together. A net of noisy elements is partially resistant to noise influence, when the net is entrained by the environmental perturbation. A net of elements influenced by an additive uncorrelated noise, also shows complete entrainment to the period of 24 hours for both types of coupling. However results obtained for the influence of environmental perturbation with 16 hours period indicate again, that the dominating period of the variables of the metabolic oscillator is different from the dominating period of the variables of the genetic oscillator. Similar as it is the case in a net with variability, the diffusion process induces the formation of spatial patterns in the net of elements influenced by additive Gaussian white noise.

6.3 Perspectives

The model for a circadian rhythm generator with its extension to environmental influences and the net of elements presented in the thesis exhibits interesting results. From a biological perspective, this model can be used to develop a more realistic model, that will account for

complex regulation and a more detailed description of the circadian machinery for specific biological organisms. Due to its simplicity, from the aspects of synthetic biology, the model can be also used for the investigation of the coupling between two biochemical clocks.
However some questions regarding the model still remain. The response of the system to an external perturbation can also be tested, but for different duration times of the perturbation to investigate transitions between different types of phase response curves. Reverse perturbation, where the system is in a day condition and is perturbed by the signals of night conditions, can be also investigated.
Considering the variability of periods of oscillators and types of coupling, it is also useful to investigate other realizations of nets, for example, a random coupling or a mutual coupling between regions of oscillators proposed for a net of SCN cells [78] and to compare the results. Furthermore, as synchronisation in the net with respect to the variability of periods and global couplings is investigated for a fixed size of the net, it would be interesting to estimate the conditions for synchronisation when the number of oscillators in the population is changed. It is expected that the size of the net induces a sharper transition from the unsynchronised to the synchronised regime, with an increase in the number of oscillators.
The investigation of the influence of additive Gaussian white noise as a stochastic source for mRNA is justified as a general case, however the model can be extended by introducing multiplicative noise. In addition, other noise sources can be implemented in the model, such as fluctuations in the constant input in the production of one of the metabolic species.
Besides, the model can be modified for the case of a single element consisting of two coupled limit cycles when the value of the coupling parameter is small and when a complete synchronisation among the genetic and the metabolic oscillator is not yet established. Again, the net of such partially coupled elements has to be investigated with respect to the influence of variability, noise or external perturbations.

Zusammenfassung

In dieser Arbeit wird ein Modell für zirkadiane Rhythmen untersucht. Chronobiologische Experimente zeigen, dass gegenwärtige Modelle nicht alle Eigenschaften zirkadianer Uhren erklären. Als Modell für eine endogene zirkadiane Uhr wird ein Einzelelement bestehend aus zwei gekoppelten biochemischen Oszillatoren (ein genetischer und ein metabolischer Oszillator) und ein Netz bestehend aus vielen gekoppelten Einzelelementen eingeführt. Es wird der Einfluss von Variabilität und Rauschen auf die Netzdynamik studiert. Um Entrainment der Uhr mit externen Faktoren wie dem Tag-Nacht-Rhythmus zu untersuchen wird das Modell erweitert, indem Parameter für Tag und Nacht eingeführt werden, die mit einer 24-bzw. 16-Stunden Periode variiert werden.
Das Einzelelement zeigt für einen bestimmten Bereich der Kopplungsstärken zwischen den beiden biochemischen Oszillatoren eine Oszillationsperiode im endogenen Bereich zirkadianer Uhren (20-28 Stunden). Die Variablen des metabolischen Oszillators (Reaktanden X, Y) können auf die Dynamik der externen Faktoren synchronisieren, während die Variablen des genetischen Oszillators (mRNA, Protein) wenig beeinflusst werden, falls sich die externe Frequenz deutlich von der endogenen Frequenz unterscheidet. Dies zeigt, dass die Variablen des metabolischen Oszillators sensitiver auf externe Störungen reagieren. Dies wird auch durch die Analyse der Phasenresponseskurven bestätigt.
In ein Netz aus Einzelelementen, die global oder diffusiv gekoppelt werden, wird Variabilität eingebracht, indem jedes Einzelelement mit einer anderen Frequenz oszilliert. Bei globaler Kopplung kommt es zur Synchronisation der Oszillationen der Einzelelemente ab einer kritischen Kopplungsstärke, die linear von der Standardabweichung der Verteilung der endogenen Oszillationsfrequenzen abhängt. Diffusive Kopplung erzeugt nur lokale Synchronisation und es kommt zur räumlichen Musterbildung. Um diese Muster zu beobachten wird eine optimale Netzgrösse verwendet. Die räumliche Ausdehnung synchron schwingender Elemente, quantifiziert mittels räumlicher Kreuzkorrelationen, wächst proportional zu der diffusiven Kopplungsstärke an.
In einem Netz aus identischen Einzelelementen können alle Variablen im Falle periodischer externer Einflüsse synchronisiert werden, falls die externe und die endogene Periode nahe beieinander liegen. Wenn beide deutlich verschieden sind, werden nur die Variablen des metabolischen nicht aber die des genetischen Oszillators synchronisiert. In einem Netz mit variablen Oszillationsperioden der Einzelelemente kommt es zum Entrainment aller Variablen (sowohl bei globaler als auch diffusiver Kopplung), wenn die externe Periode 24 Stunden beträgt. Für einen 16-Stunden Zyklus werden hingegen wieder nur die Variablen des metabolischen nicht aber die des genetischen Oszillators synchronisiert, wobei die Ergebnisse von der Art der Kopplung abhängen. Bei diffusiver Kopplung kommt es zur räumlichen Musterbildung, nicht aber bei globaler Kopplung.

Schliesslich wird der Einfluss von Rauschen untersucht, indem zusätzlich mRNA Fluktuationen eingebracht werden. Bei einem Einzelelement beeinflusst Rauschen die Ozsillationsperiode nicht sondern nur die Amplitude der metabolischen Variablen. Der Effekt von Rauschen auf Synchronisation und Entrainment im Netz hängt von der Kopplungsart ab. Netze mit globaler Kopplung synchronisieren ein wenig besser. Die Unterschiede zwischen den Kopplungsarten werden deutlicher für 16-Stunden Zyklen. Hier kommt es zur Musterbildung für diffusiv gekoppelte Elemente. Diese wird durch den Einfluss sowohl von Rauschen als auch der externen Störungen erzeugt.

Bibliography

[1] A. Goldbeter. *Biochemical Oscillations and Cellular Rhythms. The Molecular Bases of Periodic and Chaotic Behavior*. Cambridge Univ. Press, Cambridge, UK, 1996.

[2] G. Nicolis and I. Prigogine. *Self Organization in Nonequilibrium Systems. From Dissipative Structures to Order through Fluctuations*. Wiley, New York, 1977.

[3] A. Goldbeter. Computational approaches to cellular rhythms. *Nature*, 420:238–245, 2002.

[4] L. H. Hartwell, J. J. Hopfield, S. Leibler, and A. W. Murray. From molecular to modular cell biology. *Nature*, 402:47–52, 1999.

[5] H. Kitano. Computational systems biology. *Nature*, 420:206–210, 2002.

[6] H. Kitano. Systems biology: a brief overview. *Science*, 295:1662–1664, 2002.

[7] M. B. Elowitz and S. Leibler. A synthetic oscillatory network of transcriptional regulators. *Nature*, 403:335–338, 2000.

[8] E. Fung, W. W. Wong, J. K. Suen, T. Bulter, S. G. Lee, and J. C. Liao. A synthetic gene-metabolic oscillator. *Nature*, 435:118–122, 2005.

[9] A. Becskei and L. Serrano. Engineering stability in gene networks by autoregulation. *Nature*, 405:590–593, 2000.

[10] P.C. Fall, E. S. Marland, J.M. Wagner, and J.J. Tyson. *Computational Cell Biology*. Springer, New York, 2002.

[11] J. M. Bower and H. Bolouri. *Computational Modeling of Genetic and Biochemical Networks*. Computational Molecular Biology. MIT Press, Cambridge, USA, 2001.

[12] J. J. Tyson, K. Chen, and B. Novak. Network dynamics and cell physiology. *Nat. Rev. Mol. Cell. Biol.*, 2:908–916, 2001.

[13] P. Smolen, D. A. Baxter, and J. H. Byrne. Modeling transcriptional control in gene networks–methods, recent results, and future directions. *Bull. Math. Biol.*, 62:247–292, 2000.

[14] J. Stelling and E. D. Gilles. Mathematical modeling of complex regulatory networks. *IEEE Trans. Nanobioscience*, 3:172–179, 2004.

[15] J.K. Hale. *Theory of Functional Differential Equations*. Vol.3. Springer-Verlag, Berlin, 1977. Applied Mathematical Science.

[16] L.E. El'sgol'ts and S.B. Norkin. *Introduction to the Theory and Application of Differential Equations with Deviating Arguments*. Vol.105. Academic Press, New York, 1973.

[17] H. Irisawa, H. F. Brown, and W. Giles. Cardiac pacemaking in the sinoatrial node. *Physiol.Rev.*, 73:197–227, 1993.

[18] S. Schuster, M. Marhl, and T. Höfer. Modelling of simple and complex calcium oscillations. from single-cell responses to intercellular signalling. *Eur.Jour.Biochem.*, 269:1333–1355, 2002.

[19] E. D. Herzog, J. S. Takahashi, and G. D. Block. Clock controls circadian period in isolated suprachiasmatic nucleus neurons. *Nat.Neurosci.*, 1:708–713, 1998.

[20] C. Liu, D. R. Weaver, S. H. Strogatz, and S. M. Reppert. Cellular construction of a circadian clock: period determination in the suprachiasmatic nuclei. *Cell*, 91:855–860, 1997.

[21] A. Pikovsky, M. Rosenblum, and J. Kurths. *Synchronization : A Universal Concept in Nonlinear Sciences*. Cambridge University Press, Cambridge, 2001.

[22] J. García-Ojalvo, M. B. Elowitz, and S. H. Strogatz. Modeling a synthetic multicellular clock: repressilators coupled by quorum sensing. *Proc. Natl. Acad. Sci. U S A*, 101:10955–10960, 2004.

[23] H. Busch and F. Kaiser. Influence of spatiotemporally correlated noise on structure formation in excitable media. *Phys. Rev. E.*, 67:041105, 2003.

[24] H. Busch. *Pattern Formation and Synchronization in Excitable Systems under the Influence of Spatiotemporal Colored Noise*. PhD thesis, Technische Universität Darmstadt, Darmstadt, Germany, 2004.

[25] L. Gammaitoni, P. Hanggi, P. Jung, and F. Marchesoni. Stochastic resonance. *Rev. Mod. Phys.*, 70:225–287, 1998.

[26] A. Pikovsky and J. Kurths. Coherence resonance in a noise-driven excitable system. *Phys. Rev. Lett.*, 78:775, 1997.

[27] J. García-Ojalvo and J. M. Sancho. *Noise in Spatially Extended Systems*. Institute for nonlinear science. Springer, New York, London, 1999.

[28] E. Glatt, M. Gassel, and F. Kaiser. Variability-induced transition in a net of neural elements: From oscillatory to excitable behavior. *Phys. Rev. E.*, 73:066230, 2006.

[29] M.-H. Hütt, H. Busch, and F. Kaiser. The effect of biological variability on spatiotemporal patterns-model simulations for network of biochemical oscillators. *Nova Acta Leopoldina*, 332:381–404, 2003.

[30] E. Glatt, M. Gassel, and F. Kaiser. Variability-sustained pattern formation in subexcitable media. *Phys. Rev. E.*, 75:026206, 2007.

[31] M. Gassel, E. Glatt, and F. Kaiser. Doubly diversity-induced resonance. *Phys. Rev. E.*, 76:016203, 2007.

[32] M. Gassel, E. Glatt, and F. Kaiser. Noise-induced synchronization in heterogeneous nets of neural elements. *Europhys. Lett.*, 81:40004, 2008.

[33] W. Press, S. Teukolsky, W. Vetterling, and B. Flannery. *Numerical Recipes in C.* Cambridge University Press, Cambridge, UK, 2nd edition, 1992.

[34] N.G. van Kampen. *Stochastic Processes in Physics and Chemistry.* Elsevier Science Pub., Amsterdam, 1992.

[35] M. W. Young and S. A. Kay. Time zones: a comparative genetics of circadian clocks. *Nat. Rev.Genet.*, 2:702–715, 2001.

[36] M. Rosbash. Molecular control of circadian rhythms. *Curr. Opin. Genet. Dev.*, 5:662–668, 1995.

[37] T. Roenneberg and M. Merrow. Circadian clocks - from genes to complex behaviour. *Reprod. Nutr. Dev.*, 39:277–294, 1999.

[38] L. Rensing, S. Mohsenzadeh, P. Ruoff, and U. Meyer. Temperature compensation of the circadian period length: a special case among general homeostatic mechanisms of gene expression? *Chronobiol. Int.*, 14:481–498, 1997.

[39] P. Ruoff, L. Rensing, R. Kommedal, and S. Mohsenzadeh. Modeling temperature compensation in chemical and biological oscillators. *Chronobiol. Int.*, 14:499–510, 1997.

[40] T. Roenneberg and M. Merrow. The network of time: understanding the molecular circadian system. *Current Bio.*, 13:198, 2003.

[41] J. Aschoff. Exogenous and endogeous components in circadian rhythm. *Cold Spring Harbour Symp. Quant. Biol.*, 25:11–28, 1960.

[42] R.J. Knopka and S Benzer. Clock mutants of *Drosophila melangoster. Proc. Natl. Acad. Sci. USA*, 68:2112–2116, 1971.

[43] J.C. Dunlop. Molecular basis for circadian clocks. *Cell*, 96:271–290, 1999.

[44] C.R. McClung. Circadian rhythms in plants. *Ann. Rev. Plant. Physiol. Plant Mol. Biol.*, 52:139–162, 2001.

[45] M. Rosbash, R. Allada, M. Dembinska, W. Q. Guo, M. Le, S. Marrus, Z. Qian, J. Rutila, J. Yaglom, and H. Zeng. A *Drosophila* circadian clock. *Cold Spring Harb. Symp. Quant. Biol.*, 61, 1996.

[46] T. Roenneberg and M. Merrow. The circadian cycle: is the whole greater that the sum of its parts? *TRENDS in Genetics*, 17:4, 2001.

[47] C. Lee, J. P. Etchegaray, F. R. Cagampang, A. S. Loudon, and S. M. Reppert. Post-translational mechanisms regulate the mammalian circadian clock. *Cell*, 107:855–867, 2001.

[48] E. Harms, S. Kivimae, M. W. Young, and L. Saez. Posttranscriptional and post-translational regulation of clock genes. *J. Biol. Rhythms*, 19:361–373, 2004.

[49] H. Oster, A. Yasui, G. T. van der Horst, and U. Albrecht. Disruption of mCry2 restores circadian rhythmicity in mPer2 mutant mice. *Genes. Dev.*, 16:2633–2638, 2002.

[50] J. C. Dunlap. Kinases and circadian clocks: per goes it alone. *Dev. Cell*, 6:160–161, 2004.

[51] J. Tomita, M. Nakajima, T. Kondo, and H. Iwasaki. No transcription-translation feedback in circadian rhythm of KaiC phosphorylation. *Science*, 307:251–254, 2005.

[52] M. Nakajima, K. Imai, H. Ito, T. Nishiwaki, Y. Murayama, H. Iwasaki, T. Oyama, and T. Kondo. Reconstitution of circadian oscillation of cyanobacterial kaic phosphorylation in vitro. *Science*, 308:414–415, 2005.

[53] H. Zeng, Z. Qian, M. P. Myers, and M. Rosbash. A light-entrainment mechanism for the *Drosophila* circadian clock. *Nature*, 380:129–135, 1996.

[54] C. H. Johnson and J. W. Hastings. Circadian phototransduction: phase resetting and frequency of the circadian clock of gonyaulax cells in red light. *J. Biol. Rhythms*, 4:417–437, 1989.

[55] J. Aschoff. *Circadian Clocks*. North Holland, Amsterdam, 1965.

[56] T. Hiroshige and K. Honma. *Circadian Clocks from Cell to Human : 4th Symposium on Biological Rhythm*. Hokkaido University Press, Sapporo Japan, 1992.

[57] J. W. Hastings. Biochemical aspects of rhythms: phase shifting by chemicals. *Cold Spring Harb. Symp. Quant. Biol.*, 25:131–143, 1960.

[58] R. Wever. Virtual synchronization towards the limits of the range of entrainment. *J. Theor. Biol.*, 36:119–132, 1972.

[59] R.E. Kronauer. *A quantitative model for the effects of light on the amplitude and phase of the deep circadian pacemaker*. Sleep'90, Pontenagel Press, Bochum, 1990.

[60] M.E. Jewett and R.E. Kronauer. Refinement of linit cycle oscillator model of the effects of light on the human circadian pacemaker. *J. Theor. Biol.*, 192:455–465, 1998.

[61] P. Achermann and H. Kunz. Modeling circadian rhythm generation in the suprachiasmatic nucleus with locally coupled self-sustained oscillators: phase shifts and phase response curves. *J. Biol. Rhythms*, 14:460–468, 1999.

[62] H. Kunz and P. Achermann. Simulation of circadian rhythm generation in the suprachiasmatic nucleus with locally coupled self-sustained oscillators. *J. Theor. Biol*, 224:63–78, 2003.

[63] M. Amdaoud, M. Vallade, C. Weiss-Schaber, and I. Mihalcescu. Cyanobacterial clock, a stable phase oscillator with negligible intercellular coupling. *Proc.Natl.Acad.Sci.U S A*, 104:7051–7056, 2007.

[64] F. Neuf and J. Rougemont. Frequency fluctuation in circadian oscillators. *Molecular Systems Biology*, 3:98:1–7, 2007.

[65] D.K. Welsh, S.H. Yoo, A.C. Liu, and J.S. Takahashi. Bioluminescence imaging of individual fibroblasts reveals persistent, independently phased circadian rhythms of clock gene. *Current Bio.*, 14:2289–2295, 2004.

[66] B.C. Goodwin. Oscilllatory behavior in enzymatic control processes. *Adv. Enzym. Regul.*, 3:425–438, 1965.

[67] A. Goldbeter. A model for circadian oscillations in the *Drosophila* period protein (PER). *Proc. R. Soc. Lond.*, B261:319–324, 1995.

[68] A. Goldbeter and J.C. Leloup. A model for circadian rhythms in *Drosophila* incorporating the formation of complex between the PER and TIM proteins. *J. Biol. Rhythms.*, 13:70–87, 1998.

[69] D. Gonze, J. C. Leloup, and A. Goldbeter. Theoretical models for circadian rhythms in *Neurospora* and *Drosophila*. *C. R. Acad. Sci. III*, 323:57–67, 2000.

[70] D. Gonze, J. Halloy, J. C. Leloup, and A. Goldbeter. Stochastic models for circadian rhythms: effect of molecular noise on periodic and chaotic behaviour. *C. R. Biol.*, 326:189–203, 2003.

[71] J.J. Tyson, C.I.Hong, C.D. Thron, and B.A. Novak. A simple model of circadian rhythms based on dimerization and proteolysis of PER and TIM. *Biophys. J.*, 77:2411–2417, 1999.

[72] P. Smolen, Baxter D.A., and J.H. Byrne. Modeling circadian oscillations with interlocking positive and negative feedback loop. *J. Neurosci.*, 21:6644–6656, 2001.

[73] P. Smolen, Baxter D.A., and J.H. Byrne. A reduced model clarifies the role of feedback loops and time delays in the *Drosophila* circadian oscillator. *Biophys. Jour.*, 83:2349–2359, 2002.

[74] T. Scheper, D. Klinkenberg, C. Pennartz, and J. van Pelt.R. A mathematical model for the intracellular circadian rhythm generator. *J. Neurosci.*, 19:40–47, 1999.

[75] M.A. Lema, D.A. Golombek, and J. Echave. Delay model of the circadian pacemaker. *J. Theor. Biol.*, 204:565–573, 2000.

[76] P. Ruoff, S. Mohsenzadeh, and L. Rensing. Circadian rhythms and protein turnover: the effect of temperature on the period lengths of clock mutants simulated by the goodwin oscillator. *Naturwissenschaften*, 83:514–517, 1996.

[77] H. R. Ueda, K. Hirose, and M. Iino. Intercellular coupling mechanism for synchronized and noise-resistant circadian oscillators. *J. Theor. Biol.*, 216:501–512, 2002.

[78] S. Bernard, D. Gonze, B. Cajavec, H. Herzel, and A. Kramer. Synchronization-induced rhythmicity of circadian oscillators in the suprachiasmatic nucleus. *PLoS Comput. Biol.*, 3:68, 2007.

[79] S. Becker-Weimann, J. Wolf, A. Kramer, and H. Herzel. A model of the mammalian circadian oscillator including the REV-ERBalpha module. *Genome. Inform.*, 15:3–12, 2004.

[80] D. Gonze, S. Bernard, C. Waltermann, A. Kramer, and H. Herzel. Spontaneous synchronization of coupled circadian oscillators. *Biophys.J.*, 89:120–129, 2005.

[81] B. Blasius, R. Neff, R. Beck, and U. Lüttge. Oscillatory model of crassulacean acid metabolism with dynamic hysteresis switch. *Roy. Soc. Lond. B. Bio.*, 266:93–101, 1999.

[82] S. Daan and C. Berde. Two coupled oscillators: simulations of the circadian pacemaker in mammalian activity rhythms. *J. Theor. Biol*, 70:297–313, 1978.

[83] T. Roenneberg and M. Merrow. Molecular circadian oscillators: an alternative hypothesis. *J. Biol. Rhythms*, 13:167–179, 1998.

[84] K. Goto and C. H. Johnson. Is the cell division cycle gated by a circadian clock? The case of *Chlamydomonas reinhardtii*. *J. Cell. Biol.*, 129:1061–1069, 1995.

[85] K. Unsal-Kacmaz, T. E. Mullen, W. K. Kaufmann, and A. Sancar. Coupling of human circadian and cell cycles by the timeless protein. *Mol. Cell. Biol.*, 25:3109–3116, 2005.

[86] S. R. Mackey, J. S. Choi, Y. Kitayama, H. Iwasaki, G. Dong, and S. S. Golden. Proteins found in a CikA interaction assay link the circadian clock, metabolism, and cell division in *Synechococcus elongatus*. *J. Bacteriol.*, 190:3738–3746, 2007.

[87] J. Rutter, M. Reick, L. C. Wu, and S. L. McKnight. Regulation of clock and NPAS2 DNA binding by the redox state of NAD cofactors. *Science*, 293:510–514, 2001.

[88] T. Roenneberg and M. Merrow. Circadian systems and metabolism. *J. Biol. Rhythms*, 14:449–459, 1999.

[89] K. A. Stokkan, S. Yamazaki, H. Tei, Y. Sakaki, and M. Menaker. Entrainment of the circadian clock in the liver by feeding. *Science*, 291:490–493, 2001.

[90] R. Allada, P. Emery, J. S. Takahashi, and M. Rosbash. Stopping time: the genetics of fly and mouse circadian clocks. *Annu. Rev. Neurosci.*, 24:1091–1119, 2001.

[91] J. Schnakenberg. Simple chemical reaction systems with limit cycle behaviour. *J. Theor. Biol.*, 81:389–400, 1979.

[92] A. Turing. The chemical basis of morphogenesis. *Phil. Trans. R. Soc. London B*, 237:37–72, 1952.

[93] M. P. Myers, K. Wager-Smith, A. Rothenfluh-Hilfiker, and M. W. Young. Light-induced degradation of TIMELESS and entrainment of the *Drosophila* circadian clock. *Science*, 271:1736–1740, 1996.

[94] M. E. Dembinska, R. Stanewsky, J. C. Hall, and M. Rosbash. Circadian cycling of a PERIOD-beta-galactosidase fusion protein in *Drosophila*: Evidence for cyclical degradation. *J. Biol. Rhythms*, 12:157–172, 1997.

[95] Y. Kitayama, H. Iwasaki, T. Nishiwaki, and T. Kondo. KaiB functions as an attenuator of KaiC phosphorylation in the cyanobacterial circadian clock system. *Embo. J.*, 22:2127–2134, 2003.

[96] D.K. Welsh, D.E. Logothstis, M. Meister, and S.M. Reppert. Individual neurons dissociated from rat suprachiasmatic nucleus express independently phased circadian firing rhythms. *Neuron*, 14:697–706, 1995.

[97] S. M. Reppert and D. R. Weaver. Molecular analysis of mammalian circadian rhythms. *Annu. Rev. Physiol.*, 63:647–676, 2001.

[98] D.K. Welsh and S.M. Reppert. Gap junctions couple astrocytes but not neurons in dissociated cultures or rat suprachiasmatic nucleus. *Brain. Res.*, 706:30–36, 1996.

[99] S. Yamaguchi, H. Isejima, T. Matsuo, R. Okura, K. Yagita, M. Kobayashi, and H. Okamura. Synchronization of cellular clocks in the suprachiasmatic nucleus. *Science.*, 302:1408–1412, 2003.

[100] S.J. Aton, C.S Colwell, C.J. Harmar, J. Waschek, and E.D. Herzog. Vasoactive intestinal polypeptide mediates circadian rhythmicity and synchrony in mammalian clock neurons. *Nature Neuroscience*, 8:476–483, 2005.

[101] D. Gonze, J. Halloy, J. C. Leloup, and A. Goldbeter. Stochastic models for circadian rhythms: effect of molecular noise on periodic and chaotic behaviour. *C. R. Biol.*, 326:189–203, 2003.

[102] I. Mihalcescu, W. Hsing, and S. Leibler. Resilient circadian oscillator revealed in individual cyanobacteria. *Nature*, 430:81–85, 2004.

[103] H. Broda, D. Brugge, K. Homma, and J. W. Hastings. Circadian communication between unicells? Effects on period by cell-conditioning of medium. *Cell. Biophys. and Biochem.*, 8:47–67, 1986.

[104] F. Beck, B. Blasius, U. Lüttge, R. Neff, and U. Rascher. Stochastic noise interferes coherently with a model biological clock and produces specific dynamic behaviour. *Proc. Biol. Sci.*, 268:1307–1313, 2001.

[105] U. Rascher, M. T. Hütt, K. Siebke, B. Osmond, F. Beck, and U. Lüttge. Spatiotemporal variation of metabolism in a plant circadian rhythm: the biological clock as an assembly of coupled individual oscillators. *Proc. Natl. Acad. Sci. U S A*, 98:11801–11805, 2001.

[106] A. Bohn. *Analysis and simulation of circadian multi-oscillator systems in Crassulacean acid metabolism plant*. PhD thesis, Technische Universität Darmstadt, Darmstadt, Germany, 2003.

[107] H. Fukuda, J. Kodama, and S. Kai. Circadian rhythm formation in plant seedling: global synchronization and bifurcation as a coupled nonlinear oscillator system. *Biosystems*, 77:41–46, 2004.

[108] A.J Millar. *Biological Rhythms and Photoperiodism in Plants*. Bios. Scientific, Oxford, UK, 1981.

[109] A. Bohn and J. García-Ojalvo. Synchronization of coupled biological oscillators under spatially heterogeneous environmental forcing. *J. Theor. Biol.*, 250:37–47, 2008.

[110] H. H. McAdams and A. Arkin. Stochastic mechanisms in gene expression. *Proc. Natl. Acad. Sci. U S A*, 94:814–819, 1997.

[111] J. Walleczek. *Self-organized Biological Dynamics.* Cambridge Univ. Press, Cambridge, 2000.

[112] W. J. Blake, M. Kaern, C. R. Cantor, and J. J. Collins. Noise in eukaryotic gene expression. *Nature*, 422:633–637, 2003.

[113] J. M. Pedraza and A. van Oudenaarden. Noise propagation in gene networks. *Science*, 307:1965–1969, 2005.

[114] M. B. Elowitz, A. J. Levine, E. D. Siggia, and P. S. Swain. Stochastic gene expression in a single cell. *Science*, 297:1183–1186, 2002.

[115] J. Paulsson, O. G. Berg, and M. Ehrenberg. Stochastic focusing: fluctuation-enhanced sensitivity of intracellular regulation. *Proc. Natl. Acad. Sci. U S A*, 97:7148–7153, 2000.

[116] A. Neiman, L. Schimansky-Geier, F. Moss, B. Shulgin, and J. J. Collins. Synchronization of noisy systems by stochastic signals. *Phys. Rev. E.*, 60:284–292, 1999.

[117] D. Fange and J. Elf. Noise-induced Min phenotypes in *E. coli*. *PLoS Comput. Biol.*, 2:80, 2006.

[118] J. Paulsson. Models of stochastic gene expression. *Physics of Life Reviews*, 2:157–175, 2005.

[119] P. S. Swain, M. B. Elowitz, and E. D. Siggia. Intrinsic and extrinsic contributions to stochasticity in gene expression. *Proc. Natl. Acad. Sci. U S A*, 99:12795–12800, 2002.

[120] J. M. Vilar, H. Y. Kueh, N. Barkai, and S. Leibler. Mechanisms of noise-resistance in genetic oscillators. *Proc. Natl. Acad. Sci. U S A*, 99:5988–5992, 2002.

[121] D. Gonze, J. Halloy, and A. Goldbeter. Deterministic and stochastic models for circadian rhythms. *Pathol. Biol. (Paris)*, 51:227–230, 2003.

[122] N. Barkai and S. Leibler. Circadian clocks limited by noise. *Nature*, 403:267–268, 2000.

[123] C. V. Rao, D. M. Wolf, and A. P. Arkin. Control, exploitation and tolerance of intracellular noise. *Nature*, 420:231–237, 2002.

[124] M. Samoilov, S. Plyasunov, and A. P. Arkin. Stochastic amplification and signaling in enzymatic futile cycles through noise-induced bistability with oscillations. *Proc. Natl. Acad. Sci. U S A*, 102:2310–2315, 2005.

[125] M. J. Rust, J. S. Markson, W. S. Lane, D. S. Fisher, and E. K. O'Shea. Ordered phosphorylation governs oscillation of a three-protein circadian clock. *Science*, 318:809–812, 2007.

Acknowledgments

First, I would like to express my gratitude to my supervisor Professor Dr. Friedemann Kaiser for giving me possibility to work in his group. During this time I have learned a lot about the field of nonlinear dynamics, especially about its great application in biology. I am also very grateful for his support and trust of any kind. Without his enormous patience, solid criticism and constructive discussions, the ending of this thesis would not have been possible.

Furthermore, I would like to thank Deutsche Forschungsgemeinschaft (DFG) for opportunity to be a part of Graduiertenkolleg 340 "Communication in Biological Systems", providing me funding for my scientific research and thus giving me opportunity to gain knowledge in the interesting and diverse fields of biology. I owe also gratitude to Prof. Dr. Ulrich Lüttge and Heitor Monteiro Duarte for the constructive collaboration we had. I wish to thank all other members of the Graduiertenkolleg for their friendly reception, especially Prof. Dr. Felicitas Pfeifer and Monika Medina.

A special thanks goes to my colleagues and friends, Andreas Bohn, Hauke Busch and Kristian Motzek, with whom I shared not only worries about computer system and life in general, but also friendly and most of the time funny moments during my work. I would like to extend my thanks to other, "younger" colleagues, Tobias Richter, who helped me with moving "through Germany" and providing me an insight into a Linux system administration, Erik Glatt, which idea gave a turning point in my research and Martin Gassel for reading my manuscript.

Finally, a big thanks goes to my family, my brother Vojislav and my parents, Mirjana and Bogdan Žerajić, husband Vladimir and my children Jovana and Petar for their unlimited love and persistent confidence in me. Without their endless support and encouragement, I would have never finished this work. *Hvala vam dragi moji na svemu!*

Curriculum Vitae

Name	Ivona Jakovljević
Geburtsdatum	27. September 1973.
Geburtsort	Belgrad, Serbia
Familienstand	verheiratet, zwei kinder
Nationalität	Serbisch

Juni 1992	Abitur, III Belgrader Gymnasium
Juli 2001	Abschluss als Dipolm-Physikerin, Universiatät Belgrad
seit *Februar* 2002	Promotionsstudium in theoreticher Physik unter der Leitung von Prof. Dr. F. Kaiser am Institut für angewandte Physik der TU Darmstadt
2002 – 2005	Promotionsstipendium der TU Darmstadt, DFG Graduiertenkolleg 340 'Communication in Biological Systems'
2005 – 2006	Wissenschaftliche Mitarbeiterin an der TU Darmstadt

Hiermit erkläre ich an Eides statt, daß ich
die vorliegende Dissertation selbständig verfasst
und nur die angegebenen Hilfsmittel verwendet habe.
Ich habe bisher keinen Versuch unternommen, an einer
anderen Hochschule das Promotionsverfahren einzuleiten.

Darmstadt, im Februar 2010